FINAL REPORT

PROJECT B4

JANUARY 2024

Integrated Corridor Management: Cooperative Signal Control with Freeway Operations and Ramp Metering

Ali Hajbabaie, Ph.D. North Carolina State University
Lily Elefteriadou, Ph.D., University of Florida
Mohammed Hadi, Ph.D., Florida International University

STRIDE | Southeastern Transportation Research, Innovation, Development and Education Center
UF | Transportation Institute UNIVERSITY of FLORIDA

TECHNICAL REPORT DOCUMENTATION PAGE

1. Report No. Project B4	**2. Government Accession No.**	**3. Recipient's Catalog No.**
4. Title and Subtitle Integrated Corridor Management: Cooperative Signal Control with Freeway Operations and Ramp Metering		**5. Report Date** 1/28/2024 **6. Performing Organization Code**
7. Author(s) Ali Hajbabaie, Ph.D., North Carolina State University Lily Elefteriadou, Ph.D., University of Florida Mohammed Hadi, Ph.D., Florida International University		**8. Performing Organization Report No.** STRIDE Project B4
9. Performing Organization Name and Address North Carolina State University, 915 Partners Way, Raleigh, North Carolina 27695; University of Florida, 365 Weil Hall, PO Box 11680, Gainesville, FL 32605; Florida International University, 1055 W. Flagler Street, EC 3680, Miami, FL 33174		**10. Work Unit No.** **11. Contract or Grant No.** Funding Agreement Number 69A3551747104
12. Sponsoring Agency Name and Address University of Florida Transportation Institute/ Southeastern Transportation Research, Innovation, Development and Education Center (STRIDE) 365 Weil Hall, P.O. Box 116580 Gainesville, FL 32611 U.S Department of Transportation/Office of Research, Development & Tech 1200 New Jersey Avenue, SE, Washington, DC 20590		**13. Type of Report and Period Covered** 08/16/2020 to 1/28/2024 **14. Sponsoring Agency Code**

15. Supplementary Notes N/A

16. Abstract - The study aims to develop methodologies for integrated corridor management: methodologies that optimize ramp metering rates and arterial signal timing plans to improve overall traffic operation in corridor networks. Three different methodologies are developed for this purpose. The first aims to reduce queue spillbacks from on-ramps to lessen their impacts on arterial roads. The results show considerable improvement over existing conditions by at least 3% and up to 23% in overall network performance in terms of average speed. In the second methodology, an integrated control framework is developed where all signal controllers and ramp metering rates are optimized jointly to improve the overall traffic condition of the corridor. The results show that the developed control framework can reduce average delay, stops, and travel time by up to 33%, 36%, and 16%, respectively compared with benchmark conditions. In the third methodology, machine learning techniques are applied to predict capacity reduction of arterial roads due to queue spillbacks from freeway on-ramps to the arterial streets that result in lane blockages. The study developed a prediction methodology to estimate capacity reductions due to these spillbacks up to two cycles before they happen on the arterial street. The results initiate new possibilities for agencies to activate special signal timing and/or ramp metering plans to prevent the occurrence of the spillback, by constraining the number of vehicles feeding the on-ramp from the upstream intersection(s) and/or by relaxing the ramp metering to allow more vehicles to be released from the on-ramp. Overall, the developed methodologies can predict potential arterial road capacity reduction, reduce queue spillback effects, and integrate ramp metering rates with signal timing plans jointly for overall improvements of a corridor network. In real-world applications of these methodologies, the machine learning-based predictive methodology (the third methodology) can be used to continuously predict the potential for queue spillbacks from the ramps before they occur. Once a potential spillback is predicted, then a decision support software at the traffic management center will direct the controller to activate a special plan from a library of plans developed off-line using the first methodology or direct the controller to implement the developed real-time signal control strategy using the second methodology.

17. Key Words Traffic Management, Signal Control, Highway Capacity Manual, Optimization, Model Predictive Control, Machine Learning, Integrated Corridor Management	**18. Distribution Statement** No restrictions

19. Security Classif. (of this report) N/A	**20. Security Classif. (of this page)** N/A	**21. No. of Pages** 125 pages	**22. Price** N/A

DISCLAIMER

The contents of this report reflect the views of the authors, who are responsible for the facts and the accuracy of the information presented herein. This document is disseminated in the interest of information exchange. The report is funded, partially or entirely, by a grant from the U.S. Department of Transportation's University Transportation Centers Program. However, the U.S. Government assumes no liability for the contents or use thereof.

ACKNOWLEDGEMENT OF SPONSORSHIP AND STAKEHOLDERS

This work was sponsored by a grant from the Southeastern Transportation Research, Innovation, Development, and Education Center (STRIDE).

Funding Agreement Number - 69A3551747104

LIST OF AUTHORS

Lead PI:

Ali Hajbabaie, Ph.D.

North Carolina State University

ahajbab@ncsu.edu

0000-0001-6757-1981

Co-PI:

Lily Elefteriadou, Ph.D.

University of Florida

elefter@ce.ufl.edu

0000-0003-4045-3365

Co-PI:

Mohammed Hadi, Ph.D.

Florida International University

hadim@fiu.edu

ORCID: 0000-0003-2233-8283

Additional Researchers:

Abdullah Al Farabi, North Carolina State University, afarabi@ncsu.edu, 0000-0003-1843-3720

Rasool Mohebifard, North Carolina State University, rmohebi@ncsu.edu, 0000-0003-1301-9504

Leonida Kibet, University of Florida, leonidakibet@ufl.edu, 0000-0001-9443-742X

Atika Jabin, Florida International University, ajabi002@fiu.edu, 0000-0001-7924-6633

Hector Mata. Florida International University, hmata010@fiu.edu, 0000-0002-8435-0635

TABLE OF CONTENTS

LIST OF FIGURES

LIST OF TABLES

ABSTRACT

The study aims to develop methodologies for integrated corridor management: methodologies that optimize ramp metering rates and arterial signal timing plans to improve overall traffic operation in corridor networks. Three different methodologies are developed for this purpose. The first aims to reduce queue spillbacks from on-ramps to lessen their impacts on arterial roads. Based on the capacity of freeway and on-ramps, signal timing plans and ramp metering rates are adjusted off-line to improve the overall corridor performance. A balance among demand, average delays, and queue lengths must be achieved to improve performance. Two case study sites in San Mateo, CA and Miami, FL are considered, and the proposed methodology is tested using the VISSIM microscopic simulation software. The results show considerable improvement over existing conditions by at least 3% and up to 23% in overall network performance in terms of average speed.

In the second methodology, an integrated control framework is developed where all signal controllers and ramp metering rates are optimized jointly to improve the overall traffic condition of the corridor. The integrated control is formulated as a Mixed Integer Non-Linear Program (MINLP). A Model Predictive Control (MPC) framework is used. The methodology is tested in San Mateo, CA, and benchmarked with two other optimization and two simulation scenarios. The results show that the developed control framework can reduce average delay, stops, and travel time by up to 33%, 36%, and 16%, respectively compared with benchmark conditions. Besides, the integrated control balanced the congestion (in terms of delay) in the corridor network between the freeway and arterial street. With minimal impacts on freeway delays in comparison to benchmarks, the integrated control significantly reduced the arterial congestion.

In the third methodology, machine learning techniques are applied to predict capacity reduction of arterial roads due to queue spillbacks from freeway on-ramps to the arterial streets that result in lane blockages. The study developed a prediction methodology to estimate capacity reductions due to these spillbacks up to two cycles before they happen on the arterial street. Two clusters of algorithms are used to predict capacity reductions. In one cluster, capacity reduction is considered as a continuous variable while in the other cluster of algorithms capacity reduction is a categorical variable. The results show that the continuous models predict capacity reduction better than the categorical models. The results initiate new possibilities for agencies to activate special signal timing and/or ramp metering plans to prevent the occurrence of the spillback, by constraining the number of vehicles feeding the on-ramp from the upstream intersection(s) and/or by relaxing the ramp metering to allow more vehicles to be released from the on-ramp. Overall, the developed methodologies can predict potential arterial road capacity reduction, reduce queue spillback effects, and integrate ramp metering rates with signal timing plans jointly for overall improvements of a corridor network. In real-world applications of these methodologies, the machine learning-based predictive methodology (the third methodology) can be used to continuously predict the potential for

queue spillbacks from the ramps before they occur. Once a potential spillback is predicted, then a decision support software at the traffic management center will direct the controller to activate a special plan from a library of plans developed off-line using the first methodology or direct the controller to implement the developed real-time signal control strategy using the second methodology.

Keywords (up to 5):
Traffic Management, Signal Control, Highway Capacity Manual, Optimization, Model Predictive Control, Machine Learning, Integrated Corridor Management

EXECUTIVE SUMMARY

Integrated corridor management offers great potential to improve traffic operations on both freeway facilities and intersecting arterial streets. Coordinating ramp metering rates on on-ramps and signal timing plans for the interchanges and upstream intersections of the arterial street can improve both freeway and arterial operations. This research introduces three methodologies for integrated corridor management. The three methodologies can be used together in an integrated management framework to predict congestion before it occurs, then use this information to either activate a special signal plan from a library of plans or switch to a real-time signal control strategy to reduce the impacts of congestion.

The first methodology develops a queue distribution framework to reduce queue spillbacks from on-ramps and affected upstream intersections. Signal timing plans and ramp metering rates are adjusted to distribute the queues of on-ramps on multiple upstream intersections along the intersecting arterial street. The framework aims to find the most suitable timing plans and metering rates to minimize network delay while balancing individual segment and intersection delays and queues. A heuristic approach is followed to determine the signal timing plans which uses demand proportions at the on-ramp and the upstream intersections while also considering the capacity downstream of the freeway merge. The method has been applied and tested using two simulated study areas with three different traffic congestion scenarios. Results show that the method can successfully reduce the effects of queue spillbacks when compared to existing condition. Average network speed and total travel times improved by at least 3% in some scenario and up to 23% in others depending on the local traffic conditions.

The second methodology jointly optimizes ramp metering rates and signal timing plans to improve corridor network performance. This integrated control framework predicts the traffic state in near future (e.g., around two minutes in the future), and according to the prediction, updates signal timing plans as well as ramp metering plans in the corridor. The goal of the framework is to set efficient timings that maximize the numbers of completed trips in the corridor network. Therefore, this framework implements efficient timings that allow vehicles to leave the corridor network in less time resulting in shorter delays and travel times. The framework is tested in a simulation environment and the results are compared with four other scenarios including existing conditions. It is observed that the integrated control has been able to reduce delays, queues, and travel time significantly compared to the benchmark scenarios. The improvements for average delay, stops, and travel time go up to 33%, 36%, and 16%, respectively in comparison to other scenarios. At the same time, the integrated control framework reduced delays of existing heavily congested arterial street with minimum effects on freeway delays as compared to tested scenarios. Therefore, the integrated control has balanced the congestion between freeway and arterial streets in addition to overall network improvements.

The third methodology predicts the capacity reduction of arterial roads due to upcoming queue spillback from an on-ramp two cycles before it happens. This methodology allows predicting the on-set of queue spillbacks from freeway on ramps to arterial streets and resulting capacity drops on the arterial streets due to this spillback. Machine learning techniques are used to develop prediction models that enable the implementation of an integrated control strategy for signal timing and ramp metering to reduce the likelihood of queue spillback. Two clusters of machine learning algorithms (classified and continuous) are tested, including classification decision tree, fuzzy rule-based systems, M5 pruned decision tree, and two variations of the long short-term memory (LSTM) based recurrent neural network (RNN). The RNN model outperforms the other tested algorithms, achieving a mean absolute percentage error of 7.4% in predicting the capacity reduction at upstream intersections due to on-ramp queue spillback. This methodology has the potential to improve traffic flow and reduce congestion on arterial roads by predicting and mitigating the impact of on-ramp queue spillback. This framework can be integrated with arterial signal timing plans so that timings are set to avoid any disruption to regular traffic operations.

Overall, these methodologies can be used as efficient tools for integrated corridor management. While queue distribution methodology relies on manual splitting of signal timings, any algorithm to optimally distribute queues to avoid spillbacks from on-ramps has promising prospects. The integrated control framework provides a real-time control strategy that can be implemented efficiently in a corridor and improve the congestion condition of the corridor. The capacity reduction prediction models developed in the third methodology can be incorporated with any coordination methods for more efficient signal timing plans and ramp metering rates.

While the proposed methodology can be vital parts of integrated corridor management tools, there is still room for future works and improvements. The queue distribution methodology needs to be automated and also adjusted to use real-time traffic data. The developed integrated control framework would require communication and coordination among controllers for efficient and accurate implementation of signal and ramp metering plans. This study does not incorporate presence of various proportions of connected vehicles in traffic stream, which needs to be done in the future. Besides, the integrated control does not maintain specific phase sequence and common cycle times in the arterial intersections. The performances of integrated control can be studied considering specific phase and cycle timings. Finally, the prediction models developed to estimate capacity reduction are site specific. More sites are needed to generate more accurate and generalizable prediction models.

1 INTRODUCTION

Freeways and intersecting arterials often operate without coordination of their operation. However, demand at an on-ramp depends on the discharge of traffic from the upstream interchange or intersections. Innovative signal control strategies can help manage this on-ramp demand and the resulting downstream queues. Similarly, ramp metering strategies have been in place to improve the flow of traffic on freeway facilities. When the traffic congestion on the freeway facility is high, metering rates increase, resulting in longer queues along the on-ramp. Such queues may eventually spill back to the upstream intersection or interchange. When such intersections are along an arterial corridor with high traffic demands, queue spillback from ramps or downstream signals can disrupt operations on the entire facility. Flushing queued vehicles along on-ramps leads to deteriorating traffic performance on the freeway facility. Therefore, optimal operations should achieve a balance such that ramp meters hold back traffic as much as possible to avoid freeway breakdown, but not too much such that queues on the on-ramp spillback to the upstream interchange.

Such a balance can be achieved when the traffic signals at the interchange and arterial corridor leading to it (see Figure 1) are controlled considering freeway operations and work together with the ramp metering signals. The interchange and arterial corridor signals can help ramp metering signals by regulating the flow toward the freeway. Such considerations can also avoid wasting green time if they avoid allocating it to the movements entering the ramp when the on-ramp storage area is full. Strategies can be implemented such that instead of having a long queue along the on-ramp (or a downstream congested signal) that can spillback to upstream intersections, the demand can be held back upstream, and the queue can be distributed to intersections and approaches upstream along the arterial corridor. Such strategies can not only improve traffic performance on the freeway facility, but they can also improve progression on the arterial corridor.

Figure 1: Corridor arterial and freeway interchange

1.1 OBJECTIVE

The main objective of this project is to develop integrated corridor management methodologies that cooperatively coordinate the control decisions of the signalized intersections and ramp flows from the on-ramps. This project aims to reduce congestion along both the freeway facility and the arterial facility in an integrated corridor management (ICM) operation. Two different approaches are followed to achieve this:

- Rules-based optimization approach: Develop a signal control methodology that considers freeway operations in order to time the interchange and/or adjacent arterial traffic signals such that they can meter the traffic entering the freeway through on-ramps.
- Cooperative optimization-based approach: Develop a traffic responsive methodology that integrates signal timing plans and ramp metering controls to improve traffic operations of both the arterial corridor and the freeway.

In addition to these two approaches, the research team developed a machine-learning-based prediction methodology for use as part of real-time decision support tools for integrated corridor management to allow the recommendation of the activation and implementation of the appropriate signalization plans to achieve the integrated management of the freeways and arterial streets. In real-world applications, the predictive methodology can be used to continuously predict the potential for queue spillbacks from the ramps before they occur. Once a potential spillback is predicted, then a decision support software at the traffic management center will direct the controller to activate a special plan from a library of plans developed off-line using one of the two signal control approaches mentioned above (the mathematical optimization based approach and the heuristic optimization based approach)

1.2 SCOPE

The study proposes integrated corridor management methodologies that aim to reduce congestion on freeway and connected arterial roads. One of the methodologies develops a framework to distribute on-ramp queues to arterial roads to avoid queue spillback from the on-ramps. Another methodology predicts capacity reduction of arterial roads due to queue spillback from on-ramps. Therefore, these two methodologies are predominantly focused on lessening the impact of on-ramp queues on upstream arterial roads thus, they can be incorporated with arterial signal timing plans to reduce the effect of queue spillbacks. At the same time, these methodologies can be a part of any coordinated signal and ramp metering control framework for developing efficient control strategies. Furthermore, the integrated control methodology proposes a holistic control system that combines ramp metering controllers and signal controllers to generate optimum timing plans for a corridor network. As this methodology integrates signal and metering control decisions, optimal timing solutions that improves the entire corridor network are achieved. This mathematical optimization-based

methodology, however, relies on Vehicle-to-Infrastructure (V-to-I) technology for communication and coordination among controllers and accurate implementation of control decisions. Also, all three methodologies are tested in simulated networks. The first methodology is tested for two case study locations and the other two methodologies are tested on a single site. Observed improvements may be site specific and additional testing may be needed to gain better insights into performance improvements. It is also important to note that the mathematical optimization based Integrated control methodology does not consider congestions outside the study area. The effects of the methodology outside the boundary area have yet to be discovered.

2 LITERATURE REVIEW

Researchers have studied various approaches for integrated corridor management to come up with methodologies to reduce traffic congestion. While many studies integrate multiple strategies to develop efficient corridor management, the limitations of these studies are better understood when different isolated strategies are reviewed along with their effects inside the corridor. Therefore, this section reviews different literature on ramp metering strategies and queue spillback effects from freeways to urban streets. The prediction on arterial street congestion is also grouped together and reviewed. Another group of studies with perimeter control approaches to control congestion inside a control area are also studied. Finally, integrated controls of ramp metering and signal timing strategies are reviewed. Studies on network performance analysis are also grouped and reviewed.

2.1 Ramp Metering Strategies

Ramp metering strategies have been widely studied by researchers to improve the freeway traffic operation. The sole goal of these studies was to lessen freeway congestion only. Thus, these research studies do not capture the impacts of ramp metering on nearby arterial roads. Such studies are shortly described below:

Two studies (Haj-Salem and Papageorgiou, 1995; Papageorgiou and Kotsialos, 2002) analyzed the prospects of ramp metering in improving freeway operations and ramp metering effects. Similarly, a widely applied local ramp metering control algorithm, ALINEA, was studied by Smaragdis and Papageorgiou (2003). They evaluated variations of ALINEA, namely, FL-ALINEA, UP-ALINEA, UF-ALINEA, and X-ALINEA/Q in simulation and showed the prospects and limitations of these variations. Few other studies (Kan et al., 2016; Wang et al., 2014) modified traditional ALINEA with their proposed PI-ALINEA control algorithm to resolve the downstream bottleneck issue.

Again, Bellemans et al. (2006) studied ALINEA algorithm along with a MPC-based ramp metering control. During morning rush hours on a motorway, the effects of the control algorithms were tested, and they found the control algorithms improve performances over no metering. Also, some studies (Papamichail et al., 2010a, 2010b) combined MPC-based optimization with Heuristic Ramp metering coordination (HERO). They achieved significant improvement in throughput (completed number of trips of vehicles) and network travel time with their methodology. Focusing on reducing freeway bottlenecks, Kotsialos and Papageorgiou (2004) developed a non-linear optimization program for coordinating ramp metering controls. They suggested strong metering to be implemented on on-ramps near bottleneck locations. A comparison between local and global MPC-based metering controls were studied by Frejo and Camacho (2012). They found that achieving a global control is highly complex and computationally expensive. Bhouri et al. (2013) compared coordinated ramp metering with isolated ramp metering. They found improvement of travel times on a motorway as compared to isolated ramp metering strategy. They also found that travel time variabilities decrease with

coordinated metering over no metering control implementation. Han et al. (2020) developed an aggregated traffic model-based control method that uses MPC controller to meter on-ramp traffic. The optimization program meters by optimizing and distributing inflow volumes to freeway through the on-ramps.

As stated earlier, the above strategies consider freeway congestion only and do not focus on queue spillbacks or arterial traffic congestion that may occur due to implementation of ramp metering.

2.2 Queue Spillback effects from freeways to urban streets

Limited research has been reported to address freeway spillback onto signalized intersections. The HCM Merge/Diverge Segments methodology determines whether volume exceeds capacity at any critical points along the segment and estimates the maximum expected queue along each on-ramp. However, the method does not consider the effects the resultant queue may have on the upstream surface street. The HCM Ramp Terminals and Alternative Intersections procedure includes an adjustment to consider spillback from the downstream intersection to the upstream in the form of additional lost time. This lost time is estimated for each upstream movement as a function of the downstream queue length and storage availability. A similar logic can be applied in the case of spillback from the on-ramp to a local signalized intersection, as it results in additional lost time for some/all the signal phases that serve traffic movements destined for the on-ramp.

Tian (2007) analyzed the effects of ramp metering spillback onto a diamond interchange using the simulator DRIVE. Capacity reduction and delay increase were found upstream from the ramp meters due to discharging flow reductions resulting from queue spillback and intersection blockage. The authors estimated the delay incurred by the affected movements with a theoretical plot of demand over time.

For freeways without ramp metering, the queue discharge rate depends on freeway merge operations. While arrival rates at the back of the on-ramp queue are an input to HCM procedures, departure rates into the mainline during congested conditions are currently not available, and no guidance was found in the literature to provide such estimates. This is a critical aspect of evaluating spillback conditions at a merge ramp, as the discharge rate of the on-ramp traffic onto the freeway is a key parameter to calculate the queue length along the ramp over time.

Su, Lu, Horowitz, & Wang (2014) proposed a coordination strategy to integrate signal controls at an intersection that feeds the onramp with the freeway on-ramp metering. The method focuses on minimizing queue spillback and thus, delay and total travel distance of a network with an on-ramp bottleneck. The signal control approach uses demands to distribute green times while considering the intersection turn bays and the available on-ramp storage space. The authors implemented the strategy at one affected intersection and achieved an improved network performance. Distributing the on-ramp queue spillback across several upstream

intersections feeding the ramp may yield better network performance in terms of delay. Also, the approach is applicable for scenarios involving on-ramp bottlenecks only. Queue propagation could result from oversaturation at the downstream of freeway merge.

Cheng & Chang (2021) proposed an arterial friendly metering strategy that optimizes the ramp metering and the signal at the intersections that feed the traffic to the on-ramp. The authors performed numerical analyses and simulation experiment involving one case study to evaluate their method. The authors managed to prevent on-ramp queue spillback and arterial gridlock by maximizing freeway and connected arterial throughput in the study site control area. While the evaluation of the strategy focused on the performance of a bounded study site, it is important to assess effects to the performance of an extended network consisting of several interchanges both upstream and downstream of the study section. The controlled area could experience improved traffic operations at the expense of the extended network. The performance of an extended network could deteriorate because of queueing vehicles that do not enter the control area. Additionally, although a single case study area provides in-depth understanding of the model's functionality, multiple case studies are more robust for evaluation. Particularly, real world network sites with existing signal plans and different types of bottlenecks (on-ramp bottleneck, freeway merge downstream bottleneck etc.) that result in queue spillback to upstream intersections.

Reviewed studies show a growing interest in the concept of integrated corridor management to address congestion. However, there is still much to explore on the effects of queue back up from freeways to the urban streets.

2.3 Cooperative Control of Ramp Metering and Signal Timing

Researchers have been developing control methodologies that will not only reduce congestions on freeways, but also will improve traffic operations of nearby arterials and streets.

Kwon et al. (2003) developed a coordination among ramp metering controls and signal controls of nearby arterial intersections. They adjusted the signal timings and ramp metering based on traffic states on on-ramps and freeways but no optimization is implemented. Lim et al. (2011) integrated off-ramp timing with arterial intersections and developed a methodology that sets timings in a way to avoid queue spill over to the freeway. They specifically considered off-ramp queue spill back and no on-ramp metering is present in the study. Similarly, Yang et al. (2018) sets off-ramp timing using possibility of queue spill over. If there is a possible queue spillback, an off-ramp control gets activated that clears the off-ramp. Otherwise, the signal control performs as adaptive controllers. This study also focuses on off-ramp and queue spill over only with no consideration on overall network performances. Lu et al. (2013) coordinated one on-ramp and one intersection in a field test and achieved less network delay. The methodology did not consider coordination among multiple on-ramps and intersections. Su et al. (2014) proposed a methodology based on UP-ALINEA that uses ramp storage and traffic demand as

inputs. The inputs are used to meter the on-ramp traffic by coordinating with nearby arterial intersections. The proposed method did not produce significant improvement in the performance of the network. Kan et al. (2018) developed an algorithm that considers on-ramp storage to set arterial signal timings and sends small platoon to on-ramps to avoid queue spillbacks. The algorithm integrates signal timing and ramp metering, the timings are changed dynamically. The study provides better results than conventional approaches. However, the control algorithm considers on-ramp storage only to avoid queue spillback. Heavy congestion on the arterials will persist if there is high demand of vehicles that want to get into the on-ramp. So, there is a need to find a detailed coordinated approach that considers all directional movements and finds solutions optimally. On the other hand, Pang and Yang (2020) developed an optimization framework that optimizes arterial signal controllers to improve freeway operation and system network without considering any ramp metering. The study, therefore, did not consider any coordination of on-ramp metering with signal controllers. Hashemi and Abdelghany (2016) integrated four control strategies-dynamic signal plan, dynamic routing, ramp metering, and dynamic shoulder lane. The integrated control outperforms current condition in terms of travel time. The study, however, is limited in setting optimized plans. Signal plan of each intersection is selected from a preset plans based on the congestion condition on that intersection. Ramp metering also has four preset plans (25%, 50%, 75%, and 100% flow of saturation flow of on-ramps). Thus, the timings have preset plans and signal timing plans are set according to local congestion scenario of each intersection.

Overall, the mentioned studies lack in developing a global optimal framework that coordinates among all signal controllers and ramp metering controls in a corridor. An integrated demand-responsive framework that sets optimal timings in a way to achieve a common goal of producing an efficient network is still necessary.

2.4 Metered Ramp Queuing

There is extensive literature on queues resulting from on-ramp metering. Papageorgiou and Kotsialos (Markos Papageorgiou and Kotsialos, 2002) pointed to the need to address excessive queues on the ramps by using detectors at the upstream parts of the on-ramps to provide input for managing the ramp queues. The Ramp Management and Control Handbook (Jacobson et al., 2006) emphasizes that a successful implementation of ramp metering strikes a balance between freeway mainline improvements and vehicle delays and queues on the entrance ramps.

Wu et al. in (Wu et al., 2008) evaluated three methods for predicting on-ramp queues, including Kalman filter, linear occupancy (assumed a linear relationship between the time occupancy and the space occupancy), and back of queue calculated based on the Highway Capacity Manual (HCM). The study found that both the Kalman filter and linear occupancy methods can produce accurate predictions. Cheng et al. (Cheng and Chang, 2021) emphasized that the maximum

queue length has to be constrained within the ramp physical length using the arriving on-ramp volume and the optimized metering rate.

Other papers discussed the negative impacts of on-ramp queuing on adjacent street operations. They suggested allowing more vehicles to enter the freeway when there is a long queue on the ramp (Shaaban et al., 2016), (Arnold, 1998), (Smaragdis and Papageorgiou, 2003b) and (Papamichail and Papageorgiou, 2008). These studies indicate that allowing more vehicles to enter the freeway can adversely impact the freeway operations, sometimes causing the ramp metering to be ineffective. Shaaban et al. in (Shaaban et al., 2016) suggested that coordinating upstream traffic signals and ramp meters can be one way to avoid this. Kan et al. in (Kan et al., 2018b) mentioned that due to long cycle signals at the surface street in the peak periods, long platoons approach the on-ramps within a short period of time, increasing the probability of spillback to the surface street. They developed and evaluated an integrated arterial signal timing with the adjacent ramp-metering system using available on-ramp storage and the freeway ramp-metering. Mohebifard and Hajbabaie in (Mohebifard and Hajbabaie, 2018b) and (Mohebifard and Hajbabaie, 2019) developed methods to meter traffic entering urban street networks. They also observed that coordinating the traffic light signals with metering signals significantly improves traffic operations (Mohebifard and Hajbabaie, 2019).

The review in this section indicates that queueing from on-ramps have been addressed in previous studies, however, there has been no effort to predict the queues before they occur for use in proactive management.

2.5 Ramp Metering Control with Mainstream Traffic Flow Control (MTFC) Strategies

Some researchers combined ramp metering control strategies with Mainstream Traffic Flow Control strategies (MTFC) (e.g., variable speed limit) to improve freeway operations. Again, these studies focus only on freeway operation. They do not consider the impacts of ramp metering on upstream arterials and side streets. Few of notable studies are as follows:

Hegyi et al. (2005) proposed a METANET based MPC framework that integrates ramp metering control and variable speed limit to efficiently improve freeway operation. Carlson et al. (2010a, 2010b) provided two control strategies: independent variable speed limit control and an integrated control of variable speed limit and ramp metering controls. Wang et al. (2021) provided a methodology that incorporates a coordinated ramp metering along with MTFC. They applied the methodology in simulation and found significant improvement as the optimal control can eliminate freeway bottlenecks. A similar study (Wang et al. 2022) integrated cooperative ramp control with variable speed limit using deep learning algorithm. The algorithm minimizes travel time and produces promising results in freeway performance improvement.

2.6 Predicting Arterial Street Congestion

Iqbal et al. predicted the breakdown probability on an arterial street segment by combining point detection with vehicle re-identification data (Iqbal et al., 2017). The study used a decision tree approach combined with binary logistic regression. Filipovska and Mahmassani (Filipovska and Mahmassani, 2020) predicted traffic flow breakdown based on temporally and spatially lagged aggregated variables from stationary data using machine learning (ML) models, including Bayesian models, logistic models, tree models, perceptron-based models, and Support vector machine (SVM). The ML methods showed better prediction performance compared to the traditionally used methods. The neural network and the two used SVM approaches achieved the best performance considering class-balanced accuracy, true positive rate (recall), true negative rate (specificity), and positive predictive value (precision) as performance measures.

Massahi et al. (Massahi et al., 2017) developed and assessed two models to estimate the capacity reduction at the incident location and upstream intersection using regression models. Tariq et al. (Tariq et al., 2020) utilized a combination of recursive partitioning and regression decision tree (RPART) and fuzzy rule-based system (FRBS) for the preparation of a ML model to capture the historic responses of the traffic signal engineers to automate the process of updating the signal timing plans during non-recurrent conditions.
Rahman and Hasan developed a data-driven real-time queue length prediction technique using a deep learning approach in (Rahman and Hasan, 2021). To capture the time dependent patterns of queue of a signal, a long short-term memory (LSTM) neural network was utilized. Comert et al. developed and compared six short-term queue length prediction models for adaptive traffic signal control using six variations of Grey systems (Comert et al., 2021). They reported that the Greys models performed better than the complex ones like LSTM and NN. Mata and Hadi in (Mata and Hadi, 2021) combined data mining and machine learning with HCM procedures for the assessment of the level of service (LOS) variation in time and space throughout the year. To measure the LOS, this study showed how the HCM processes could be used in conjunction with a bi-level clustering approach, mining of association rules, artificial neural network (ANN), and visualization.

The review in this section indicates that previous studies have successfully used machine learning to predict the congestion on arterial streets in near real-time operation. Therefore, such techniques can be used to predict the reduction in capacity at upstream intersections due to queue spillbacks from on-ramps.

2.7 Perimeter Control and Signal Timing optimization

A set of studies focus on improving traffic condition by restricting the flow of vehicles inside the network by perimeter control. These studies can solely be perimeter control approaches as well as perimeter control plus signal timing optimization. These methodologies keep vehicles outside

the protected region to improve the congested condition inside the network. Such methodologies can be divided into two types: Macroscopic Fundamental Diagram (MFD) based control system and Optimization-based approaches.

A group of studies (Geroliminis et al., 2013; Keyvan-Ekbatani et al., 2015; Ramezani et al., 2015) developed methodology using MFD to control traffic at the perimeter level. No integration with signal timing is considered in these studies. On the other hand, some studies (Keyvan Ekbatani et al., 2016; Kouvelas et al., 2018) developed an integrated control among perimeter control and signal timings using MFD.

Apart from those approaches, few studies (Hajbabaie and Benekohal, 2011; Medina et al., 2013) analyzed the effects of metering in perimeter control with dynamic signal timings for the intersections inside the network. Mohebifard and Hajbabaie (2018a, 2018b) studied the effects of signal timing parameters due to various metering rates in perimeter control. Hajbabaie (2012) proposed genetic algorithm to jointly optimize perimeter metering and signal timing in a grid network. Mohebifard et al. (2019) developed to a cooperative signal and perimeter metering control using Distributed Optimization and Coordination algorithm (DOCA). The studies consider various penetration rates of connected vehicles and showed the effectiveness of the proposed methodology.

These studies provide methodologies to control inflow of vehicles inside the protected region. Such approaches are mostly applicable to grid networks. However, the methodologies may be applied to few entry points except freeways. It is important that these methods cause congestion outside the protected region. Therefore, such perimeter control approaches may not be suitable to corridor networks with freeways.

2.8 New HCM Chapter 38 on Network Analysis

This section discusses on Highway Capacity Manual provided methods on network analysis. A recently completed project (NCHRP 15-57) developed new materials for the HCM to modify the freeway analysis methods and the urban street methods so that the effects of operations from one facility to the other can be evaluated. The research developed a new chapter (Chapter 38) which was recently approved for publication in HCM version 7, which was released in 2021. The new methods can be used to evaluate operations along networks that include both freeways and urban streets. The methods can also evaluate the impact of spillback into freeways and into urban streets from downstream facilities.

The new procedures consider queue spillback into the freeway, which occurs due to insufficient capacity in at least one element of the off-ramp: either the ramp proper, or the downstream ramp terminal. The blockage of one or more freeway lanes adversely affects performance, and the extent of the blockage effects depend on various factors including the design of the facility, the cause of the blockage, and the length of the queue. The methodology developed is based on the calculation of demand and capacity at the downstream ramp terminal using the respective Interrupted Flow methods. It expands the Oversaturated Segment Evaluation for

freeway facilities (HCM Chapter 25) and accounts for spillback and its effects by lane along the freeway mainline.

The procedures also consider queue spillback into urban streets, which occurs due to insufficient discharge capacity into the freeway merge. It may occur due to oversaturated conditions at the merge segment or the presence of ramp metering. The methodology integrates the Interrupted Flow methodologies with the Freeway Facilities procedure to account for constraints of the on-ramp capacity. Several adjustments were developed to estimate the impacts of queue spillback from an on-ramp into upstream signalized and unsignalized intersections, including roundabouts.

2.9 Summary

The reviewed literature shows that studies on ramp metering (and ramp metering along with MTFC) only aim to improve freeway operations. These research studies do not consider the impact of ramp metering on upstream roads. Some studies provide methods to integrate ramp metering and signal timing but, these studies either limited in eliminating specific issues such queue spillbacks or partially coordinates signal control with metering controls. A demand-responsive holistic control system has yet been developed to optimize signal timings and ramp metering rates jointly. Another group of studies cover perimeter control strategies, but these studies are mostly suitable for grid networks. Also, such studies produce unnecessary congestion outside the study area. At the same time, in some studies, queuing from on-ramps has been studied but no attempt has been made to predict the queues on the ramp before they occur for use in proactive management. Although the recent edition of the HCM includes a new chapter that provides procedures to estimate the impacts of queue spillback from an on-ramp into upstream facilities, there is still limited research on the effects of queue back up from freeways to the urban streets.

Therefore, this study covers multiple lacking in previous research:

- This research proposes a new methodology that mitigates the impact of queue spill back from the on-ramp to the arterial intersection of the connected arterial road while improving the network performance.
- This study fulfils the need of a demand responsive real-time control system by developing an integrated control framework that combines all signal controllers and ramp metering controllers in a corridor. An optimization framework is developed that provides optimal timings of signal controllers and optimal metering rates of on-ramps to achieve an overall improvement of the corridor network.
- The study proposes a plan to reduce the impact of the ramp queues by predicting the queue spillback before it occurs. Such prediction can be an important component of proactive management strategies for mitigating the effects of queue spillbacks. A combined signal timing and ramp metering control method could be used to lessen the likelihood of queue spillback.

- The review of machine learning applications for arterial streets indicates that previous studies have successfully used machine learning to predict the congestion and performance on arterial streets in near real-time operation. However, none of these studies used machine learning to predict spillbacks from on-ramps utilizing data from multiple sources including those that can be considered as high resolution as was done in this study.

3 RUELS_BASED OPTIMIZATION OF ARTERIAL SIGNAL CONTROL AND RAMP METERING SIGNALS

3.1 Introduction

This chapter focuses on developing a signal control plan to mitigate the effects of queue spillback from the freeway on-ramp while improving the network performance. The proposed methodology determines the location where oversaturation occurs and then adjusts the signal control at the upstream intersections of the intersecting arterial and/or ramp metering rates in order to maintain a balance of queue lengths and to optimize the overall network performance.

The next subsection describes the proposed methodology, while the third subsection discusses three case studies used to apply the proposed methodology using simulation. The last subsection provides the overall conclusions and recommendations.

3.2 Methodology

Figure 2 below provides the overall methodology flowchart which was developed to adjust ramp metering rates and/or signal control for the intersecting arterial. Each of the steps in the flowchart are discussed in more detail in the following paragraphs.

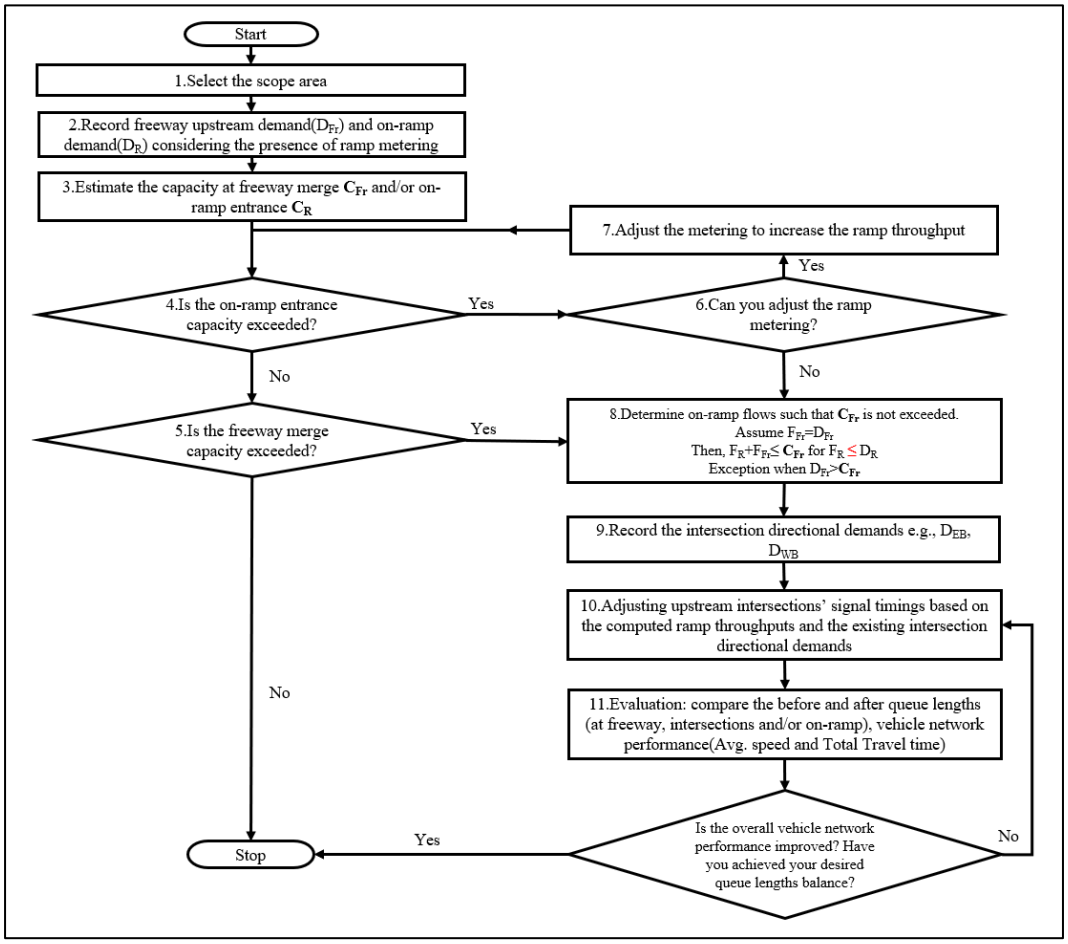

Figure 2: Strategy to Mitigate the Effects of Queue Spillback Due to On-Ramp Congestion

Notation and description

C_{Fr}: Freeway Capacity (veh/h)

F_{Fr}: Freeway flow(veh/h)

C_R: On-ramp Entrance Capacity(veh/h)

F_R: Ramp flow(veh/h)

D_{Fr}: Freeway Upstream Demand(veh/h)

D_R: On-ramp Demand(veh/h)

Step 1 - Select the Scope Area: The process begins by selecting the scope area considering both time and space limits. The scope area includes a merge/on-ramp and the intersecting arterial with as many signalized intersections as may be affected by the spillback. The analysis should also include all intersections that may contribute to the on-ramp demand. The time-period of analysis should include the onset and dissipation of congestion.

Step 2 - Record Freeway Upstream Demand (D_{Fr}), and On-ramp Demand (D_R) Considering the Presence of a Ramp Meter: This step involves recording the traffic demands from the mainline freeway and from the on-ramp. The step also considers whether a ramp meter is in place at the subject on-ramp and if yes, obtain the metering rate during the analysis period.

Step 3 - Estimate the Capacity of the Freeway Merge (C_{Fr}) and/or On-ramp Entrance (C_R): The capacity can be estimated either using field data or through simulation. When field data are used, it is recommended to use at least 30 breakdown events during the analysis period. When simulation is used, the capacity estimation involves collecting the speed and flow data over several (10-20) simulation runs and drawing a time series graph with time intervals in the horizontal axis, flow in the primary vertical axis and speed in the secondary vertical axis. The average breakdown flow value is then used as the estimated capacity (Elefteriadou, 2014).

Step 4 - Is the On-ramp Capacity Exceeded? and Step 5, Is the Freeway Merge Capacity Exceeded? This step identifies the location of the bottleneck based on checks of demand to capacity at two locations: the entrance to the on-ramp, and at the freeway merge. The bottleneck is the on-ramp entrance when demand exceeds the capacity at that location. In this case there would be minimal congestion on the freeway. This type of bottleneck is often due to the presence of a restrictive ramp meter. If the demand greatly exceeds the capacity at the freeway merge causing congestion and eventually queue spillback, then the bottleneck is at the freeway merge. Thus, if the bottleneck is at the on-ramp entrance, the process continues to step 6, and if it is at the freeway merge, it continues to step 8.

Step 6 - Can you Adjust the Ramp Metering? This step checks whether the ramp metering rate can be increased by determining whether the on-ramp demand plus the mainline freeway demand exceed the capacity of the freeway merge. If there is no oversaturation at the freeway merge, then the metering rate can be increased and thus the process continues to step 7. If there is oversaturation at the freeway merge, the process continues to step 8.

Step 7 - Adjust the Metering Rate to Increase the Ramp Throughput: During this step, the ramp metering rate is increased to approach the capacity of the merge. If after adjustment of the metering rates the capacity is not exceeded at either the freeway merge or the on-ramp entrance, then the process ends. In the case that the on-ramp metering rate cannot be adjusted, the process continues to step 8. In the case that adjusting the on-ramp metering rate cannot improve the overall network performance, the process continues to step 8.

Step 8, Determine the Ramp Flows such that the Freeway Merge Capacity is not Exceeded:

In either case of the bottlenecks, the desired on-ramp throughput (F_R) is computed such that the sum of the ramp and mainline freeway throughputs must be less than the capacity of the freeway merge as in the Equations 1 and 2 below.

$$F_R + F_{Fr} \leq \boldsymbol{C_{Fr}} \quad \forall F_R \leq D_R, \tag{1}$$

This is equivalent to:

$$F_R = (\boldsymbol{C_{Fr}} - F_{Fr}) \leq D_R \tag{2}$$

When using the above equations, if the freeway mainline throughput (F_{Fr}) exceeds the freeway merge capacity even when the on-ramp throughput is set to zero, the traffic can be regulated at the interchange further upstream. However, this is not within the scope of this project.

Figure 3 illustrates the calculation for obtaining the on-ramp throughput such that the freeway merge capacity is not exceeded.

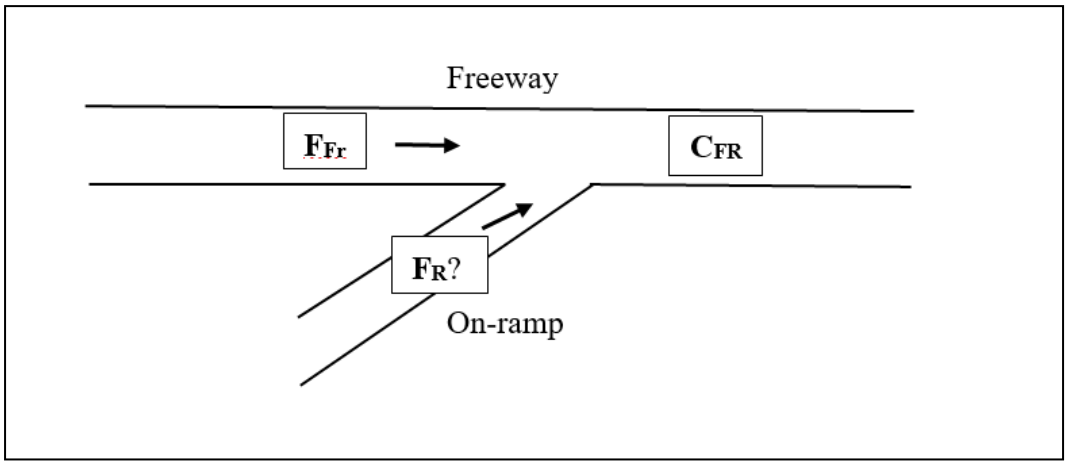

Figure 3: Illustration of the On-Ramp Flow Calculation

Step 9 - Record the Intersection Directional Demands: The directional demands consist of the different movements such as northbound, eastbound, southbound, and westbound right, through or left.

Step 10 - Adjusting Upstream Intersections' Signal Timings Based on the Computed Ramp Throughputs and the Existing Intersection Directional Demands: Once the F_R is calculated it

can be used to estimate how much green time can be allocated at the upstream intersection signal control phases that feed the on-ramp demand. If the freeway is not congested and can accommodate a higher on-ramp demand the signal timings for the feeder movements can be adjusted to maximize the throughput. If the freeway is congested and there is spillback from the on-ramp, the signal timings can be adjusted to limit the throughput while ensuring the other movements in the intersection do not experience greater delay. Readjusting the signal timings may involve a change in cycle length, a change in phases, or a change in green time durations. For example, the signal timings may be adjusted to reduce the green for the movements that feed the ramp and increase the green for the remaining movements. Such adjustments can be made for several intersections along an arterial, considering the origin-destinations of the demands, as well as queue spillback due to signal control adjustments. This step ensures that the vehicles released from the upstream intersection(s) to the on-ramp will result to a value equal to or less than the estimated capacity.

Step 11 - Evaluation: Compare the before and after Queue Lengths (at Freeway, Intersections and/or On-ramp), Vehicle Network Performance (Average Speed and Total Travel Time): After implementing the adjusted signal control plans, the network is evaluated by comparing the queue lengths on the freeway, and at the upstream intersections , and the overall network performance (average speed and total travel time per vehicle over the analysis period) for the base conditions and after adjusting the signals.

The process stops when improved performance (based on the analyst's criteria) has been achieved.

3.3 Case Studies

This section covers three case studies. The first and the second cases use the San Mateo Testbed network in San Mateo County near San Francisco Int. Airport in California. The overall network consists of 8.5 mile of the US 101 freeway and State Route 82 (El Camino Real) (see Figure 4 below). The site was modelled with VISSIM. We obtained the San Mateo data from the USDOT open-source site[1] which included the VISSIM files[2].

[1] https://rosap.ntl.bts.gov/view/dot/32698
[2] https://doi.org/10.21949/1500857

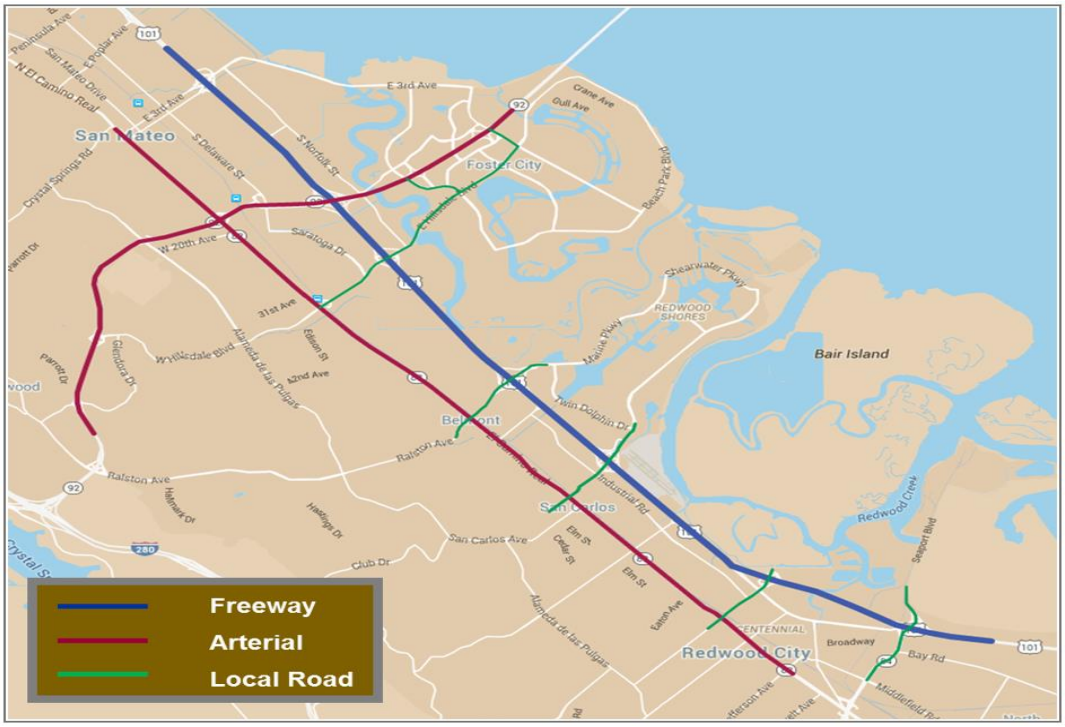

Figure 4: The San Mateo Testbed

The first case study focuses on one of the interchanges i.e., US 101 freeway @ Ralston Avenue but the evaluation of the performance measures looks at the entire network of the test bed. Also, VISSIM simulation indicates congested conditions in the northbound direction of the freeway at the interchange that causes spill back to the onramp and the connected upstream intersections.

The second case is the Truncated San Mateo Test Bed. The section with the US 101 freeway @ Ralston Avenue interchange was completely cut off from the rest of the network, and the end evaluation considered only the isolated interchange. Like case study one, this case considers the northbound direction of the US 101 freeway. However, based on the VISSIM simulation animation, the traffic congestion pattern in the truncated section of the test bed was different from the first case study. The freeway was free flowing whereas the presence of the ramp metering resulted in queue spillback on the on-ramp to the end of the Ralston Avenue.

Case study three's network is the Florida I-95 @ NW 119th St in Miami Dade County in Florida. Like case studies one and two, the network was modelled in VISSIM. Queues emanates from the onramp and spill back to the NW 119th St while there is minimal congestion on the freeway. The study considers the southbound direction of the I-95.

3.3.1 Case Study 1: San Mateo Test Bed in California

The study section is an interchange; US 101 freeway @ Ralston Avenue as part of the entire network (See Figure 5 below).

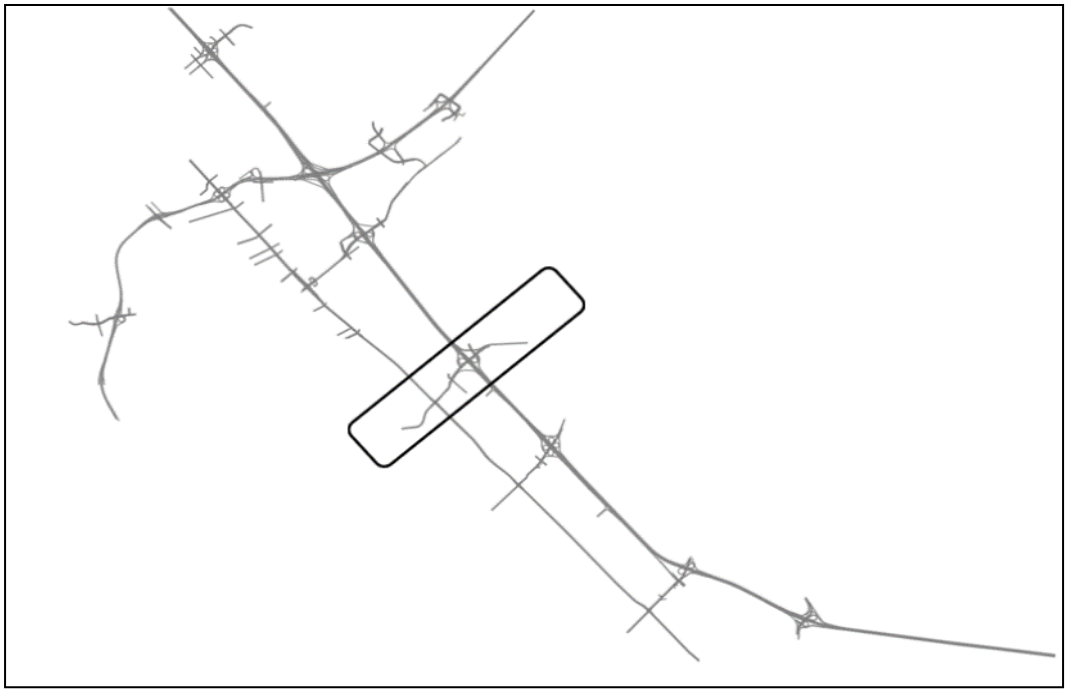

Figure 5: Case Study 1; The Study Section as Part of the San Mateo Testbed

This section comprises of two merge sections, one upstream intersection to the right and three to the left as shown in Figure 6, and the northbound direction was considered.

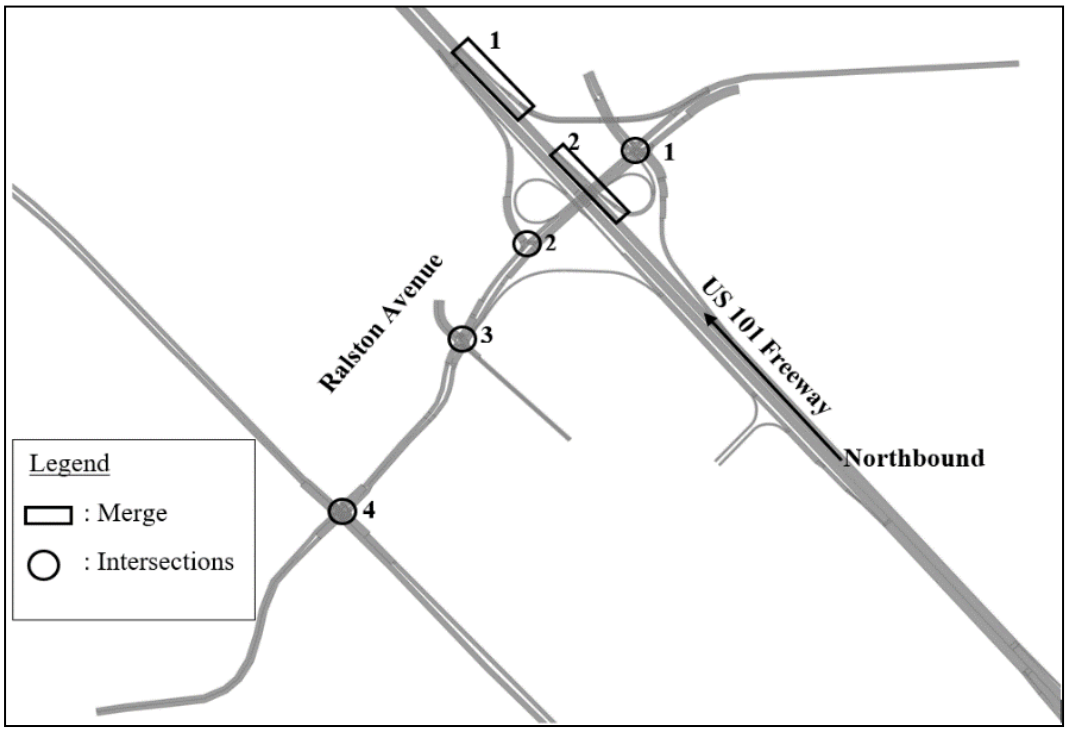

Figure 6: The Interchange; US 101 Freeway and Ralston Avenue

At this location there exists congestion on the freeway and queue spillback into the arterial as shown in Figure 7. We will be testing the developed method to mitigate the effects of the spillback by balancing queue lengths and optimizing the overall network performance through adjusting the signal controls at the affected intersections.

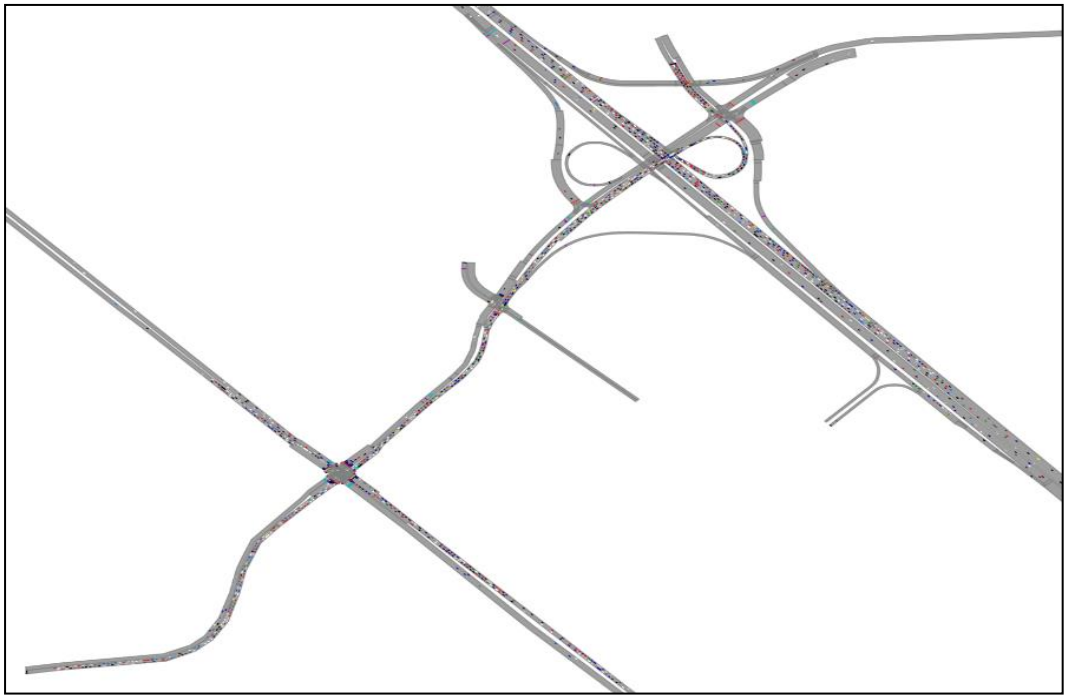

Figure 7: Congestion and Queue Spillback

The Figure 8 below shows the intersections' northbound, southbound, eastbound and westbound approaches as used in the signal groups for the signalized intersections as in Figure 9 to Figure 11.

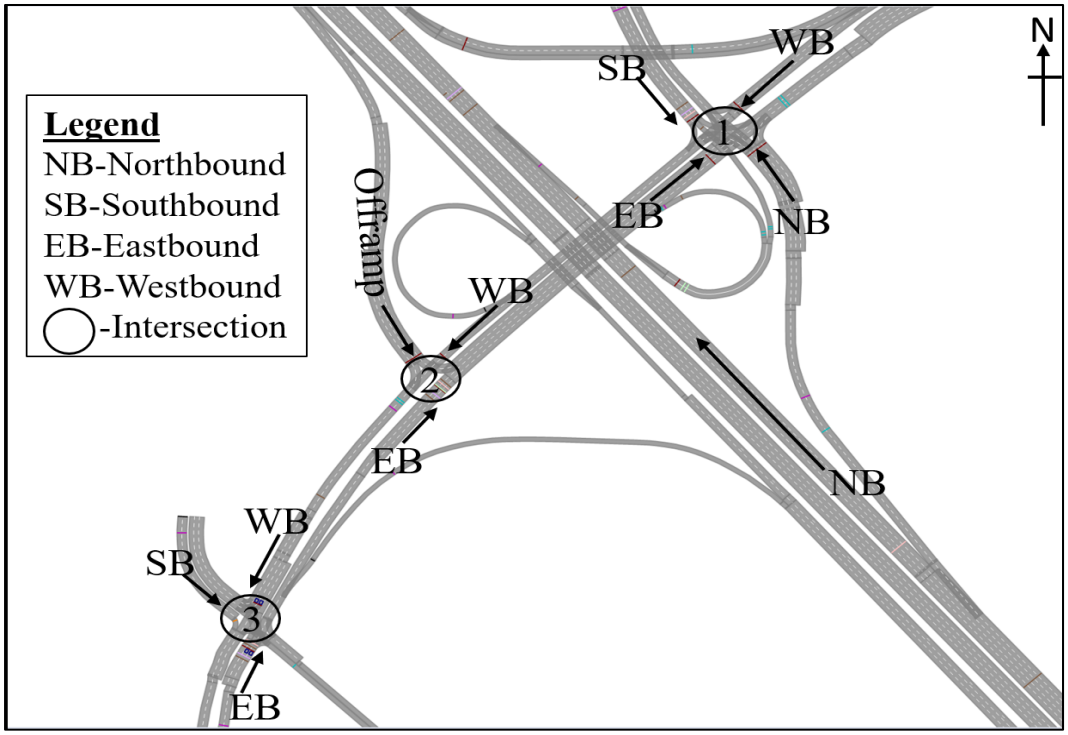

Figure 8: The Approaches at Intersections 1,2 and 3.

Figure 9 to Figure 11 show the existing signal timing splits at intersections 1,2 and 3, and the phasing sequence before any adjustments (base conditions). The splits have been provided for the different approaches of the intersections.

Signal Group	**2**	3	4	6	8
Signal Group Name	**SB**		WB	NB	EB
Splits (s)	**40**	15	25	40	40

Figure 9: Signal Phasing Sequence at Intersection 1

Signal Group	2	4	**8**
Signal Group Name	Offramp	WB	**EB**
Splits (s)	50	70	**70**

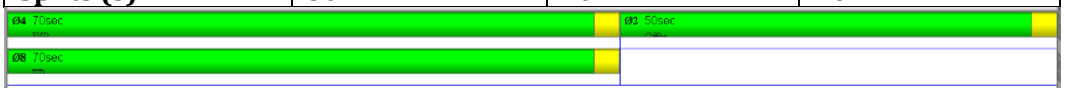

Figure 10: Signal Phasing Sequence at Intersection 2

Signal Group	1	2	4	**8**
Signal Group Name	Other		WB	**EB**
Splits (s)	40	40	40	**40**

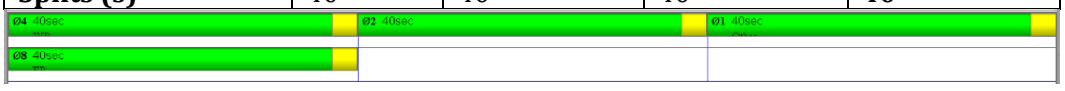

Figure 11: Signal Phasing Sequence at Intersection 3

Step 1: Select the Scope Area

The scope included a network consisting of an on-ramp and the intersecting Ralston Avenue with 4 intersections (see Figure 6) affected by queue spillback and a study period of 6 hours. However, the evaluation of the network performance will involve the entire San Mateo test bed as previously discussed.

Step 2: Record Freeway Upstream Demand (D_{Fr}), and On-ramp Demand (D_R) Considering the Presence of a Ramp Meter

The freeway upstream demand and the on-ramp demands were recorded and are provided in Table 1 . The study on-ramp has ramp metering during the analysis period. The values were obtained from the VISSIM network using the vehicle routing object over the 6-hour simulation period.

Table 1: Demands for the Mainline Freeway and the O*n-ramp.*

Time periods (minutes)	0-30	30-60	60-90	90-120	120-150	150-180	180-210	210-240	240-270	270-300	300-360
D_{Fr} (4 lanes) (veh/h)	3216	3216	5900	5900	6276	6595	6995	8002	7458	7458	5621
D_R (1 lane) (veh/h)	363	375	655	668	717	717	709	709	550	550	447
D_{Fr} (4 lanes) + D_R (veh/h)	3579	3591	6555	6568	6993	7312	7704	8711	8008	8008	6068

Step 3: Estimate the Capacity of the Freeway Merge (C_{Fr}) and/or On-ramp Entrance (C_R)

For this case study, the freeway merge was oversaturated causing spill back to the on-ramp and the upstream intersections of the connected arterial. Thus, the freeway merge capacity was estimated.

The freeway merge capacity was determined downstream of the freeway merge location 2 (see Figure 6). Using the data collection tool in VISSIM, we obtained the speed and flow data of the network over 20 simulation runs. The speed and flow data for each run were collected over a 6-hour simulation period in VISSIM. The breakdown flow was obtained for each run and the average value used as the freeway merge capacity. According to the Highway Capacity Manual (HCM) chapter 26, a breakdown occurrence is defined when the speed drops by 25% compared to the previous 15-min period. Therefore, the estimated capacity value was 1683 veh/h/ln.

Figure 12 shows a timeseries graph for one of the simulation runs. The primary axis represents the flowrate of the freeway mainlines immediately downstream of the merge, the secondary axis represents the speed, and the x-axis represents the time (15-minute periods) over which the data were collected.

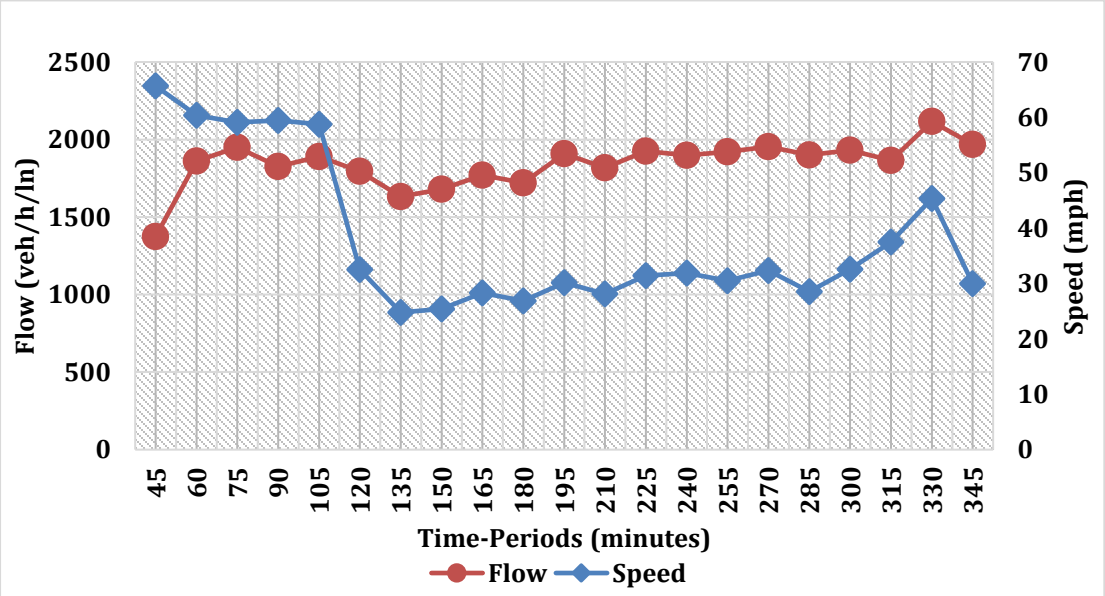

Figure 12: Time Series Graph of Flow Speed Data

As shown, breakdown occurred between 105 and 120 minutes. The desired freeway speed was modeled as 60-70 mph. For this simulation run, the speed drops from 58.77 mph to 32.51 mph. The breakdown flow is 1795 veh/h/ln.

After determining the freeway merge capacity, the process continues to step 5.

Step 5: Is the Freeway Merge Capacity Exceeded?

The estimated freeway merge capacity was 1683 veh/h/ln which translates to 6732 veh/h since the freeway section at the merge has 4 lanes. The freeway merge capacity was exceeded (as it can be seen in Table 1) between 120-300 minutes of the simulation. The oversaturated conditions can also be seen in the time series graph in Figure 12 which shows the breakdown and subsequent congestion for one of the 20 simulation runs. The high demand resulting in the freeway bottleneck originated largely from the upstream intersections along the Ralston Avenue Arterial.

From step 5, we established the freeway merge capacity was exceeded, thus the process continued to step 8 as shown in the flowchart.

Step 8: Determine the Ramp Flows such that the Freeway Merge Capacity is not Exceeded.

The ramp throughput (F_R) that can be accommodated given the demand from the freeway mainline and the capacities of the freeway and the on-ramp was calculated using equations 1 and 2.

When the upstream freeway mainline demand already exceeds the freeway merge capacity, the resulting ramp throughput is theoretically zero for that time-period. During the time intervals when the ramp throughputs are theoretically zero, the congestion will still exist since the freeway mainline throughput control is beyond the scope area for this study. Additionally, during these time intervals, since it is impractical to have splits of zero seconds for the phases contributing to the freeway flow, splits values will be assigned as per the signal timing manual specifications to ensure that a recommended minimum green time for an arterial with a certain range of average speed serves the movement (Urbanik et al., 2015).

The Equation 1 was applied across the entire study period as shown in *Table 2*. As shown, the equation yields F_R as zeros for the time-periods when the F_{Fr} exceeded the freeway merge capacity.

Table 2: On-ramp Throughput

Time periods (minutes)	0-30	30-60	60-90	90-120	120-150	150-180	180-210	210-240	240-270	270-300	300-360
Freeway merge capacity (veh/h)	6732	6732	6732	6732	6732	6732	6732	6732	6732	6732	6732
Upstream freeway throughput (veh/h)	3216	3216	5900	5900	6276	6595	6995	8002	7458	7458	5621
On-ramp throughput F_R (veh/h)	363	375	655	668	456	137	0	0	0	0	447

Further, at this site the single lane on-ramp is formed by two ramps that merge upstream. Each of these ramps is connected to a signalized intersection. Therefore, we need to compute the proportion of throughput from the two ramps.

Let the two ramps be labeled R_A and R_B where R_A is the ramp connected to the eastbound arterial and R_B is the ramp connected to the southbound arterial as shown in Figure 13.

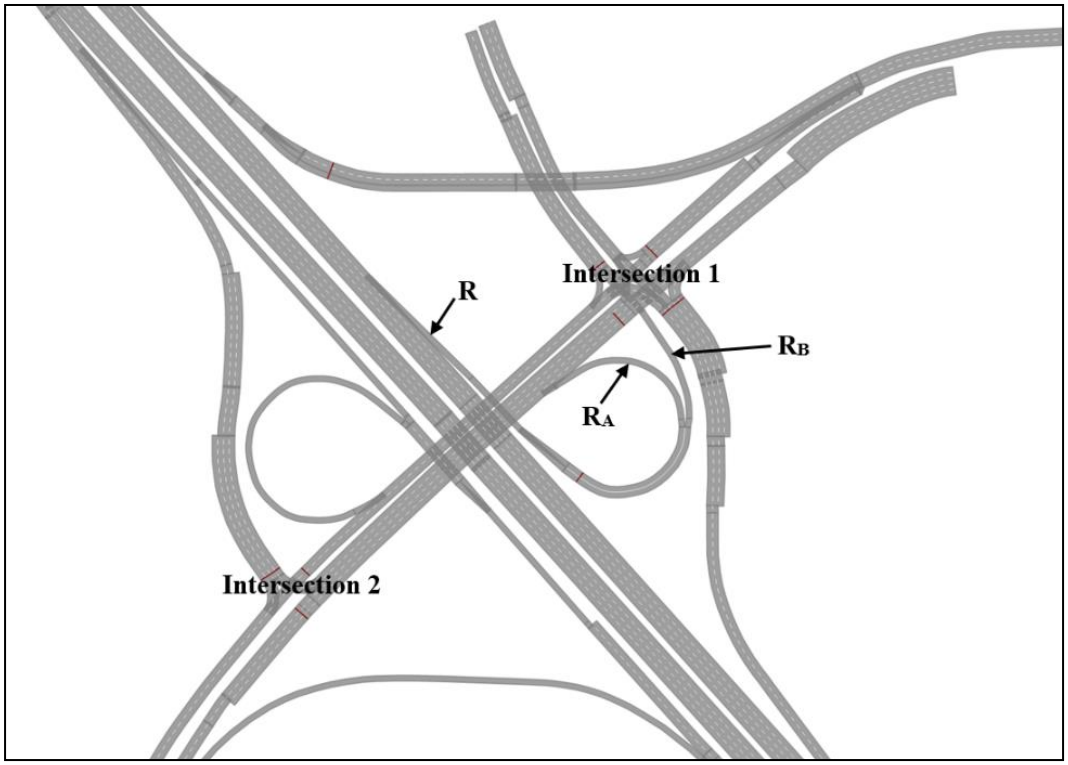

Figure 13: The On-ramp is Formed by the Merging of R_A and R_B

The throughputs of ramps R_A and R_B were computed based on the proportions of their existing demands. Table 3 show the demands for each ramp recorded from the VISSIM network file.

Table 3: Demands at Ramps R_A and R_B

Time periods (minutes)	0-30	30-60	60-90	90-120	120-150	150-180	180-210	210-240	240-270	270-300	300-360
D_{RA} (veh/h)	150	162	300	313	350	350	350	350	250	250	200
D_{RB} (veh/h)	213	213	355	355	367	367	359	359	300	300	247
$D_{RA} + D_{RB}$ (veh/h)	363	375	655	668	717	717	709	709	550	550	447

The sum of the demands from R_A and R_B should total up to the demand at the on-ramp R when the two ramps merge.

Thus.

$$D_{RA}+D_{RB}=D_R$$

Where:

D_{RA} is the existing demand on ramp R_A

D_{RB} is existing demand on ramp R_B

The ramp throughput proportions were calculated as follows:

Let the proportions related to R_A be denoted as X_{RA} and for R_B be X_{RB}, then.

$$X_{RA} = \frac{D_{RA}}{D_R} \times 100\%$$

$$X_{RB} = \frac{D_{RB}}{D_R} \times 100\%$$

Table 4 shows the proportions (%) used for computing the ramp throughputs at R_A and R_B

Table 4: Proportions Used to Compute the Throughputs at Ramps R_A and R_B

Time periods (Minutes)	0-30	30-60	60-90	90-120	120-150	150-180	180-210	210-240	240-270	270-300	300-360
X_{RA} (%)	41	43	46	47	49	49	49	49	45	45	45
X_{RB} (%)	59	57	54	53	51	51	51	51	55	55	55

The ramp throughputs were computed by multiplying the proportions (X_{RA} and X_{RB}) by the throughput at the main on-ramp (F_R) from Table 2.

Table 5 shows the computed throughput from each of the ramps.

Table 5: Throughput at Ramps R_A and R_B

Time periods (minutes)	0-30	30-60	60-90	90-120	120-150	150-180	180-210	210-240	240-270	270-300	300-360
F_{RA} (veh/h)	150	162	300	313	223	67	0	0	0	0	200
F_{RB} (veh/h)	213	213	355	355	233	70	0	0	0	0	247

Step 9: Recording the Intersections' Directional Demands

In this case study, three upstream intersections i.e., intersections 1,2 and 3, were considered (Figure 6). The recorded directional demands at each intersection are those that affect the signal timing phases.

For intersection 1, based on the vehicle routing network object within the VISSIM file only the southbound movement contributes to the on-ramp R_B flow. Table 6 shows the recorded directional demands at intersection 1.

Table 6: Directional Demands for Intersection 1

Time-periods	0-30	30-60	60-90	90-	120-	150-	180-	210-	240-	270-	300-

(minutes)				120	150	180	210	240	270	300	360
EB existing demands (veh/h)	307	307	511	511	484	484	528	528	577	577	488
WB existing demands (veh/h)											
NB existing demands (veh/h)	50	50	50	50	50	50	50	50	50	50	50
SB existing demands (veh/h)	213	213	355	355	367	367	359	359	300	300	247

For intersection 2, the vehicle routing network object within the VISSIM file shows that the eastbound movement is the only one that contributes to the on-ramp R_A flow. *Table 7* shows the recorded directional demands at intersection 2.

Table 7: Directional Demands at Intersection 2

Time-periods (minutes)	0-30	30-60	60-90	90-120	120-150	150-180	180-210	210-240	240-270	270-300	300-360
Off-ramp Demands (veh/h)	613	613	1022	1022	968	968	1056	1056	1154	1154	976
WB Demands (veh/h)	50	50	50	50	50	50	50	50	50	50	50
EB Demands (veh/h)	150	162	300	313	350	350	350	350	250	250	200

For intersection 3, the vehicle routing network object within the VISSIM file shows that the eastbound movement is the only one that contributes to the on-ramp R_A flow. *Table 8* shows the recorded directional demands at intersection 3.

Table 8: Directional Demands at Intersection 3

Time-periods (minutes)	0-30	30-60	60-90	90-120	120-150	150-180	180-210	210-240	240-270	270-300	300-360
WB Demands (veh/h)	331	331	536	536	509	509	553	553	602	602	513
EB Demands (veh/h)	151	261	300	354	368	400	444	365	342	270	280

Step 10: Adjusting Upstream Intersections' Signal Timings Based on the Computed Ramp Throughputs and the Existing Intersection Directional Demands

In this step the existing signal timings for the selected intersections were first recorded. Each upstream intersections had one signal time pattern over the entire simulation 6-hour simulation period and a cycle length of 120sec. The process of signal timing adjustment is demonstrated using intersection 1. Then, a summary of the new signal timings for each intersection is provided at the end of this step.

Intersection 1 connects to ramp R_B. The base condition of the network has southbound approach consisting of only southbound through movement. The southbound through movement directly leads to the on-ramp. Figure 14 provides the existing signal groups/phases,

assigned group name and the splits. The signal group in bold represents the phase that contributes flows to the on-ramp.

At intersection 1, the SB approach was modelled with only southbound through movement. The NB approach consisted of northbound left and right movements, and the EB approach had only eastbound through movement. The WB approach was not assigned any demand/routing in the existing VISSIM file.

Signal Group	**2**	3	4	6	8
Signal Group Name	**SB**		WB	NB	EB
Splits (s)	**40**	15	25	40	40

Figure 14: Signal Phasing Sequence at Intersection 1

From the time series graph in Figure 12, congested conditions with low speed begin at time 120min and lasts throughout the study period. This is a good start point to estimate the new signal timings to restrict the number of vehicles flowing to the freeway. However, for a new signal timing pattern to be effective, it needs to be implemented earlier, such that flow restrictions can be effective. Previous research has found that this time period needs to be at least 30 minutes before the congestion (Urbanik et al., 2015). Thus, for this case study, the signal timings will be estimated using demands for time-period 120-150 minutes, then implemented beginning from time-period 90-120 min.

Therefore, the computations for signal timing settings for the time-period between 120-150 minutes are as follows:

Estimate the split for the 2nd phase labelled SB, which is basically the southbound through movement that leads to the on-ramp as per the base network conditions: If 40s allows 367 veh/h (the existing SB demand at intersection 1, see *Table 6*), how many seconds will be required to allow only 233 veh/h (the ramp R_B throughput at 120-150 minutes, see *Table 5*)? The result is about 25s, and this is the value used as the new split for the SB signal group. The remaining 15s i.e., (40-25=15) are distributed to the 1st and 3rd phases based on the proportions of the existing critical per lane demands for the other movements (either the EB or WB whichever is greater (in this case the EB is greater)), and the NB.

Distribute the remaining time: At intersection 1, the 1st phase consists of the WB and EB approaches, but the EB approach has a greater demand (484veh/h). The 2nd phase consists of the SB approach, and the third phase consist of the NB approach with a demand of 50 veh/h (see *Table 6* and Figure 14).

The proportions for the time-period 120-150 min were calculated as:

1st phase: (EB approach demand) / (EB approach demand + NB approach demand) i.e., 484/ (484+50) =0.91

3rd phase: (NB approach demand) / (EB approach demand + NB approach demand) i.e., 50/ (484+50) =0.094.

This proportion was multiplied by the extra split time (which in our case is 15s) as follows:

1st phase: 0.91×15s=14s

3rd phase: 0.094×15s=1s

Thus, the new estimated green time splits for the time-period 120-150 min would be as follows (also see Figure 15).

Phase 1: 40+14=54s, and 25+14=39s

Phase 2: 25s

phase 3: 40+1= 41s

Signal Group	**2**	3	4	6	8
Signal Group Name	**SB**		WB	NB	EB
Splits (s)	**25**	15	39	41	54

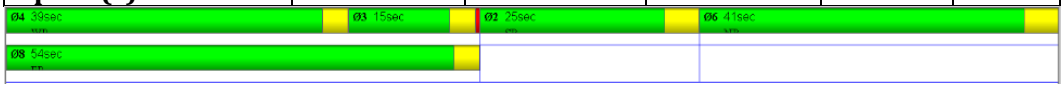

Figure 15: Adjusted Signal Timings at Intersection 1

The same procedure was applied to the remaining time-periods, and at the other upstream intersections. The implementation and results from the scenarios with signal timing adjustments at the selected intersections are discussed in the following subsection.

Step 11, Evaluation: Compare the before and after Queue Lengths (at Freeway, Intersections and/or On-ramp), Vehicle Network Performance (Average Speed and Total Travel Time)

This subsection discusses the scenarios implemented in simulation to test the proposed methodology, and provides the results obtained from the initial adjustments calculated above, as well as additional adjustments that were made to achieve a balance in improved freeway operations and arterial operations without compromising the performance of the entire network. The scenarios tested follow a series of trial-and-error steps to adjust the green time splits while considering queue lengths and the network performance. For each scenario, we provide the signal timing plans implemented at each upstream intersection, the respective queue lengths, the overall network performance, and the latent demand which refers to the number of vehicles that could not enter the VISSIM network due to congestion.

3.3.1.1 Scenario 1 Implementation, Results and Discussion

This scenario was based on the theoretical calculations described earlier, to obtain splits at different time periods. During some of the time-periods, the computed allowable ramp throughputs were zero, which suggested that no vehicles should be allowed into the freeway. However, since a split time of zero was not practical, slight modifications were made by increasing the split from 0s to 15s to accommodate the recommended minimum green of 7s-10s as per the signal timing manual (Urbanik et al., 2015). The first scenario comprised of three different signal timing plans over the 6-hour simulation period for each intersection as shown in Figure 16 to Figure 24 below.

Intersection 1

Plan 1 (0 mins-90 mins and 250 mins-360 mins)

Signal Group	**2**	3	4	6	8
Signal Group Name	**SB**		WB	NB	EB
Splits (s)	**40**	15	25	40	40

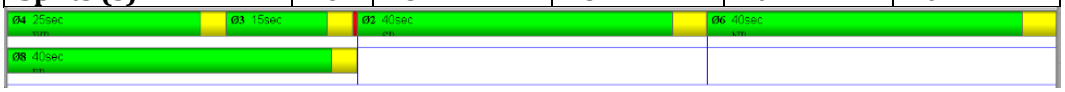

Figure 16: Scenario 1-Plan 1 Signal Phasing Sequence at Intersection 1

Plan 2 (90 mins-120 mins)

Signal Group	**2**	3	4	6	8
Signal Group Name	**SB**		WB	NB	EB
Splits (s)	**27**	15	37	41	52

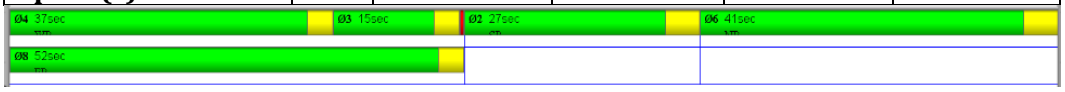

Figure 17: Scenario 1-Plan 2 Signal Phasing Sequence at Intersection 1

Plan 3 (120 mins-250 mins)

Signal Group	**2**	3	4	6	8
Signal Group Name	**SB**		WB	NB	EB
Splits (s)	**15**	15	48	42	63

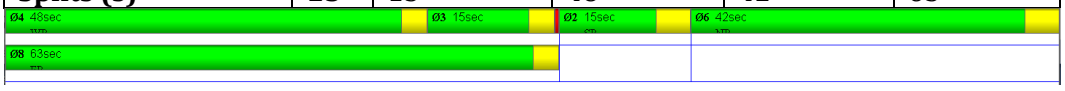

Figure 18: Scenario 1-Plan 3 Signal Phasing Sequence at Intersection 1

Intersection 2

Plan 1(Starts at 0mins-90mins and 250 mins-360 mins)

Signal Group	2	4	**8**
Signal Group Name	Offramp	WB	**EB**
Splits (s)	50	70	**70**

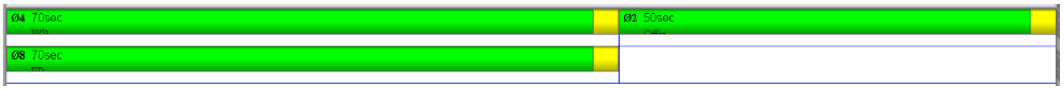

Figure 19: Scenario 1-Plan 1 Signal Phasing Sequence at Intersection 2

Plan 2(Starts at 90mins-120mins)

Signal Group	2	4	**8**
Signal Group Name	Offramp	WB	**EB**
Splits (s)	73	47	**47**

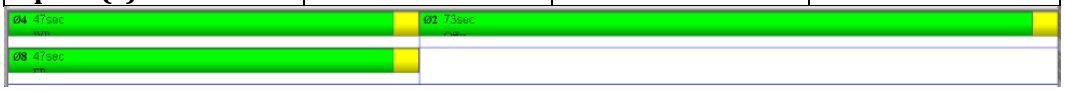

Figure 20: Scenario 1-Plan 2 Signal Phasing Sequence at Intersection 2

Plan 3 (Starts at 120-250 min)

Signal Group	2	4	**8**
Signal Group Name	Offramp	WB	**EB**
Splits (s)	105	15	**15**

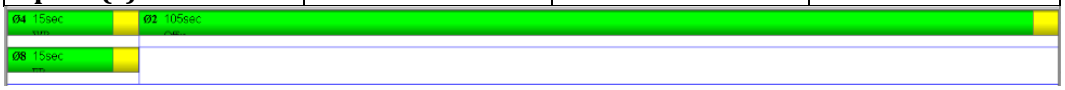

Figure 21: Scenario 1-Plan 3 Signal Phasing Sequence at Intersection 2

Intersection 3

Plan 1(Starts at 0mins-90mins and 250 mins-360 mins)

Signal Group	1	2	4	**8**
Signal Group Name	Other		WB	**EB**
Splits (s)	40	40	40	**40**

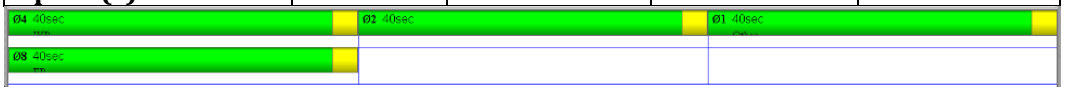

Figure 22: Scenario 1-Plan 1 Signal Phasing Sequence at Intersection 3

Plan 2 (Starts at 90mins-120mins)

Signal Group	1	2	4	**8**
Signal Group Name	Other		WB	**EB**
Splits (s)	46	46	28	**28**

Figure 23: Scenario 1-Plan 2 Signal Phasing Sequence at Intersection 3

Plan 3 (Starts at 120-250 min)

Signal Group	1	2	4	**8**

Signal Group Name	Other		WB	EB
Splits (s)	53	52	15	15

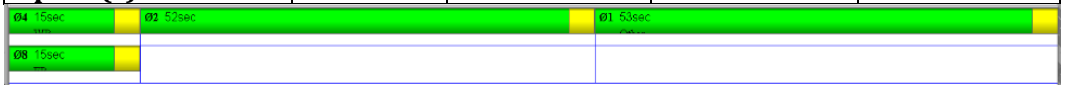

Figure 24: Scenario 1-Plan 3 Signal Phasing Sequence at Intersection 3

The first signal plans as in Figure 16, Figure 19, and Figure 22 were implemented between time 0min-90 minutes for the three intersections and the splits were the same as the original timings as previously shown in Figure 9 to Figure 11. 0min-90min was the time-period before the flow breakdown and thus maintaining the existing signal plan was assumed to be a good starting point (see Figure 12 for breakdown flow).

The second and the third plans were designed to be more restrictive to the phases with movements leading to the freeway i.e., the SB phase for intersection 1, and the EB phases for the intersections 2 and 3 as shown in bold in Figure 16 to Figure 24. Signal timings were calculated for the congested periods as discussed in the example in step 10, and it begins from time 90min-120 min for plan 2 (see Figure 17, Figure 20 and Figure 23 below) and 120-250min for plan 3 (see Figure 18, Figure 21 and Figure 24). Plan 3 was the most restrictive as it was implemented about the same time-periods; 180min-270min where the computed ramp throughput was zero as previously shown in *Table 5* (step 8: calculating the ramp throughput).

Note how, for example at intersection 1, the southbound phase has a split of 40s in plan 1(0min-90min), the gradually decreases to 27s in plan 2(90min-120min) to 15s in plan 3(120min-250min) and back to 40s; plan 1 from time 250min-360min (see Figure 16 to Figure 18). The SB phase split was reduced, and the remaining time was distributed to the other phases. This is the same trend for this scenario at intersection 2 and 3. The minimum green was set to 10s and the maximum green were set as the difference between the split time and the yellow and red time. Additionally, since the three intersections were actuated, the restricted phases and were set to minimum recall and the others to maximum recall. This ensured that the restricted phases only served the assigned the minimum green time and the other phases maxed out to ensure that the flow not leading to the freeway achieves the maximum possible flow for the available split.

These plans are expected to reduce the queue lengths at the freeway while balancing queues at the upstream intersections to achieve an improved network performance.

The queue length data were obtained using the queue counter tool in the VISSIM network Figure 25 shows the position of the queue counters at the freeways and the upstream intersections at the arterial. The queue counters at the intersections were placed behind the signal heads of the movement that lead to the freeway. At the freeway, the queue counter was placed at the bottleneck location. Queue lengths are measured from the downstream position of the queue counter to the furthest upstream vehicle that has entered queueing conditions.

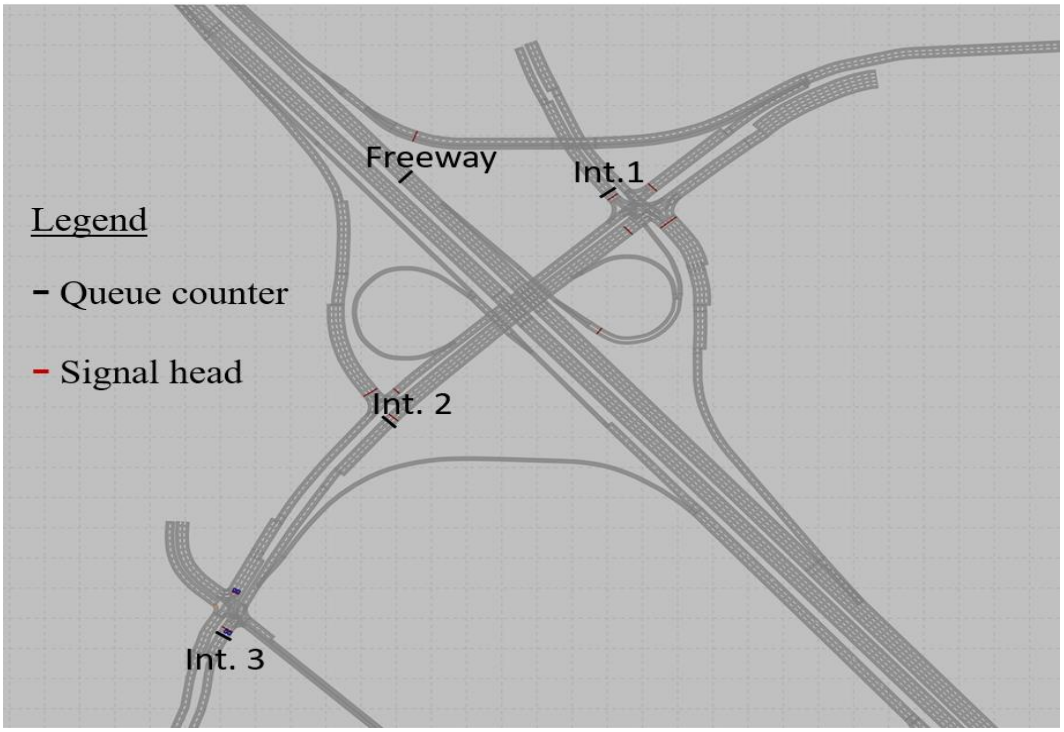

Figure 25: Position of the Queue Counters in VISSIM

The graphs in Figure 26 to Figure 29 show the comparisons of queue lengths at the freeway and the signalized intersections before and after implementing the scenario 1 signal timing plans.

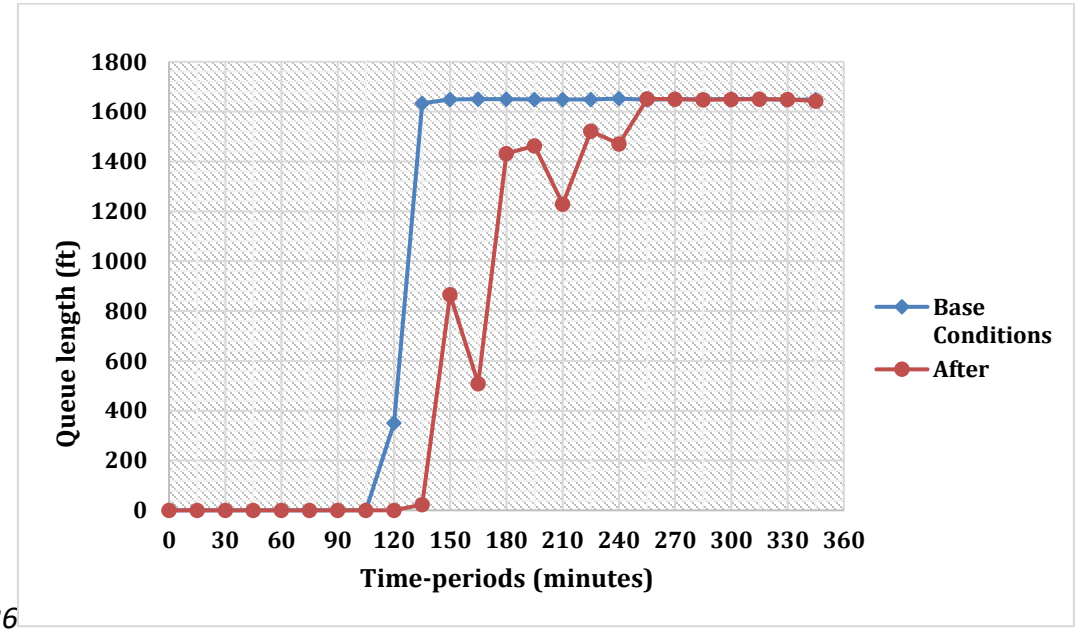

Figure 26

Figure 26: Case Study 1 Scenario 1 Comparison of the Freeway Queue Length

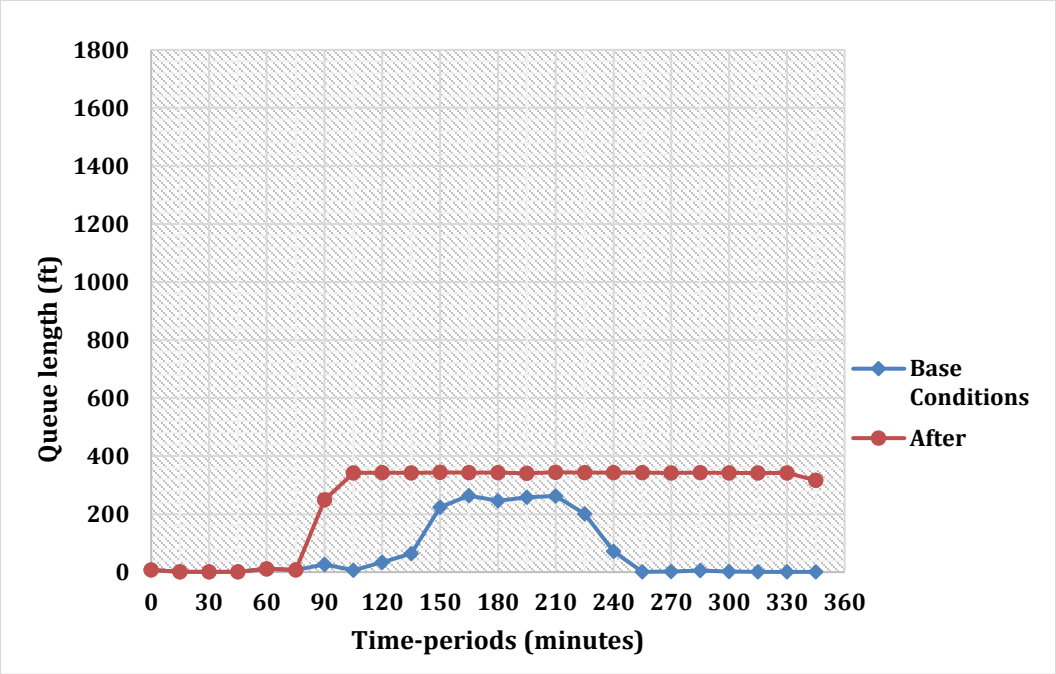

Figure 27: Case Study 1 Scenario 1 Comparison of the Queue Lengths at Intersection 1 (SB)

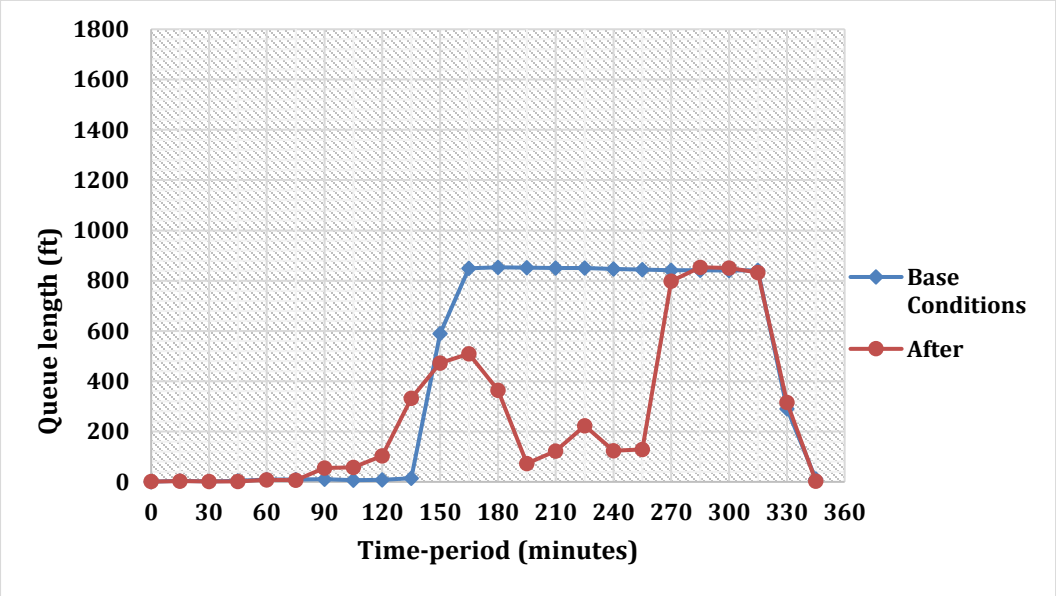

Figure 28: Case Study 1 Scenario 1 Comparison of the Queue Lengths at Intersection 2(EB)

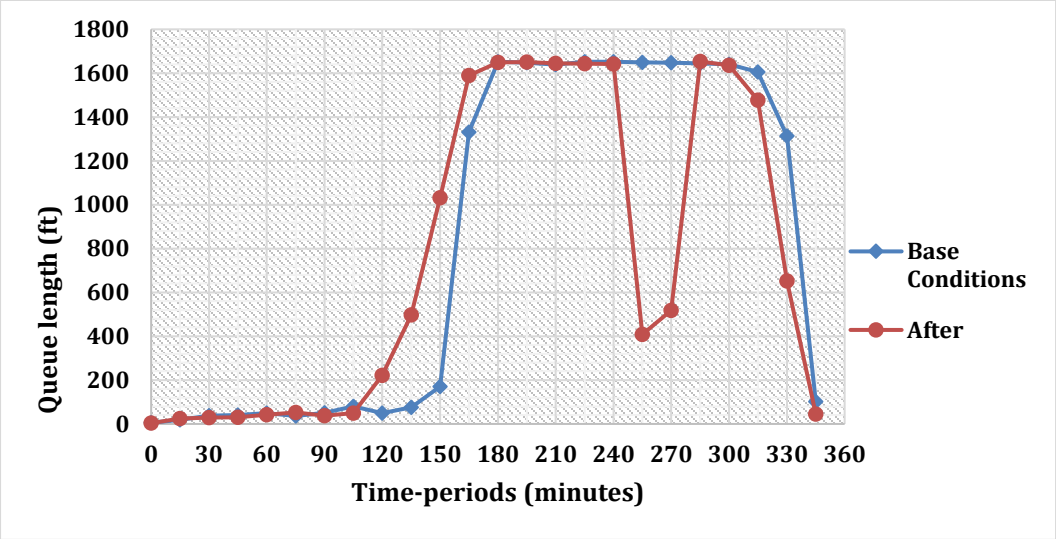

Figure 29: Case Study 1 Scenario 1 Comparison of the Queue Lengths at Intersection 3 (EB)

In Figure 26 to Figure 29 we first observe a trend where the queue caps after a certain length. This could be the end of the queuing conditions that the vehicles entered; the end of the link in which the queue counter could capture the queues.

In Figure 26, after signal plan adjustments, we see that the queue build-up at the freeway begins about 30 minutes later than the original plan. From time-period 255min-360 minutes, the queue length is like that of the before condition which is probably because the queue reached the end of the link in which it could be captured. This is also the period towards the end of the simulation when plan 1 was implemented to ensure most vehicles are served before the end of the study period. Compared to all the other plans, plan 1 allows more vehicles through the upstream intersections into the freeway.

The queues formation at the upstream intersections was as expected. At intersection 1, the queue length was longer than the before conditions. This was because of the restrictive signal timing plans. However, looking at the coordinated intersections 2 and 3, while the queue begins early at intersection 3 and remain long, the intersection 2 seem to experience less queue for longer time(see Figure 28 and Figure 29). At intersection 2, the queue length builds up when the restrictive signal timing plans 2 and 3 were implemented between time 90min- 250min. When plan 1 which was less restrictive was implemented from time 250min, the queue began to increase due to the vehicles proceeding from intersection 3 during that period. In Figure 29, the dip at time-period 240min-270min could be because of changing from one plan to another. To balance the queues in these two intersections, scenario 2 was implemented.

The Figure 30 and Figure 31 show the network performances in terms of average speed and total travel time per vehicle, respectively.

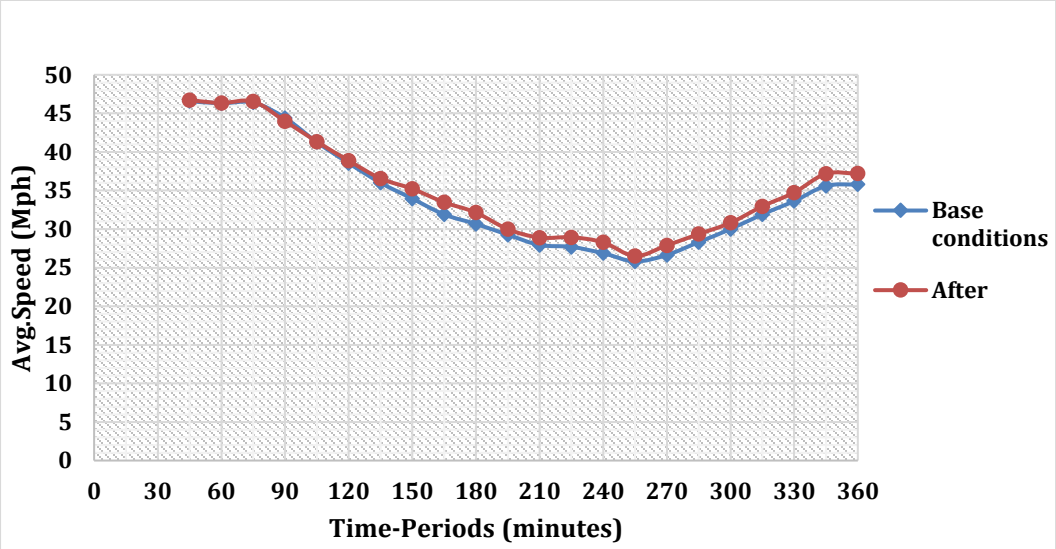

Figure 30: Case Study 1 Scenario 1 Comparison of the Network Average Speed

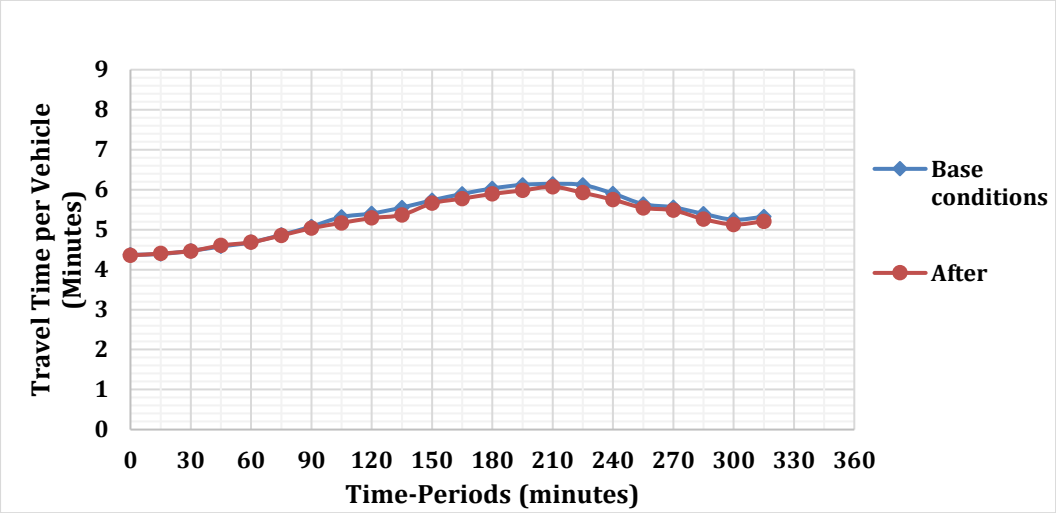

Figure 31: Case Study 1 Scenario 1 Comparison of the Network Travel Time per Vehicle

The signal plan implementation in this scenario led to a slight improvement; an average of 2.7% in the overall network performance in terms of average speed and the total travel time per vehicle (see Figure 30 and Figure 31).

3.3.1.2 Scenario 2 Implementation, Results and Discussion

Following scenario 1, scenario 2 strives to balance the queues at intersections 2 and 3 between time-period 150min-255min as in the previous Figure 28 and Figure 29. The plan 3 from scenario 1 was very restrictive for the EB phase in both intersections 2 and 3, and this was eliminated in scenario 2, leaving only two plans over the 6-hour simulation study period. By eliminating the most restrictive plan at intersection 3, more vehicles were expected proceed to intersection 2 which could result in reduced queue at intersection 3 and longer at intersection 2. Plan 1 was implemented at the beginning and towards the end of the simulation, i.e.,

between 0min-90min, and 250min-360min, and plan 2 was implemented at time-period 90min-250min.

Table 9 below shows the summary of the signal timings used for scenario 2 for the different plans at the three intersections.

Table 9: The Signal Plans for Scenario 2

Intersection 1									
			SB		WB		NB		EB
Plans	Time Period (min)	1	**2**	3	4	5	6	7	8
1	0-90		40	15	25		40		40
2	90-120		27	15	37		41		52
3	120-250		15	15	48		42		63
1	250-360		40	15	25		40		40
Intersection 2									
			Offramp		WB		NB		**EB**
Plans	Start (min)	1	2	3	4	5	6	7	**8**
1	0-90		50		70				70
2	90-250		73		47				47
1	250-360		50		70				70
Intersection 3									
		OTHER			WB		NB		**EB**
Plans	Start (min)	1	2	3	4	5	6	7	**8**
1	0-90	40	40		40				40
2	90-250	46	46		28				28
1	250-360	40	40		40				40

Like scenario 1, the phases consisting of movements leading to the freeway were set to minimum recall and the rest to maximum recall. The minimum green was set to 10s and the maximum green for the phases not contributing to the freeway flow were set as the difference between the split time and the yellow plus red time.

The graphs in Figure 32 to Figure 35 show the comparisons of queue lengths at the freeway and the signalized intersections before and after implementing the scenario 2 signal timing plans.

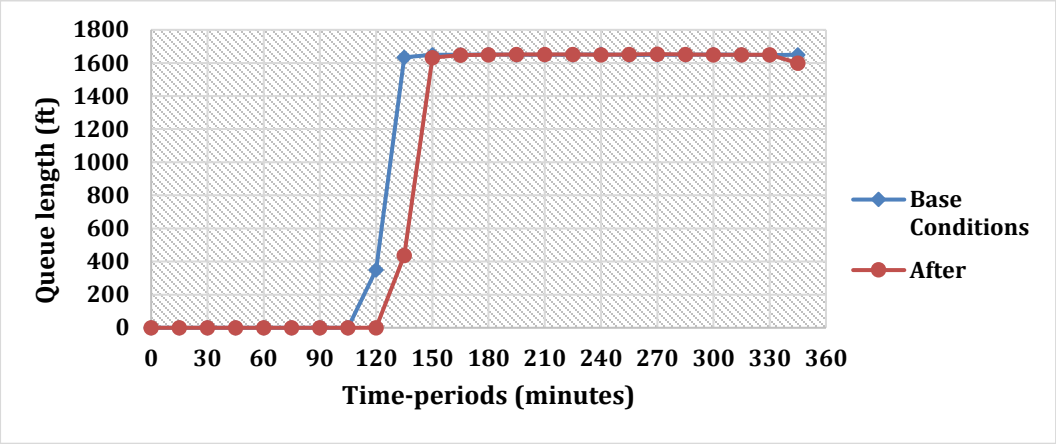

Figure 32: Case Study 1 Scenario 2 Comparison of the Freeway Queue Length

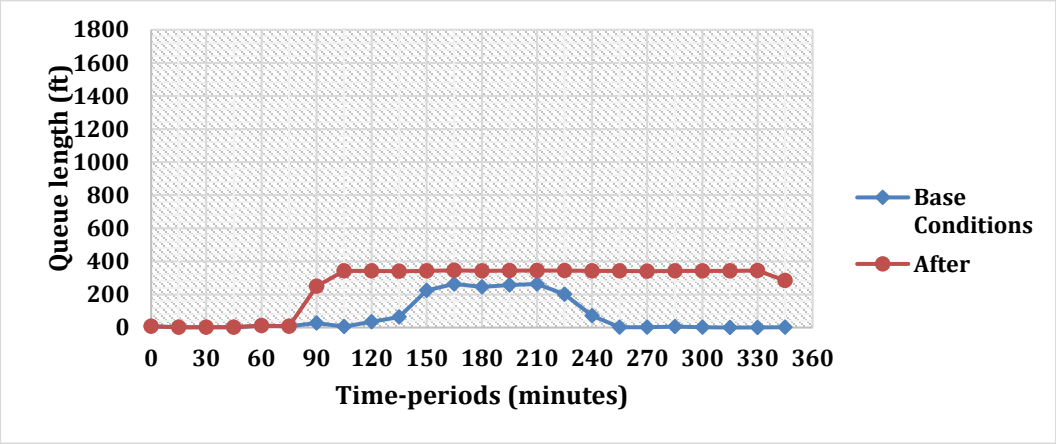

Figure 33: Case Study 1 Scenario 2 Comparison of the Queue Lengths at Intersection 1 (SB)

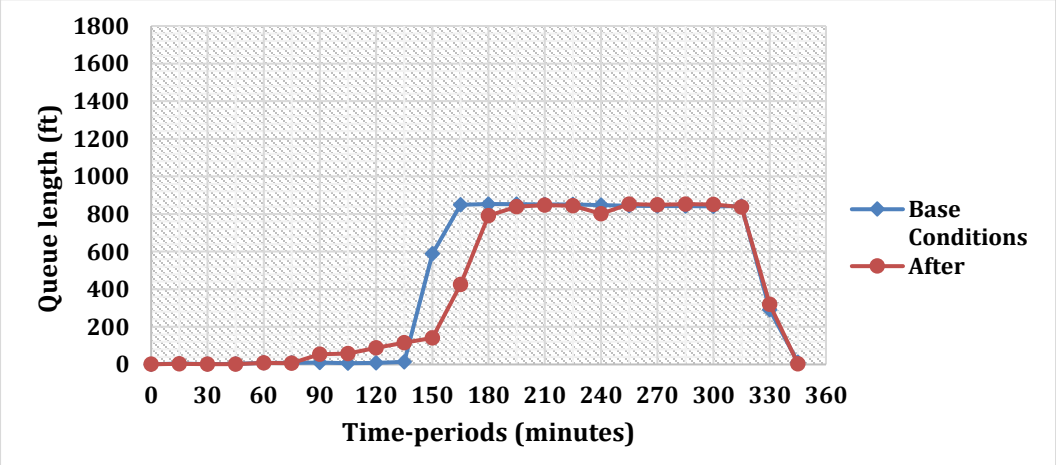

Figure 34: Case Study 1 Scenario 2 Comparison of the Queue Lengths at Intersection 2 (EB)

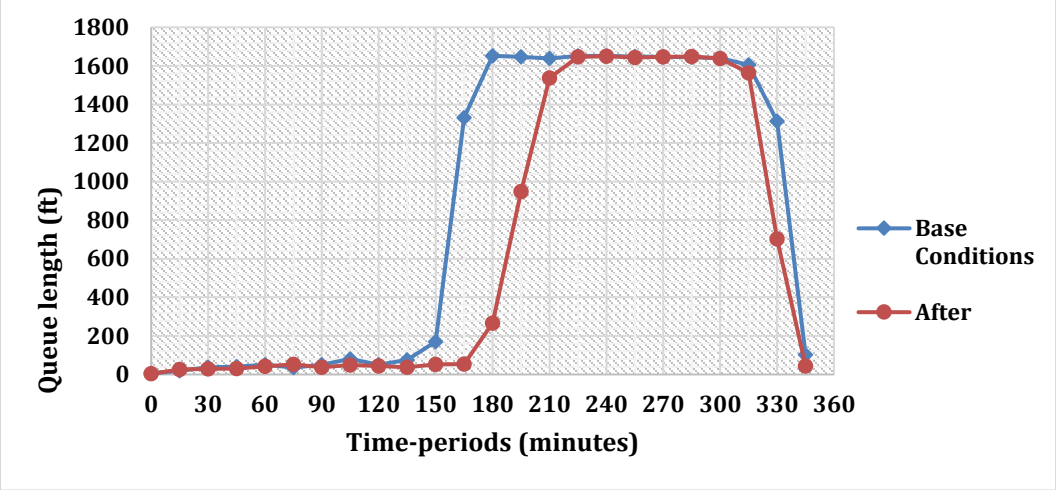

Figure 35: Case Study 1 Scenario 2 Comparison of the Queue Lengths at Intersection 3 (EB)

Like scenario 1, the queue lengths in Figure 32 to Figure 35 caped at the end of the link in which the counter could record the queues.

The queue length at intersection 1 remained similar to that of scenario 1. We observe that freeway congestion begins 15 minutes later than the before conditions (Figure 32). As in Figure 34 and Figure 35, similar to the freeway, the queues at intersections 2 and 3 begin some minutes later than the base conditions. Note that the starvation experienced at intersection 2 has been slightly balanced with that of intersection 3.

Figure 36 and Figure 37 show the overall network performance after implementing the signal timings in scenario 2.

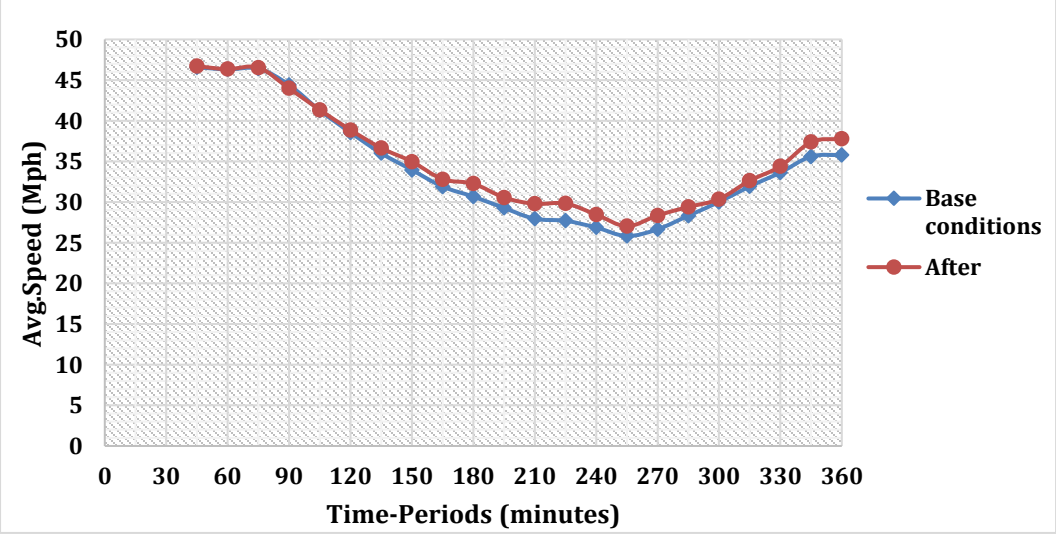

Figure 36: Case Study 1 Scenario 2 Comparison of the Network Average Speed

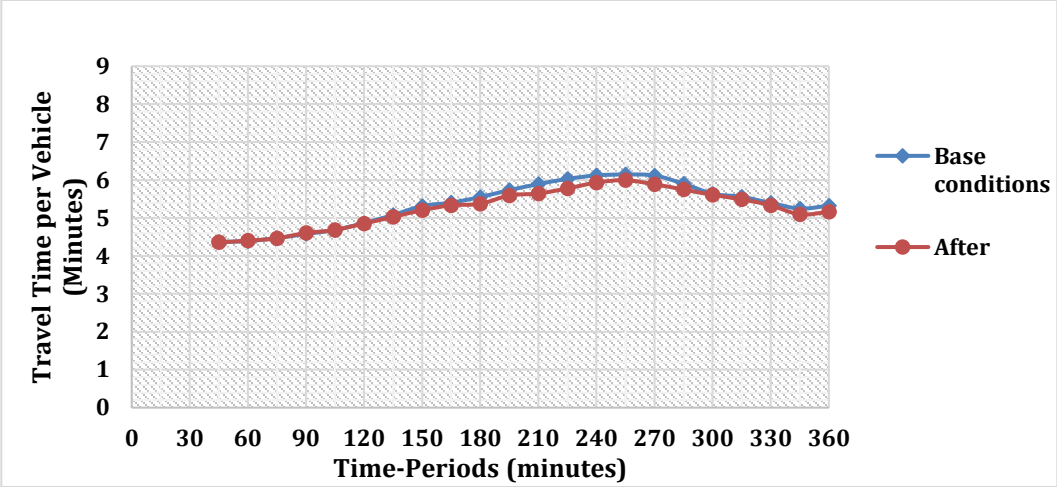

Figure 37: Case Study 1 Scenario 2 Comparison of the Network Travel Time per Vehicle

The overall network performance was improved by an average of about 3.1%.

Latent demand is an important attribute in this methodology as the method involves restricting the number of vehicles accessing the freeway at certain times during the simulation and this might result to some vehicles not being served. *Table 10* provides the comparisons of the network's latent demands over the entire simulation period for the base conditions and two scenarios discussed above.

Table 10: Comparisons of the Latent Demands for the Three Scenarios in Case Study 1

		After adjusting signals at upstream intersections	
Time- interval (minutes)	**Base conditions (Vehicles)**	**Scenario 1 (Vehicles)**	**Scenario 2 (Vehicles)**
30-45	0	0	0
45-60	0	0	0
60-75	0	0	0
75-90	0	0	0
90-105	20	20	20
105-120	114	133	133
120-135	252	297	297
135-150	403	478	473
150-165	570	705	678
165-180	774	954	918
180-195	941	1154	1116
195-210	1228	1468	1363
210-225	1357	1644	1510
225-240	1465	1712	1577
240-255	1573	1838	1638
255-270	1703	1761	1625
270-285	1778	1660	1600
285-300	1742	1596	1588

300-315	1631	1463	1466
315-330	1491	1382	1362
330-345	895	823	801
345-360	455	423	393

In both scenarios 1 and 2, between periods 105-255 min, after adjusting the signals at the upstream intersections, we see that more vehicles were not served at the end of the simulation compared to the base conditions. This was mainly because the process involved restricting the numbers of vehicles getting to the freeway to decrease the freeway merge congestion and thus the signal plans were more restrictive. However, between times 270-360 minutes the scenario 2 showed a great improvement in latent demand overall. Generally, before any adjustments in the signal timing at the upstream intersections, the latent demand data shows that 455 vehicles were not served at the end of the simulation while this number decreased to 423 vehicles in scenario 1 and 393 vehicles in scenario 2.

In this case study 1, the bottleneck was identified as the downstream of the freeway merge resulting in queue spillback to the onramp and eventually affecting the upstream intersections. Signal timings at these upstream were adjusted to regulate/restrict the flow leading to the on-ramp to minimize the congestion while balancing the queue lengths at the affected intersections and ensuring the overall network performance was not impacted negatively. Time was reduced for the approaches that contribute to the on-ramp flows and the remainder added to the other phases. The phases with movements that do not contribute to the onramp received additional split time and were not negatively impacted in terms of additional delays and extended queues. Eventually desired balance in queue lengths, improved overall network performance and latent demand was achieved.

3.3.2 Case Study 2: The Truncated San-Mateo Testbed

The truncated San-Mateo Testbed is obtained from the San Mateo Testbed in case study 1. This site particularly refers to the interchange; US 101 freeway @ Ralston Avenue completely isolated from the rest of the San Mateo Network. This network also represents the scope area which consists of freeway merge and affected upstream intersections (see Figure 38).

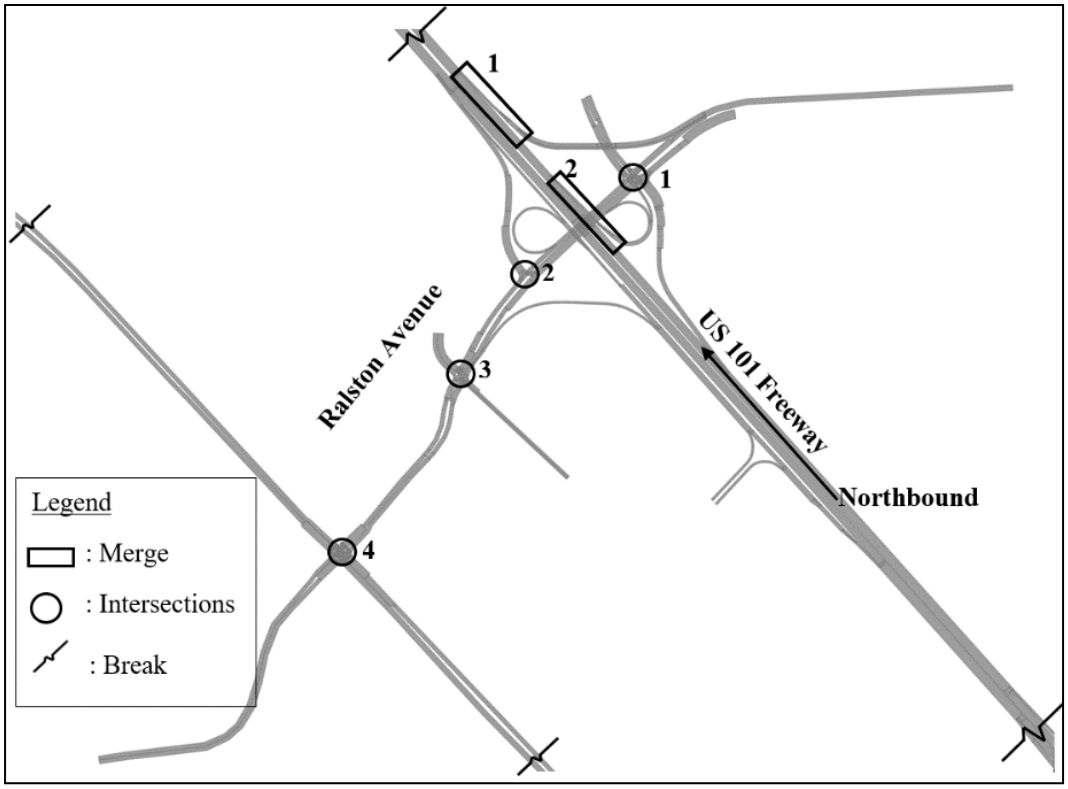

Figure 38: The Truncated San-Mateo Testbed

The truncated San Mateo area experiences congestion at the on-ramp due to the presence of ramp metering that results in queue spillback affecting the upstream intersections. However, the freeway mainlines and downstream of the freeway merge experiences no congestion. In this case study will be testing whether regulating the ramp throughput would mitigate the effect of spill back and improve the overall network performance.

The existing signal timing plans at the 3 intersections of the affected intersections are like those presented in case study 1.

Step 1: Select the Scope Area

Like case study one, the scope area consisted of an onramp and an intersecting arterial with four upstream intersections affected by queue spillback due to congestion. The simulation study period was 6hours. However, the evaluation of the performance only considers the truncated/isolated network as previously discussed.

Step 2: Record Freeway Upstream Demand (D_{Fr}), and On-ramp Demand (D_R) Considering the Presence of a Ramp Meter

The inputs were like those of the case study 1 since the same VISSIM network file was used (see *Table 1* and *Table 3*).

Step 3: Estimate the Capacity of the Freeway Merge (C_{Fr}) and/or On-ramp Entrance (C_R).

The on-ramp entrance capacities were estimated as 315 veh/h for R_A which connects to intersection 2,3 and 4, and 273veh/h for R_B which connects to intersection 1. Figure 39 and Figure 40 below shows the times series graphs of flow and speed for ramps R_A and R_B for one of the simulation runs. The breakdown flow value in Figure 39 is approximately 245veh/h at time 75min and in Figure 40, it is 270 veh/h. After the breakdown, we observe that the vehicles operate at lower speeds in congested conditions for about 2 hours at each ramp.

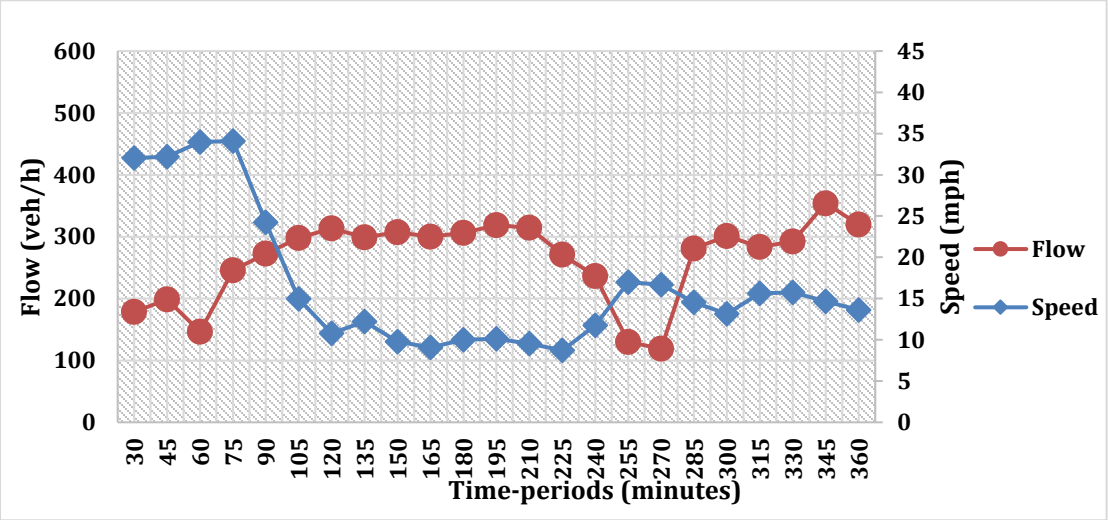

Figure 39: Case Study 2 Time Series Graph of Speed and Flow Data for Ramp R_A

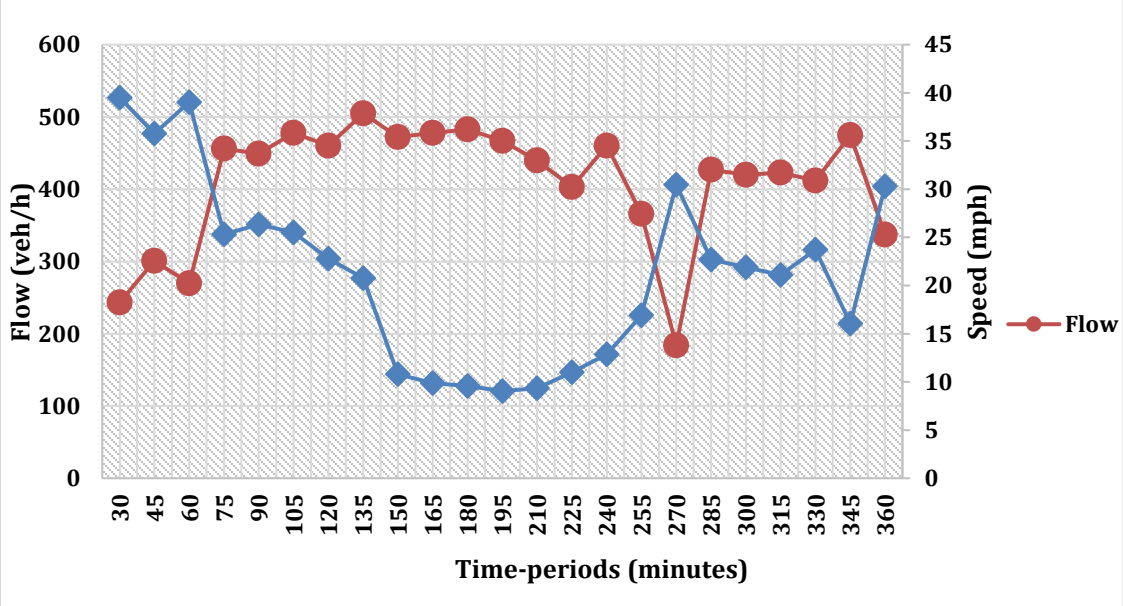

Figure 40: Case Study 2 Time Series Graph of Speed and Flow Data for Ramp R_B

Step 4: Is the On-ramp Entrance Capacity Exceeded?

The allotted volumes at ramps R_A and R_B for the various time intervals indicate that the estimated ramp capacity is already exceeded between times 120-310 min for ramp R_A and

between time 60-270min for ramp R_B (see *Table 3*). The simulation animation also indicates an on-ramp entrance bottleneck with minimal congestion in the freeway. Thus, the following steps will aim to maximize the ramp throughput and manage the upstream intersections queues.

After establishing that the on-ramp entrance capacity was exceeded, the process continues to step 6.

Step 6: Can you Adjust the Ramp Metering?

For this case study, since there was minimal congestion on the freeway while the was queue backed up on the on-ramp and the upstream arterial intersections, there was need to maximize the ramp throughputs.

Step 7: Adjust the Metering to Increase the Ramp Throughput.

In adjusting the ramp metering to increase the ramp throughput, the best plan for this case was when the ramp signal controllers were set to free running mode. This formed the basis of our scenario 1. Evaluation was conducted to gauge the network's performance after setting the signal controllers to free running which will be discussed as **scenario 1** in the results and discussion subsection of step 11.

However, to explore further possibility of improving the network operations, we resorted to **scenario 2** where we eliminated the ramp metering and regulated the traffic throughput at the upstream signalized intersections. Thus, the following steps describe the continuation for scenario 2.

Step 8: Determine the Ramp Flows such that the Freeway Merge Capacity is not Exceeded.

The ramp throughputs were computed as per equation 3 across the entire study period and the results are as shown in the *Table 11* below.

Table 11: Case Study 2 Throughputs from Ramps R_A and R_B

Time periods (minutes)	0-30	30-60	60-90	90-120	120-150	150-180	180-210	210-240	240-270	270-300	300-360
F_{RA} (veh/h)	150	162	300	313	315	315	315	315	250	250	200
F_{RB} (veh/h)	213	213	273	273	273	273	273	273	273	273	247

Step 9: Recording the Intersections' Directional Demands

The upstream intersections demand considered were similar to those in the case study 1 (see *Table 6* to *Table 8*).

Step 10: Adjusting Upstream Intersections' Signal Timings Based on the Computed Ramp Throughputs and the Existing Intersection Directional Demands

Each upstream intersections had one signal time pattern with a cycle length of 120s over the entire 6-hour simulation period. The existing signal timings for the selected intersections were first recorded, then the splits for the phases leading to the freeway were increased in small increments to ensure a maximized throughput.

An example for scenario 2

The splits for the signal groups of the approaches with movements contributing to the freeway flow were made to be more than 50% of the total cycle length. The remaining time was distributed to the other signal groups based on their demand proportions.

For example, Figure 41 below shows the existing signal timing plan for intersection 1.

Signal Group	**2**	3	4	6	8
Signal Group Name	**SB**		WB	NB	EB
Splits (sec)	**40**	15	25	40	40

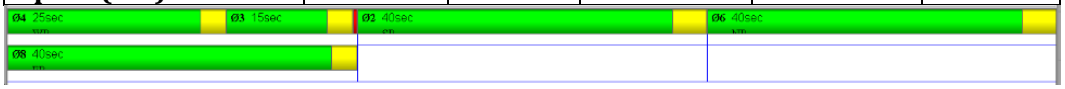

Figure 41: The Existing Signal Timing Plan at Intersection 1

At intersection 1, the SB approach signal group consisted of the southbound through movement that connects to the on-ramp. Referring to the directional demands for intersection 1 (see *Table 6*), at the first time-period 0-30min the demands for the NB and the EB approaches are 50veh/h and 307veh/h, respectively. If the split for the southbound approach signal group is increased to 80s which is approximately 67% of the cycle length, the remaining time, 40s is distributed as follows:

NB approach demand / (NB approach demand +EB approach demand) * 40s.

50/ (50+307) *40s=6s for the NB approach phase.

This leaves 34s for the EB approach phase.

However, to attain a minimum green of 7-15s, the split for the NB phase was increased to at least 10s, and thus the EB approach phase remained with a split of 30s.

The revised signal timings were as shown in the Figure 42 below:

Signal Group	**2**	3	4	6	8
Signal Group Name	**SB**		WB	NB	EB
Splits (sec)	**80**	15	15	10	30

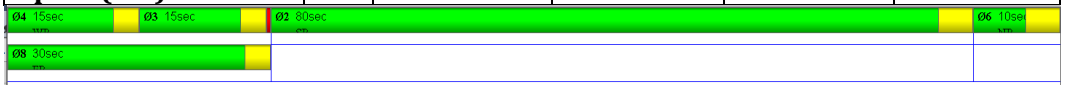

Figure 42: Revised Signal Timing Plan at Intersection 1

Step 11: Evaluation: Compare the before and after Queue Lengths (at Freeway, Intersections and/or On-ramp), Vehicle Network Performance (Average Speed and Total Travel Time)

The following are the results and discussions for each scenario that was implemented featuring the signal timing plans at each upstream intersections, the queue lengths, the overall network performance, and the latent demand.

3.3.2.1 Scenario 1 implementation, Results and Discussion

In this scenario, signal controllers at the ramps were set to free running mode. In free running mode, there is no defined cycle length, and the signal controller times the assignment of the right of way independent of other signals. The following paragraphs discus the result after implementing scenario 1.

Figure 43 to Figure 47 shows the queue lengths recorded over the 6-hours simulation at the freeway merge downstream and at the upstream intersections' movements that contribute to the freeway flow. The comparison is based on results of the original plans and when only the onramp meters were adjusted and set to free running mode.

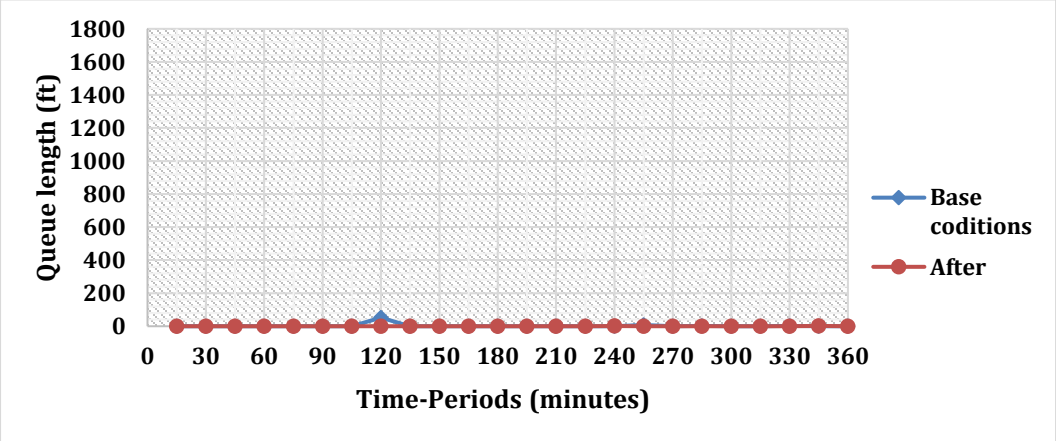

Figure 43: Case Study 2 Scenario 1 Freeway Queue Length Comparison

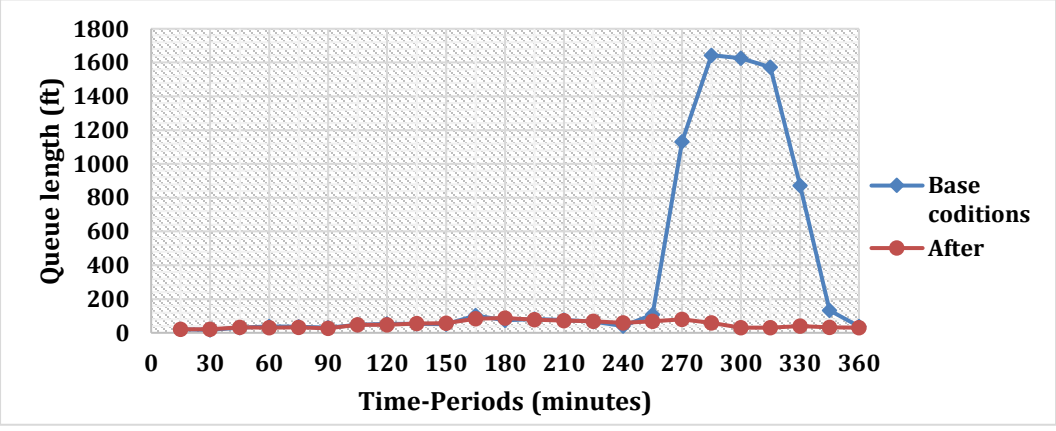

Figure 44: Case Study 2 Scenario 1 Queue Lengths Comparison at Intersection 4 (EB)

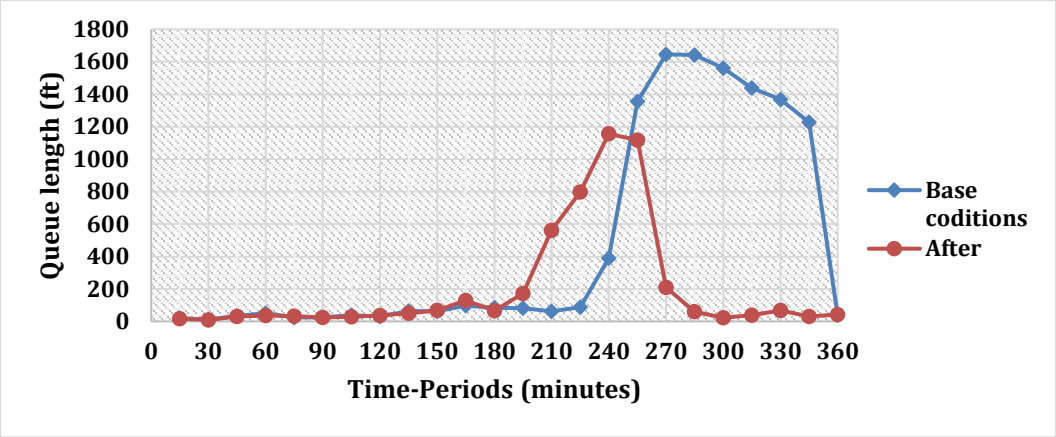

Figure 45: Case Study 2 Scenario 1 Queue Lengths Comparison at Intersection 3(EB)

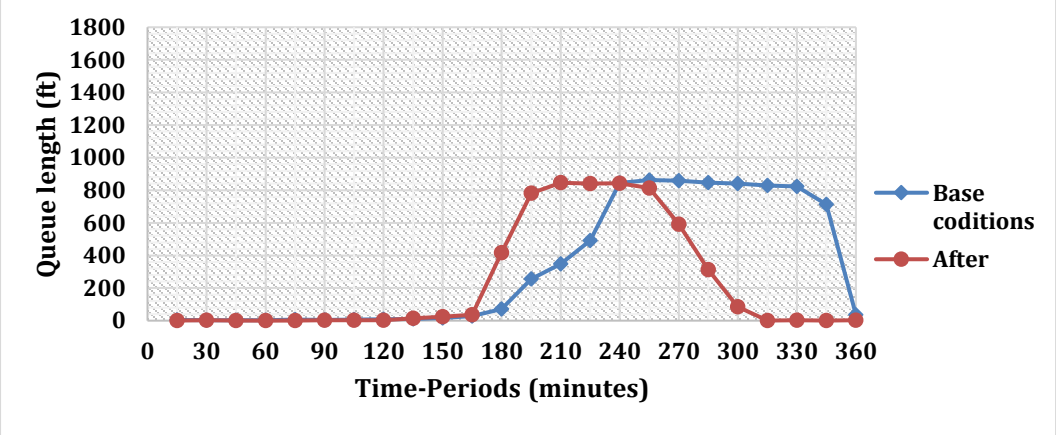

Figure 46: Case Study 2 Scenario 1 Queue Lengths Comparison at Intersection 2(EB)

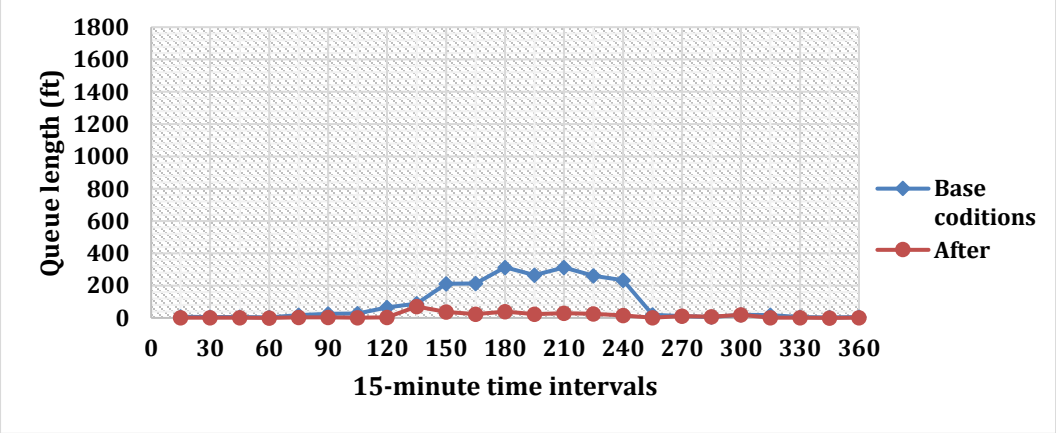

Figure 47: Case Study 2 Scenario 1 Queue Lengths Comparison at Intersection 1 (SB)

In both conditions, i.e., base conditions and after adjusting the ramp meters, there were no queues at the downstream of the freeway merge.

There was a great improvement in queue length at the intersection 4 and a slight improvement at intersections 3,2 and 1.

After adjusting the ramp metering, the queues at intersections 2 and 3 begun and dissipated earlier in the simulation compared to before. This was because most vehicles that were queued at intersection 4 were cleared and proceeded to intersection 2 and 3.

When the signal controllers at the ramp were set to free running, vehicles were released to the freeway in the optimal way possible thus leading to reduced upstream queue lengths.

Figure 48 and Figure 49 below shows the comparisons of the overall network performance in terms of average speed, total travel time and latent demands.

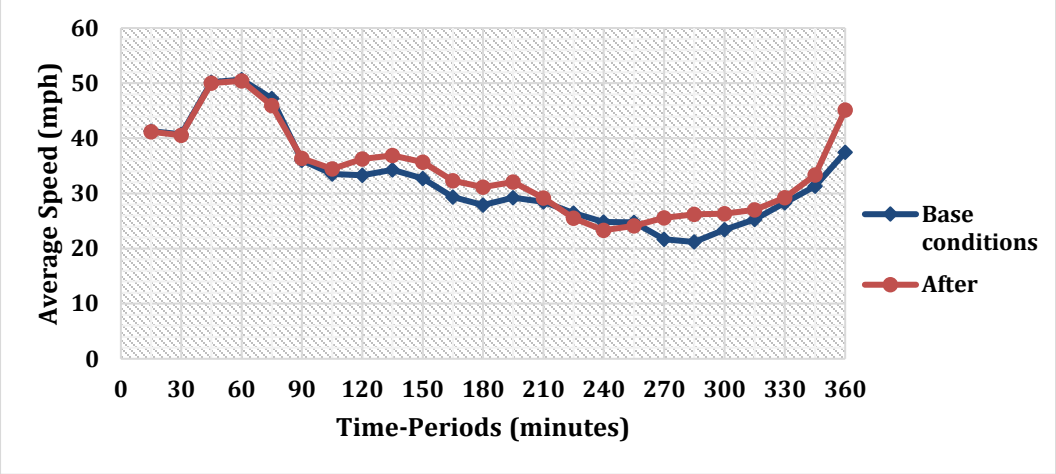

Figure 48: Case Study 2 Scenario 1 Comparison of the Network (Vehicle) Average Speed

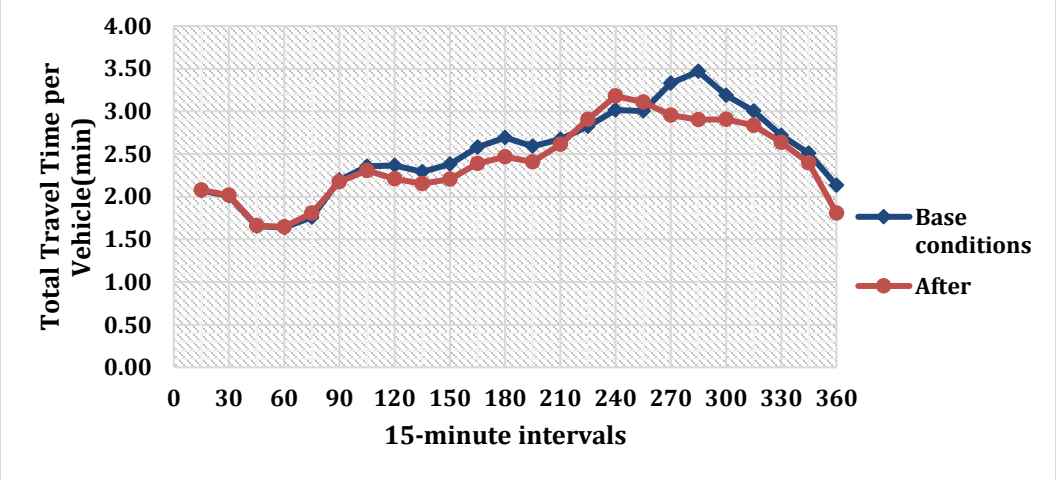

Figure 49: Case Study 2 Scenario 1 Comparison of the Network's Total Travel Time per Vehicle

Generally, there was an improvement in the vehicle average speed within the network by an average of 5.8% and thus lower travel times as compared to the original conditions.

3.3.2.2 Scenario 2 Implementation, Results and Discussion

In this scenario, the signal controls at the ramp were eliminated and the flow into the freeway was regulated at the upstream signalized intersections. The splits for the phases containing movements that lead to the freeway were increased to maximize the ramp throughputs as discussed in the example in step 10 of this case study. Each intersection had one signal timing plan throughout the entire simulation period with every phase set to minimum recall.

Table 12 below shows the signal timing plans implemented at the three of the affected upstream intersections in scenario 2.

Table 12: Signal Timing Plans for Scenario 2

Intersection 1									
			SB		WB		NB		EB
Plans	Start(min)	1	**2**	3	4	5	6	7	8
1	0		80	15	15		10		30
Intersection 2									
			Offramp		WB		NB		**EB**
Plans	Start(min)	1	2	3	4	5	6	7	**8**
1	0		35		80				80
Intersection 3									
		OTHER			WB		NB		**EB**
Plans	Start(min)	1	2	3	4	5	6	7	**8**
1	0	80	80		20				20

Figure 50 to Figure 54 show the comparisons of queue lengths at the freeway and at the freeway. Before and after adjusting the signal timing at the upstream intersections.

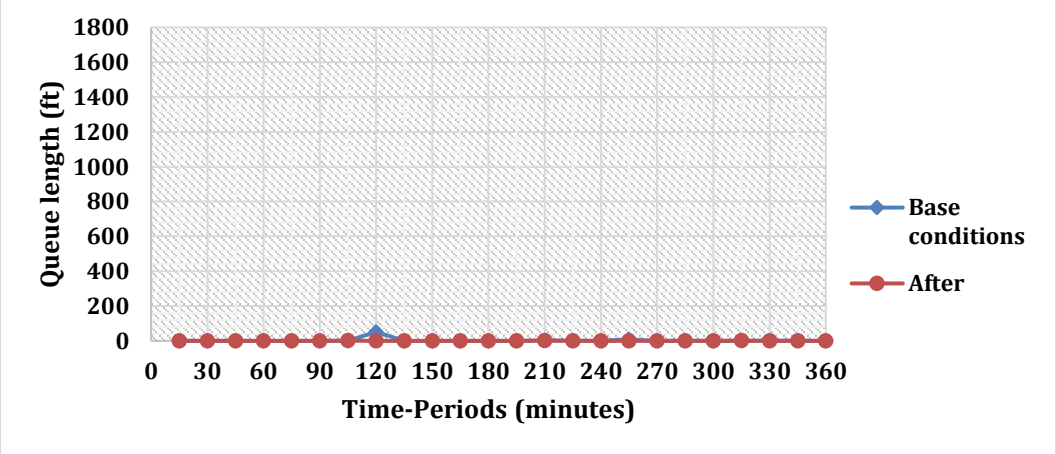

Figure 50: Case Study 2 Scenario 2 Freeway Queue Length Comparison

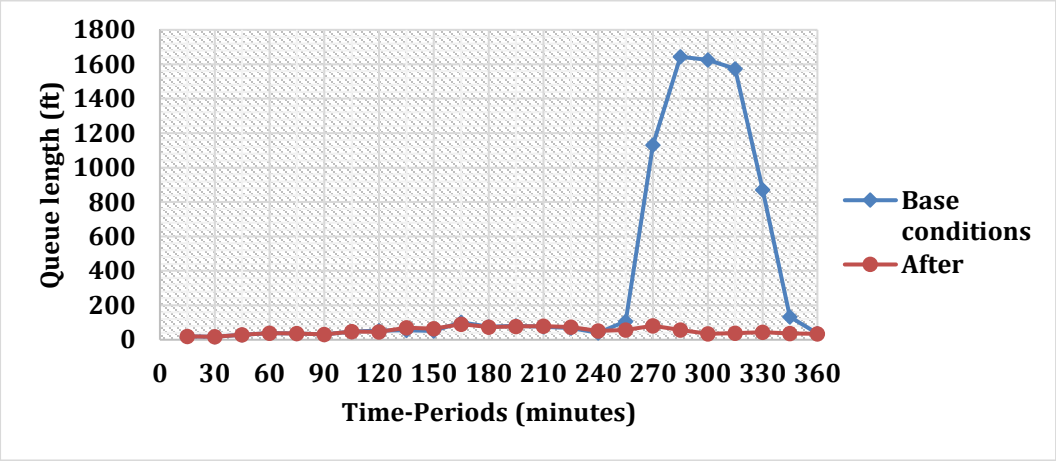

Figure 51: Case Study 2 Scenario 2 Queue Lengths Comparison at Intersection 4(EB)

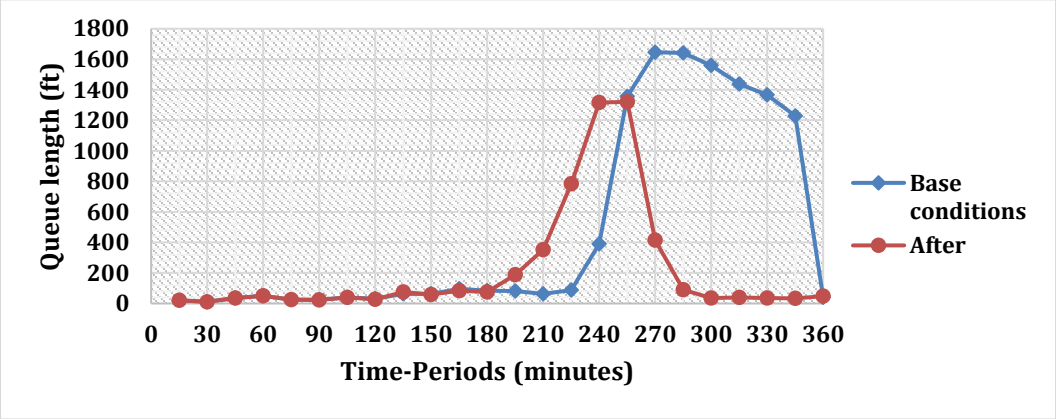

Figure 52: Case Study 2 Scenario 2 Queue Lengths Comparison at Intersection 3(EB)

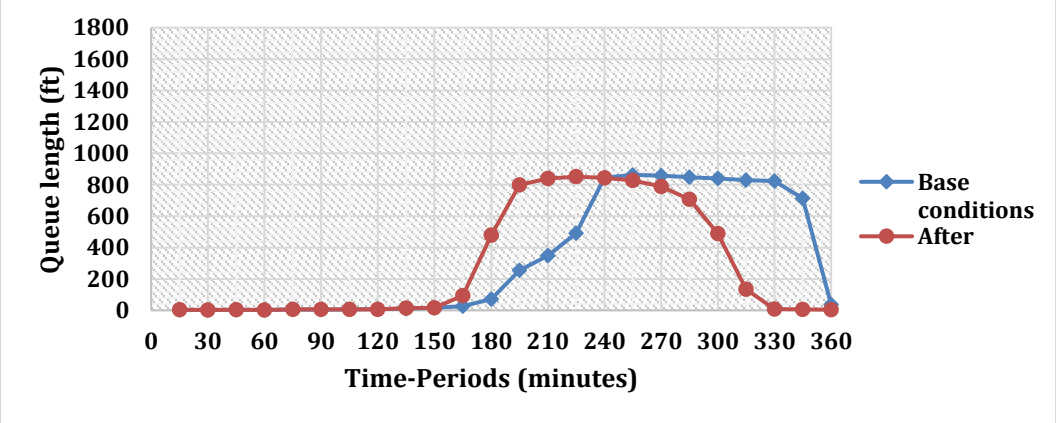

Figure 53: Case Study 2 Scenario 2 Queue Lengths Comparison at Intersection 2 (EB)

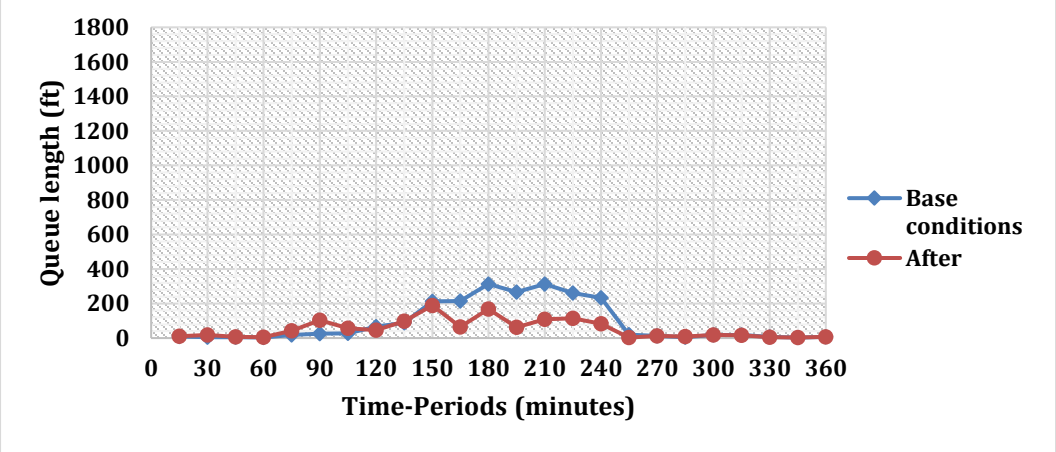

Figure 54: Case Study 2 Scenario 2 Queue Lengths Comparison at Intersection 1(SB)

After adjusting the signal timing, we observe that there was no queue formation at downstream of the freeway merge and at intersection 4. However, queues began and dissipated early at intersections 3 and 2. This could be because the queue at intersection 4 dissipated faster due to the increase in green time at intersection 3 for the affected phases that possibly maximized the throughput. At intersection 1, the queue length is lower than before due to the increase in the split for the phase with the movement leading to the on-ramp i.e., SB.

Figure 55 and Figure 56 represent the overall network performance in terms of average speed and total travel time per vehicle over the entire study period. The performance deteriorated between time 120-255min and then improved towards the end of the simulation from 255-360 min. Generally, there was an average improvement by 3.4%.

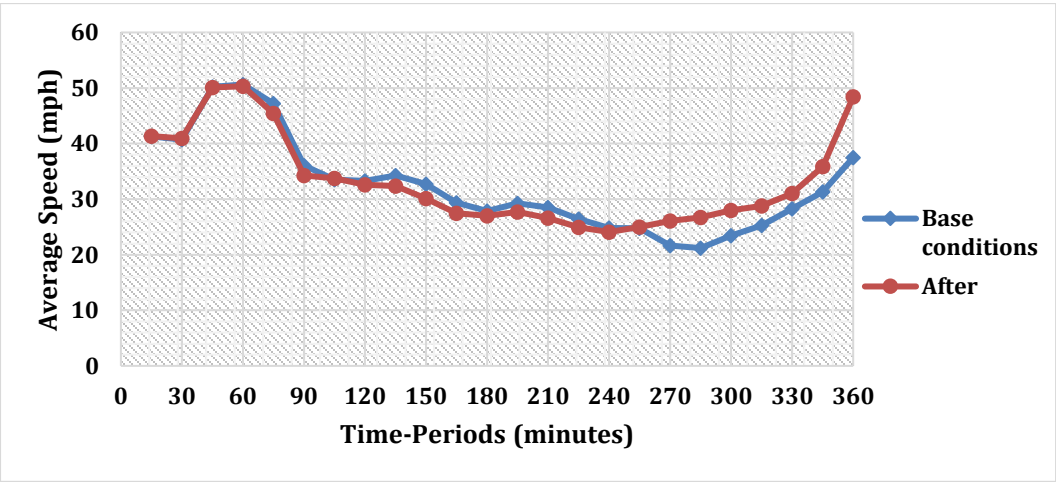

Figure 55: Case Study 2 Scenario 2 Comparison of the Network (Vehicle) Average Speed

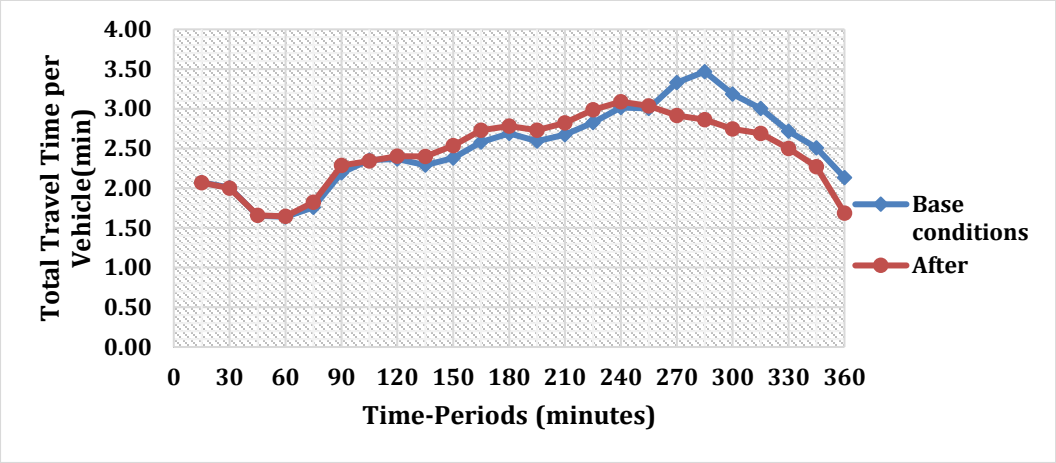

Figure 56: Case Study 2 Scenario 2 Comparison of the Total Travel Time per Vehicle

3.3.2.3 Scenario 3 Implementation, Results and Discussion

The presence queue at intersections 2 and 3 appeared to impact the overall network performance in scenario 2. The signal plans implemented in this scenario 3 were such that at intersection 1, the signal control was more restrictive between time 90min-250min and more unrestricted at intersection 2 for the same time-period. This scenario is expected to decrease the queue at intersections 2 and 3 and increase the queue at intersection 1. This action could possibly improve the overall performance of the network.

The *Table 13* below shows the signal timing plans implemented in scenario 3 for the three intersections. The plan 1 at each intersection was set to minimum recall. In plan 2 at intersection 1, the SB phase had decreased split time of 27s to restrict the flow onto the on-ramp during time-period 90min-250min. The SB and NB that were set to dual entry were set to minimum recall and the WB and EB to maximum recall. Meanwhile in plan 2 at intersection 2, the EB and WB phase were set to minimum recall and the SB phase set to maximum recall.

Table 13: Signal Timing Plans for Scenario 3

Intersection 1									
			SB		WB		NB		EB
Plans	Start(min)	1	**2**	3	4	5	6	7	8
1	0		40	15	25		40		40
2	90		27	15	37		41		52
1	250		40	15	25		40		40
Intersection 2									
			Offramp		WB		NB		**EB**
Plans	Start(min)	1	2	3	4	5	6	7	**8**

1	0		50		70				70
2	90		35		85				85
1	250		50		70				70
Intersection 3									
		OTHER			WB		NB		**EB**
Plans	Start(min)	1	2	3	4	5	6	7	**8**
1	0	40	40		40				40

Figure 57 to Figure 61 show the queue lengths comparisons at the freeway downstream and the signalized upstream intersections for scenario 3 of case study 2.

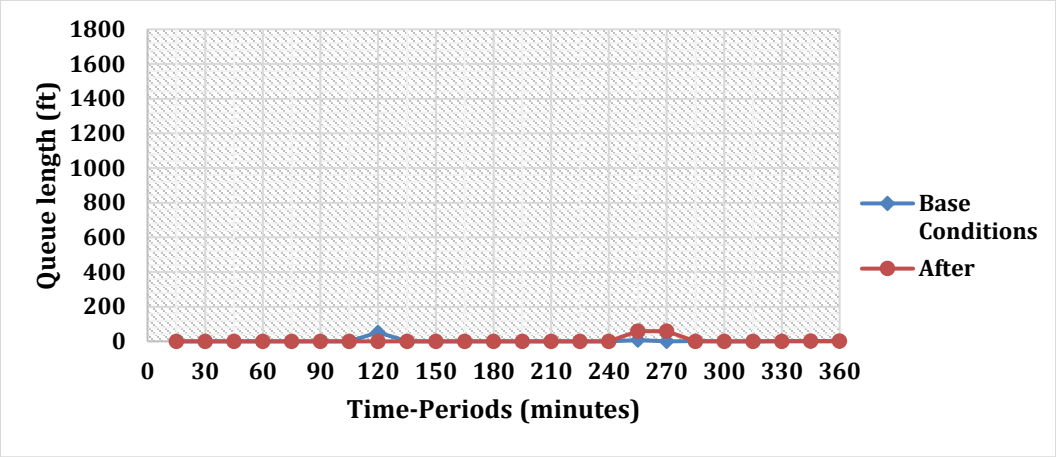

Figure 57: Case Study 2 Scenario 3 Freeway Queue Length

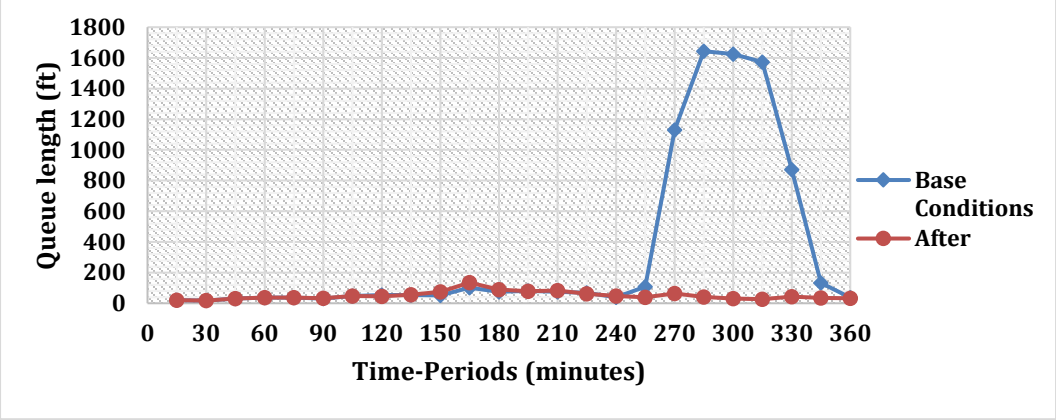

Figure 58: Case Study 2 Scenario 3 Queue Lengths Comparison at Intersection 4 (EB)

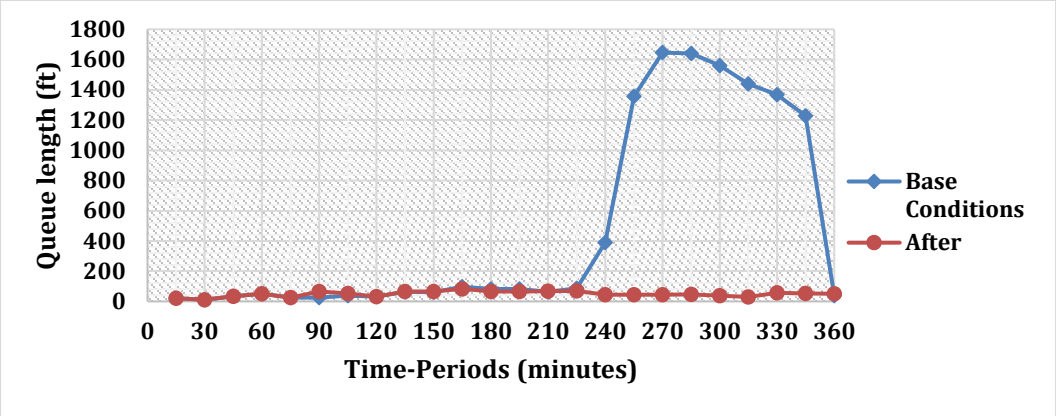

Figure 59: Case Study 2 Scenario 3 Queue Lengths Comparison at Intersection 3(EB)

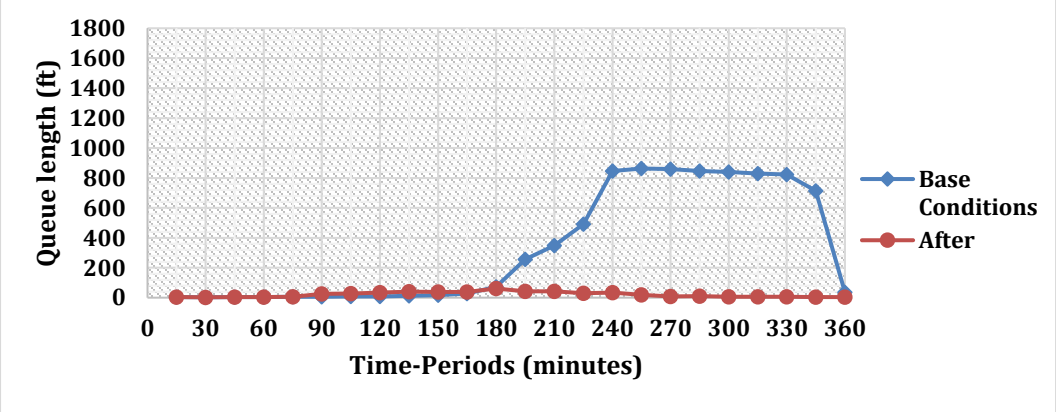

Figure 60: Case Study 2 Scenario 3 Queue Lengths Comparison at Intersection 2 (EB)

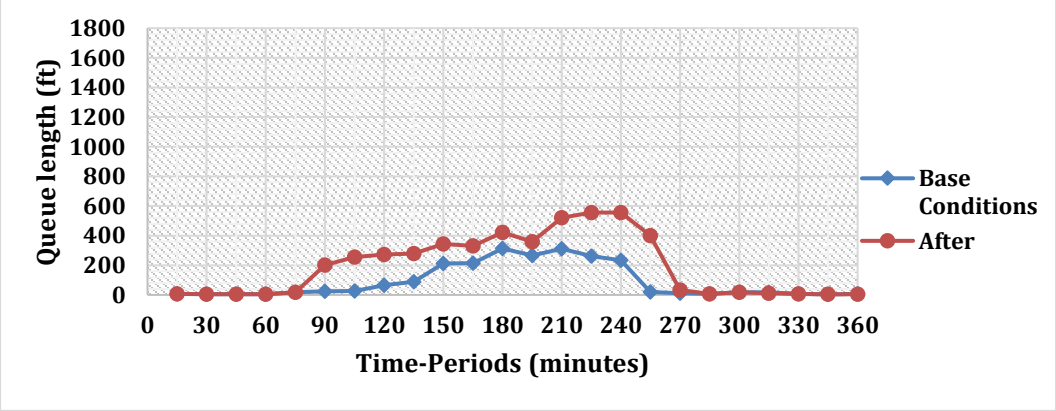

Figure 61: Case Study 2 Scenario 3 Queue Lengths Comparison at Intersection 1(EB)

The was no queue length at the freeway downstream before and after adjusting the signal timings at the upstream intersections.

Intersections 4, 3 and 2 had no queues after adjusting the signals. However, the queue at intersection 1 was longer than before. This was due to the adjustment of the green time at intersection 1 that was more restrictive at the expense of intersection 2.

Releasing as much vehicles as possible to the freeway by adjusting the signals at the upstream intersections led to reduced queue lengths in the network.

Figure 62 and Figure 63 are graphs showing the average speed and the total travel time per vehicle in the network over the entire study period. The average speed remained higher throughout the simulation period starting from 60 minutes which corresponds to the reduced total travel times. The improvement was by an average of 23%. Clearly, a balance was achieved between the queue lengths and the network performance.

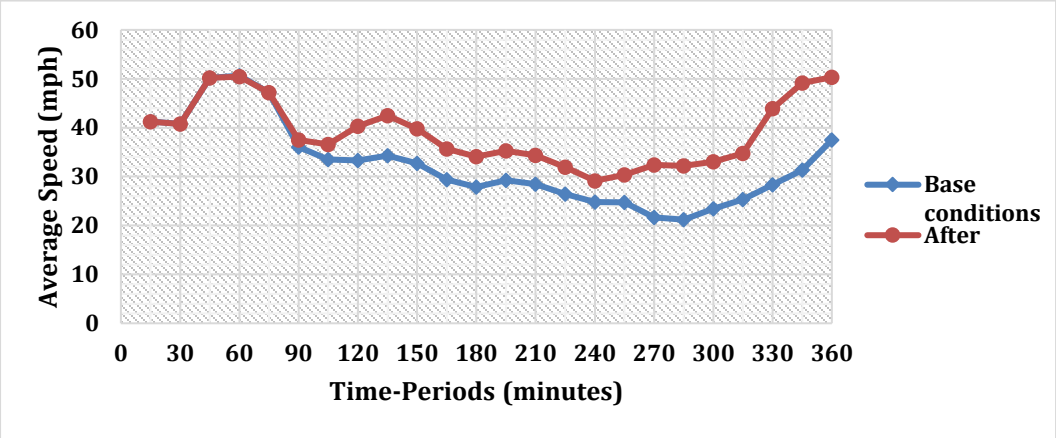

Figure 62: Case Study 2 Scenario 3 Comparison of the Network Average Speed

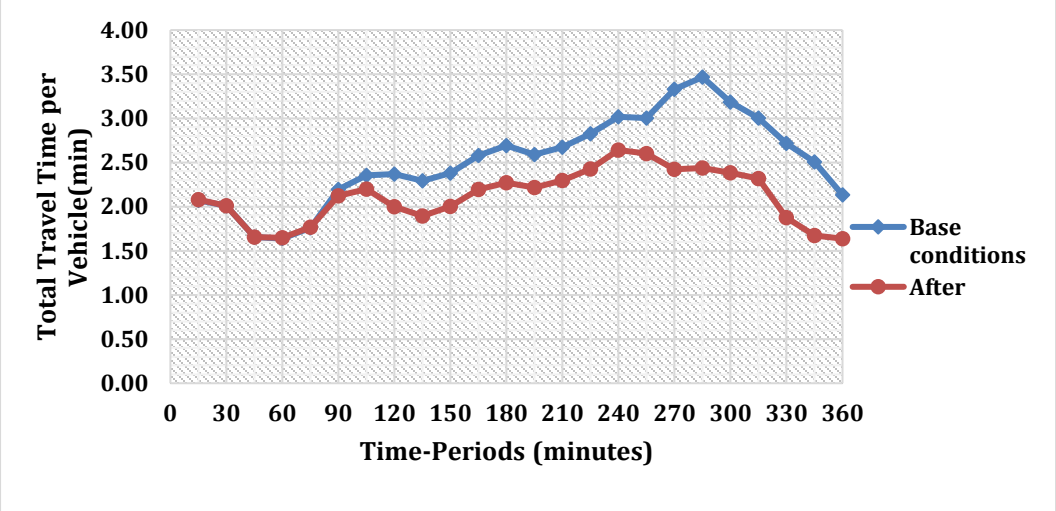

Figure 63: Case Study 2 Scenario 3 Comparison of the Network Total Travel Time per Vehicle

Latent demand

Table 14 below provides the comparisons of the network's latent demands over the entire simulation period for the three scenarios discussed above.

Table 14: Comparisons of the Latent Demands for the Various Scenarios in Case Study 2

Time- interval (minutes)	Base Conditions (vehicles)	Scenario 1 (vehicles)	Scenario 2 (vehicles)	Scenario 3 (vehicles)
0-15	0	0	0	0
15-30	0	0	0	0
30-45	0	0	0	0
45-60	0	0	0	0
60-75	20	0	0	0
75-90	114	0	70	0
90-105	252	0	40	0
105-120	403	0	0	0
120-135	570	0	0	0
135-150	774	0	11	0
150-165	941	0	17	0
165-180	1228	3	3	3
180-195	1357	11	11	11
195-210	1465	0	0	4
210-225	1573	29	121	12
225-240	1703	269	268	200
240-255	1778	263	272	210
255-270	1742	342	358	258
270-285	1631	226	265	130
285-300	1491	208	243	92
300-315	895	103	127	0
315-330	455	79	101	0
330-345	0	0	0	0
345-360	0	0	0	0

In this case study, there was an on-ramp bottleneck causing queue spillback to the end of the arterial in the VISSIM network while the freeway congestion was minimal. This created high latent demand as most vehicles from the input flows and any available parking lots were not used. Thus, setting the ramp signal controllers to free running as in scenario 1, and adjusting the signals at the intersections such that the flow into the freeway was increased as in scenarios 2 and 3 reduced the latent demand. Overall, in the scenario 3, most vehicles were used throughout the simulation. Also, at the end of the simulation period, all vehicles were successfully used.

In case study 2, the on-ramp entrance bottleneck resulted in queue spillback that affected the performance of the network. The case focused on applying the developed method to mitigate the effects of queue spill back by maximizing the on-ramp throughput onto the freeway through adjustment of upstream signal timing. Since the freeway experienced minimal congestion, the method aimed to maximize the ramp throughputs by increasing the splits for the phases with

movements that lead to the on-ramp. This meant that the splits for the other approaches that do not contribute to the ramp were reduced and may have resulted to delays. However, this trade off led to improved queue conditions and the overall network performance in terms of speed travel time and latent demand. Also, by maximizing the ramp throughputs, any the effect to the freeway's measures of effectiveness such as the freeway mainline speed, occupancy and delay did not deteriorate the performance of the network.

3.3.3 Case Study 3: The Florida Site (I-95 @ NW 119th Street)

Case study 3 is a site in Florida along the I-95 with an intersecting arterial NW 119th Street. Figure 64 below shows the Florida site and the selected scope for study. Congestion and the queues beginning from the on-ramp and spilling to the upstream intersections can be seen in Figure 65.

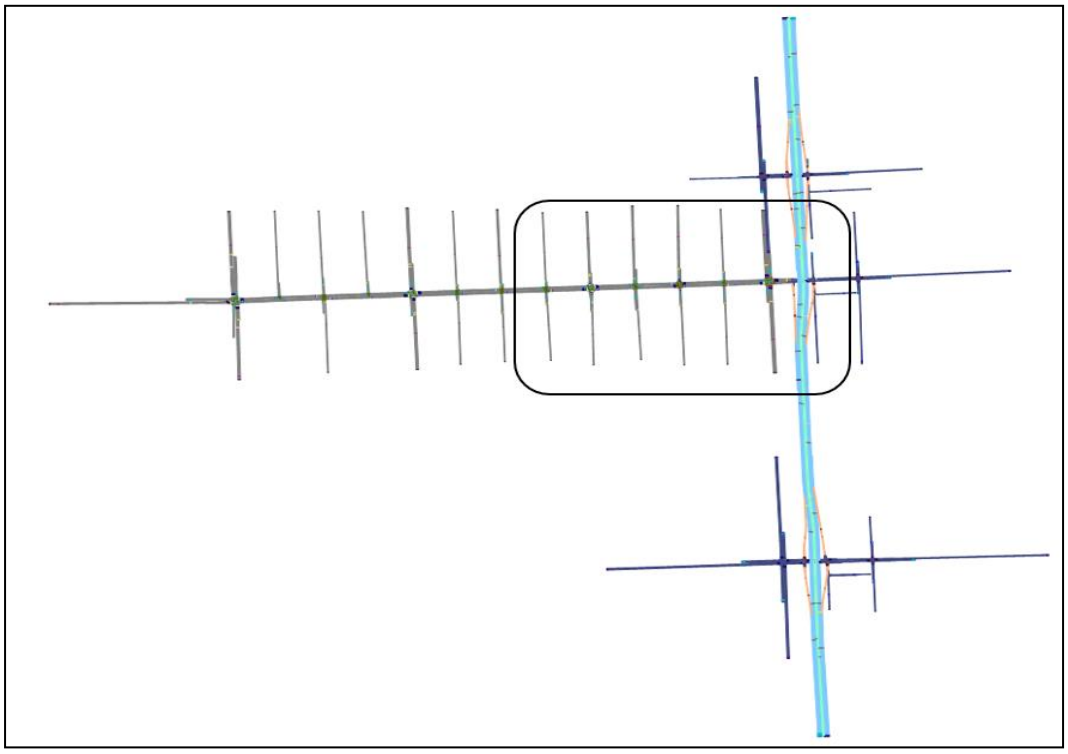

Figure 64: Case Study 3; The Florida I-95 at NW 119th Avenue

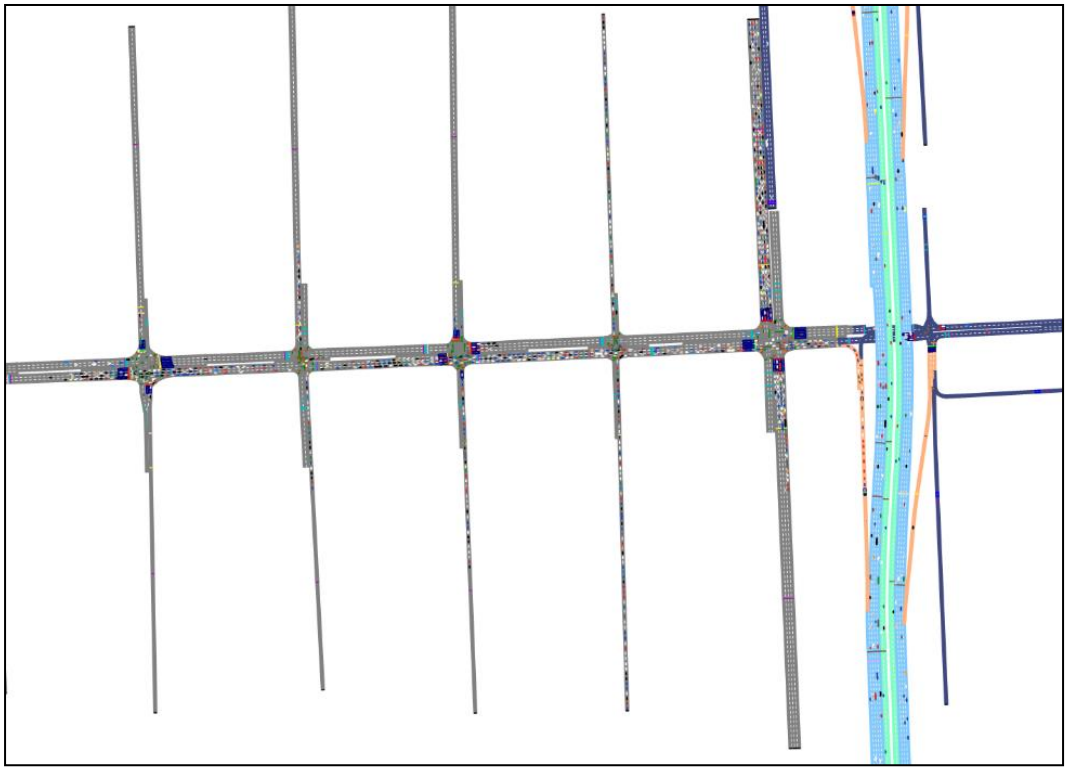

Figure 65: Congestion and Queue Spillback

Step 1: Select the Scope Area

The area of study is the Florida I-95 at NW 119th Avenue. The scope for the study included an on-ramp, one signalized intersection to the right and three to the left, and a 5.5-hour simulation duration. Figure 66 shows the four signalized intersections and the on ramp in the southbound direction.

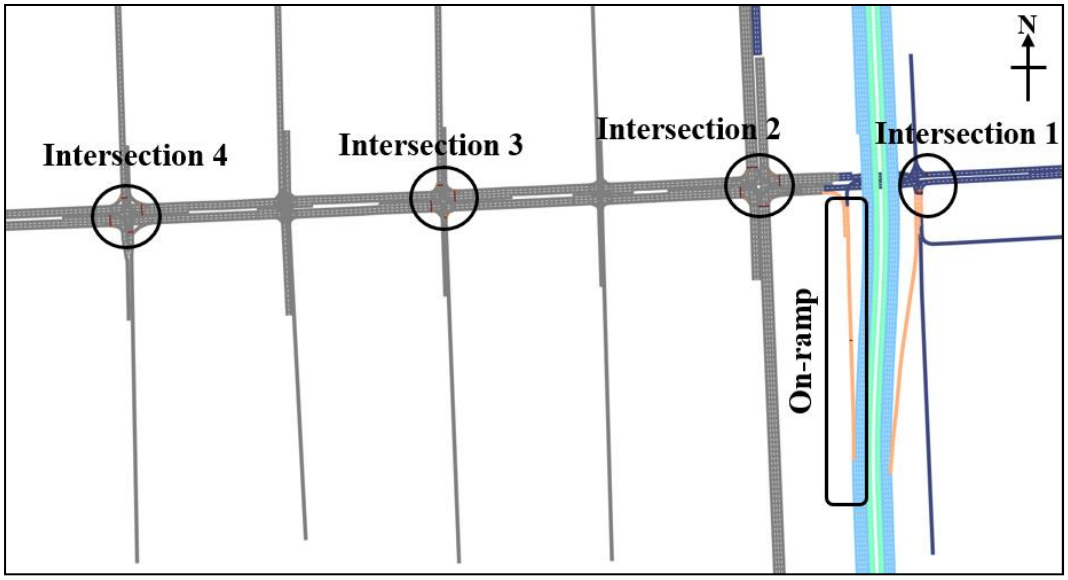

Figure 66: The on-ramp and the Four Signalized Intersections

Step 2: Record Freeway Upstream Demand (D_{Fr}), and On-ramp Demand (D_R) Considering the Presence of a Ramp Meter

The ramp demands were recorded at intervals of 15 minutes as shown in the *Table 15* below and the presence of a ramp metering facility was noted.

Table 15: The 15-minute On-ramp Demands Over 5.5-hour Simulation Period

Time periods (minutes)	Demand from Int.1(veh/h)	Demand from Int. 2 (veh/h)	Total onramp Demand
0-15	73	74	147
15-30	83	83	166
30-45	139	139	278
45-60	8	0	8
60-75	0	0	0
75-90	47	187	234
90-105	75	301	376
105-120	97	389	486
120-135	155	618	773
135-150	259	1034	1293
150-165	226	902	1128
165-180	230	918	1148
180-195	239	954	1193
195-210	249	997	1246
210-225	223	892	1115
225-240	169	676	845
240-255	167	666	833
255-270	130	521	651

270-285	157	629	786
285-300	148	593	741
300-315	145	580	725
315-330	120	481	601

Step 3: Estimate the Capacity of the Freeway Merge (C_{Fr}) and/or On-ramp Entrance (C_R)

The capacity was estimated at the on-ramp entrance which was the critically congested location following the observation of the simulation animation. The estimated capacity value was 167 veh/h/ln. Figure 67 below shows a time series graph of flow and speed data at the on-ramp entrance for one of the simulation runs with a breakdown flow value of approximately 172 veh/h/ln.

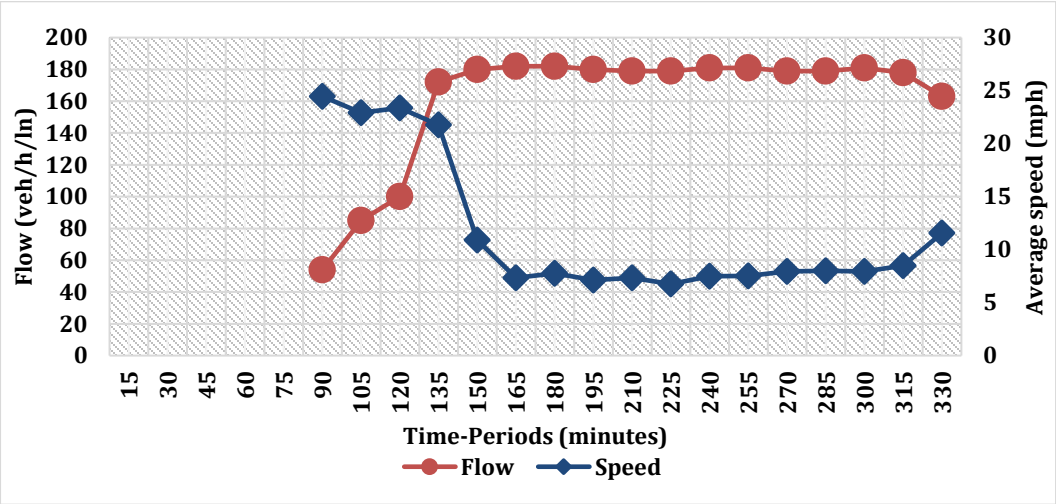

Figure 67: Time Series Graph of Flow Speed Data at the On-ramp Entrance

Step 4: Is the On-ramp Entrance Capacity Exceeded?

The estimated capacity was 167 veh/h/ln, and the on-ramp entrance has two lanes thus 334 veh/h. The share of volume allocated to access the ramp exceeds the estimated capacity at the on-ramp entrance (see *Table 15* under recording inputs step). Also, the time series graph shows breakdown of flow which represents congestion and low traffic speed for longer period during simulation, thus creating an on-ramp entrance bottleneck.

After establishing that the on-ramp entrance capacity was exceeded, the process continues to step 6.

Step 6: Can you Adjust the Ramp Metering?

In this case study, the downstream of the freeway merge was not in oversaturated conditions and thus the ramp metering could be adjusted by increasing the rate to maximize the ramp throughput.

Step 7: Adjust the Metering to Increase the Ramp Throughput.

The ramp metering facility was located at the point where the on-ramp became a single lane. The existing metering rate was 720 veh/h which was more restrictive to vehicles entering the freeway and thus contributing to queue spillback. A 720 veh/h rate implies one vehicle is released every 5s. Thus, increasing the metering rate was a possibility to decrease the queue spillback at the upstream intersections. For instance, for 800 veh/h a vehicle is released every 4.5s and for 900 veh/h, one vehicle every 4s.

The metering rates were increased to 800veh/h and 900 veh/h which formed the basis for scenarios 1 and 2 respectively for this case study. After adjusting the metering rates, evaluation was conducted to gauge the performance of the network which leads us to step 11.

Step 11, Evaluation: Compare the before and after Queue Lengths (at Freeway, Intersections and/or On-ramp), Vehicle Network Performance (Average Speed and Total Travel Time)

This step discusses two scenarios implemented for this case study, and the results of the simulation including the queue lengths, the overall network performance, and the latent demand which refers to the number of vehicles that could not enter the VISSIM network due to congestion.

Scenarios 1 and 2 Implementation, Results and Discussion

The base conditions had a ramp metering rate of 720veh/h. In scenarios 1 and 2, the metering rates were increased to 800veh/h and 900veh/h respectively.

The queue lengths were recorded at the freeway downstream of the merge, the on-ramp, and the upstream intersections, specifically for approaches containing the movements that contribute to the on-ramp flow. Based on the VISSIM network design, the following approaches at upstream intersections had movements that contribute to the on-ramp flow: at intersection 1, NB and the WB approaches, at intersection 2, the EB approach, and at intersection 3, the NB, EB, and SB approaches, and at intersection 4, the NB, EB and SB approaches (see Figure 66). To record the queues, the queue counters were placed downstream of the freeway merge, immediately behind the ramp meter and the signal heads at the upstream intersections.

Table 16 below shows the average queue lengths at the on-ramp and at the intersections.

Table 16: The Average Queue Lengths at the On-ramp and the Affected Upstream Intersections.

		Average queue lengths before and after adjustment of on-ramp metering rates		
No.	**Direction**	**Base conditions (metering rate 720 veh/h)**	**Scenario 1 (Metering rate 800veh/h)**	**Scenario 2 (metering rate 900 veh/h)**

1	Freeway	0.00 ft	0.00 ft	0.00 ft
2	Ramp	569.03 ft	418.37 ft	341.36 ft
3	Int. 1 WB	66.58 ft	66.57 ft	66.51 ft
4	Int. 1 NB	24.53 ft	24.50 ft	24.55 ft
5	Int. 2. EB	904.18 ft	740.13 ft	589.72 ft
6	Int. 2 NB	264.77 ft	187.60 ft	111.29 ft
7	Int. 3 NB	304.82 ft	12.19 ft	0.77 ft
8	Int. 3 EB	461.06 ft	118.76 ft	40.66 ft
9	Int. 3 SB	0.57 ft	0.45 ft	0.44 ft
10	Int. 4 NB	1.59 ft	0.59 ft	0.473 ft
11	Int.4 EB	79.80 ft	57.77 ft	58.91 ft
12	Int.4 SB	3.67 ft	3.84 ft	3.13 ft
13	Int. 2 SB	1025.09 ft	1025.92 ft	1025.22 ft

- We can observe that there was no queue at the freeway both before and after adjusting the ramp metering rates.
- The average queue length at the ramp meter is decreased subsequently fooling the increase in metering rates.
- At intersection 1, both the NB and WB queues remain almost the same. This could be due to the less volume of vehicle allotted to the on-ramp route, thus experiencing lesser effect of the on-ramp entrance bottleneck.
- All the movements at intersections 2 to 4 experience a decrease in queue lengths after increasing the metering rates.
- From Figure 65 there was congestion in the SB direction of intersection 2. However, the average queue length results barely show any change after increasing the metering rates. This is because the vehicle routing decision does not lead to the onramp in the VISISM network and thus, it is beyond the scope of the objective and the methodology of this study.

Figure 68 and Figure 69 show the comparisons of the network(vehicle) average speed and the total travel time per vehicle over the 5.5-hour simulation period for the base conditions (720 veh/h) versus two scenarios of adjusting the ramp metering rates (800 veh/h and 900 veh/h).

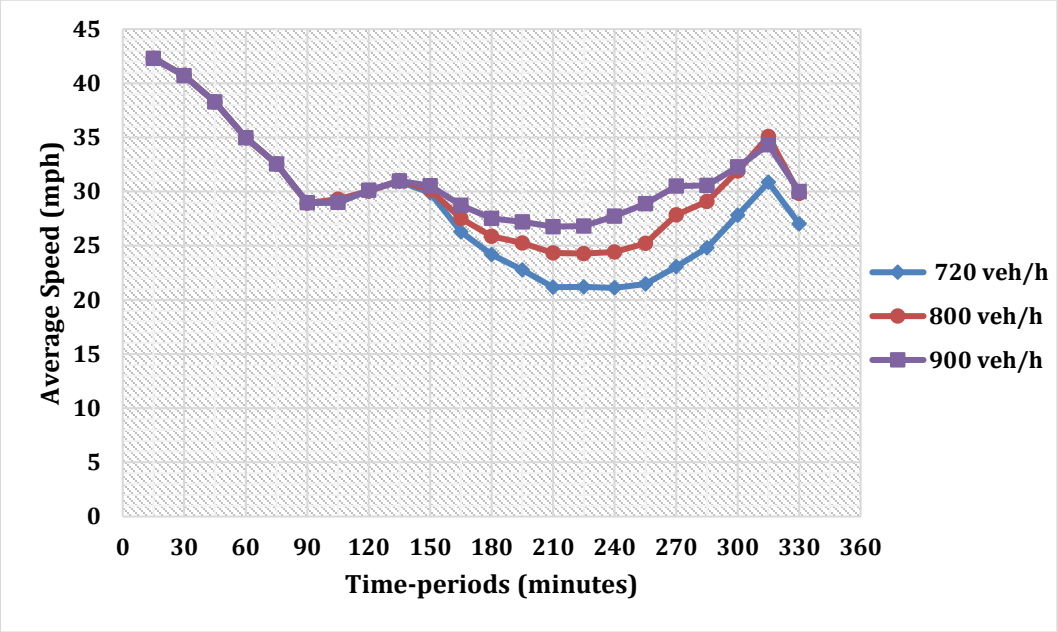

Figure 68: Case Study 3 Comparison of the Network (Vehicle) Average Speed

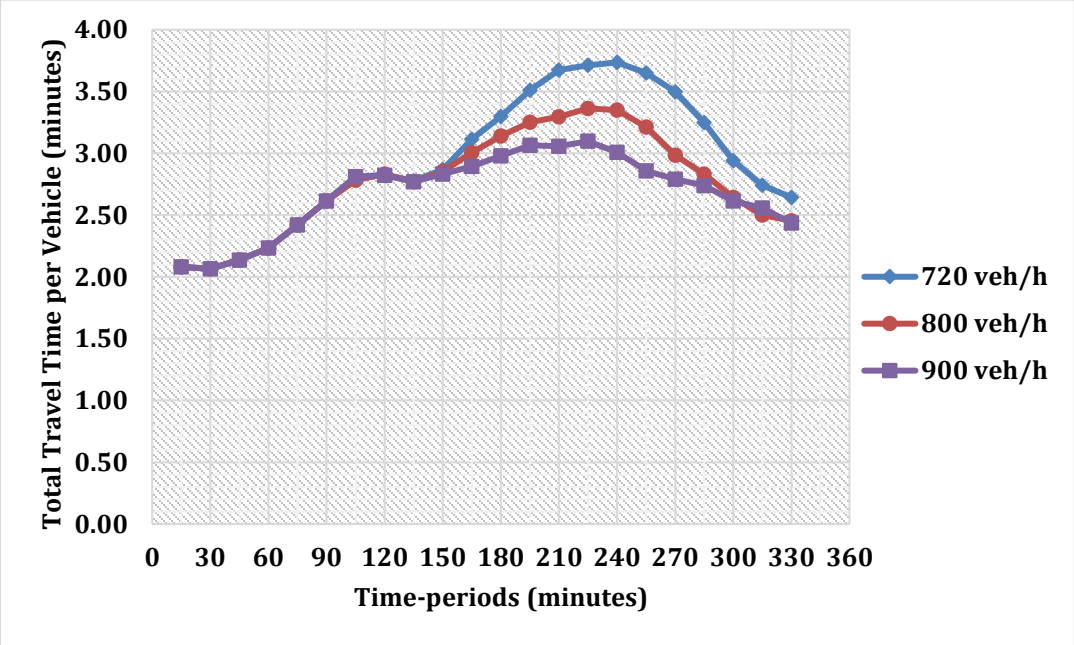

Figure 69: Case Study 3 Comparison of the Network's Total Travel Time per Vehicle (minutes)

The trend for the average speed and the total travel time per vehicle for the two scenarios remain the same as the original metering rate between time 0 to around minute 135. With

metering rate 720 veh/h, the network performance begins to deteriorate at around 150 minutes as congestion build up, and then improves towards the end of the simulation. Increasing the metering rate improves this dip in average speed and thus reducing the travel time per vehicle. The overall improvement was by an average of 7.5% with the 800 veh/h metering rate and 11.7 % with the 900 veh/h metering rate. With the 900veh/h metering rate, the low speeds between time 150min to 300min were improved to a range of 28-30mph compared to the range of 25mph to 30mph with the 800veh/h metering rate.

Latent demand

Table 17 below provides the comparison of the network's latent demand before and after adjusting the ramp metering rates.

Table 17: Comparisons of Latent demand

Time- interval (minutes)	Base conditions; (Vehicles)	Scenario 1 (Vehicles)	Scenario 2 (Vehicles)
0-15	0	0	0
15-30	0	0	0
30-45	1	1	1
45-60	0	0	0
60-75	0	0	0
75-90	45	45	45
90-105	284	284	284
105-120	500	500	500
120-135	631	631	631
135-150	781	781	781
150-165	883	893	843
165-180	1075	1092	985
180-195	1264	1265	1125
195-210	1459	1396	1244
210-225	1441	1407	1198
225-240	1459	1428	1182
240-255	1425	1336	969
255-270	1307	1167	896
270-285	1205	910	797
285-300	1019	831	737
300-315	810	809	729
315-330	716	809	749

By increasing the metering rates, the latent demand gradually decreases for the most part of the simulation. Metering rate 900veh/h has better latent demand overall as it can be observed between time 165min to around time 315min.

Generally, in case study 3, the on-ramp entrance bottleneck due to the presence of a ramp metering facility caused queue spillback to the upstream intersections deteriorating the overall

performance of the network. Increasing the ramp metering rates increased the on-ramp throughput resulting in decreased queues at the on-ramp and the affected intersections. This also resulted in improved overall network performance in terms of speed, travel time and latent demand.

Increasing ramp metering rates may affect the freeway's mainline speed, occupancy, and delays. However, since the selected scope are does not include interaction of traffic from further upstream and downstream interchanges of the freeway, the improved overall network performance indicates that by maximizing the ramp throughputs, any the effect to the freeway's measures of effectiveness such as the freeway mainline speed, occupancy and delay were minimal.

3.4 Conclusions and Recommendations

This chapter proposed a methodology to determine locations with oversaturation then balance queue lengths and optimize the overall network performance. The methodology develops a strategy to mitigate the effects of queue spillback by adjusting metering rates and or signal timings at the affected intersections considering the existing demands and computed throughputs. It was assessed using VISSIM microsimulation involving three selected case studies.

Based on the three case studies the following are concluded:

- The method comes with tradeoffs in terms of latent demands, delays, queue lengths and better operations of the freeway segment. A balance that leads to improvement of the overall network performance is considered better.
- The methodology developed cannot address bottlenecks outside the scope area. Therefore, it is important to establish the scope area such that all areas affected are included in the analysis.
- Ensure to observe reasonable minimum green values; the typical values given in the Chapter 10 of FHWA Signal Timing Manual
- Future research could investigate the effects of the method on the traffic progression for coordinated intersections.
- Also, an automated approach/ an algorithm to generate optimal split values and cycle lengths for the desired throughputs at the affected signalized intersections can be considered in the future.

4 COOPERATIVE ADAPTIVE CONTROL OF SIGNAL AND RAMP METERING

4.1 Introduction

Traffic operation in urban freeways tend to deteriorate each year due to a gradual increase in the Average Annual Daily Traffic (AADT) numbers over the years. In an urban setting, it is not always economically feasible to widen the road to meet the growing demand. Thus, efficient traffic management to improve traffic operation has always been under study and these management tools have shown great prospects in coping with the day-to-day stochastic traffic demands (Papageorgiou et al., 2003).

Ramp metering (Papageorgiou and Kotsialos, 2002), Variable Speed Limit (Hadiuzzaman and Qiu, 2013), dedicated HOV lanes (Menendez, 2010), Reversible lanes (Frejo et al., 2016) are some common strategies for congestion management in freeway traffic operation. Among these strategies, ramp metering can control the entry flow of vehicles into the freeway, and thus, this strategy is a proven efficient tool for freeway traffic management.

While ramp metering can protect the demand-capacity balance of freeways (Bogenberger and May 1999), such strategy is susceptible to excessive delays on the upstream on-ramps, arterial roads, and side streets (Geroliminis et al., 2010). As the impacts of ramp metering decision can affect freeway operations as well as nearby arterials, researchers have been developing efficient ways to come up with coordinating ramp metering strategies with signal timings of arterial road intersections.

It is a complex decision-making process to integrate traffic signal timings with ramp metering decisions that can serve a common purpose of improving traffic operations of an entire network. Previous studies on such coordination methods are developed in ways that achieve specific purposes such as avoiding freeway bottlenecks, queue spillbacks to arterials etc. While only a few studies partially integrate ramp metering controls with traffic signals, there exists a gap in formulating an integrated solution framework where each optimal decision is set to fulfill a common objective of improving the operations of the entire road network. Thus, this study covers the research gap by developing a methodology to integrate traffic signal timings with ramp metering decisions for an urban corridor network.

The study develops an optimization program that takes current traffic states as inputs and provides optimal signal timings and ramp metering decisions. The optimization model is a Mixed Integer Linear Program (MILP) with an objective to maximize the number of completed trips of vehicles. Cell Transmission Model (CTM) network loading concept (Daganzo, 1995, 1994) is used to estimate traffic states as required for the MILP. As the optimization program is complex and traffic is stochastic, a Model Predictive Control (MPC) framework is used that predicts the traffic states based on CTM simulation, solves the MILP, and implements the optimized signal timings and ramp metering decisions at each timestep during the study

period. A receding horizon scheme ensures that the optimized decisions are implemented at each timestep and rolls on to the next timestep until the end of the study period.

The rest of the paper is organized as follows: A literature review is presented in the next section. Subsequent sections discuss problem formulation and solution technique, respectively. Afterwards, a detailed case study is presented. The last two sections discuss the results and concluding remarks.

4.2 Methodology

4.2.1 Problem Formulation

The study proposes a mixed integer linear program (MILP) as an optimization model. The aim of this program is to set optimal decisions (signal timings and ramp metering indications) in a way that maximizes the number of completed trips during the entire study period. The model takes inputs of initial traffic states from a macroscopic CTM model of the corridor network and generates optimal decisions.

CTM model divides the entire corridor network into homogeneous cells and links. The homogeneous cells of CTM are classified as: ordinary, merge, diverge, intersection, source, and sink cells. Vehicles start from the source cells (the entry points of vehicles for the corridor) and reaches their destinations by entering sink cells. The flow of vehicles from cell to cell is discretized in time, and the number of vehicles inside each cell at every timestep can be known using CTM vehicle propagation rules.

The MILP has two sets of decision variables: signal timing states, g_i^t and ramp metering decisions, g_m^t. These decision variables are binaries and refer to the fact that each decision variable makes decision to either initiate, continue, or terminate control indications at each time step, t. The objective function sets the decision variables that maximizes the number of vehicles of sink cells ($\sum_{\forall i \in C_s} \sum_{\forall t \in T} x_i^t$) over the study period.

$$\max\ Z = \sum_{\forall i \in C_s} \sum_{\forall t \in T} x_i^t \tag{3}$$

A detailed list of all the sets, parameters, and variables can be found in Table 18.

The objective function satisfies a few sets of constraints and maximizes the throughput.

Constraints (4) present the flow conservation constraints. At timestep $t+1$, the number of vehicles, x_i^{t+1} in any cell $i \in C$ is equal to the number of vehicles in cell $i \in C$ at timestep t, plus the entry flow of vehicles to cell i (D_i^t for source cells and $\sum_{k \in P(i)} y_{ki}^t$ for other cells), minus outgoing flow of vehicles from cell, i ($\sum_{j \in S(i)} y_{ij}^t$ for all cells except sink cells). It is also important to note Kronecker delta (if $i = j$, $\delta_{ij} = 1$; otherwise, $\delta_{ij} = 0$) in constraints (4) which is used to facilitate the representation of flow conservation for different types of cells.

$$x_i^{t+1} = x_i^t + (\delta_{io} + \delta_{is}) \sum_{k \in P(i)} y_{ki}^t - (\delta_{ir} + \delta_{io}) \sum_{j \in S(i)} y_{ij}^t + \delta_{ir} D_i^t \tag{4}$$

$$\forall t \in T, \forall i \in C, \forall o \in C \backslash \{C_s, C_r\}, \forall r \in C_r, \forall s \in C_s$$

The signal timing related constraints are presented by constraints set (5) - (10). The definition of lane groups used in formulating signal timing constraints and ramp metering constraints can be found in Figure 70.

Constraints (5) stem from a set of left and through movements of an intersection (see Figure 70). These constraints ensure that at most two-lane groups from this set can receive green time at the same time. Constraints (6) considers through and right turning movements as a lane group, and ensure these movements are served simultaneously. Constraints (7) ensure only one movement among the pairs of conflicting movements can receive green signal at a time.

Table 18: List of notations used in the study

Sets	
T	set of all time steps
C	set of all network cells
C_o	set of all ordinary cells
C_r	set of all resource cells
C_s	set of all sink cells
C_m	set of all merged cells
C_d	set of all diverge cells
C_i	set of all intersection cells
C_M	set of all metering cells
L	set of all network links
I	set of all intersections
M	set of all on-ramps
$S(i)$	set of all successor cells of cell $i \in C$
$P(i)$	set of all predecessor cells of cell $i \in C$
$E(k)$	set of all intersection cells of intersection $k \in I$ with through and left-turning movements
$O(i)$	set of all cells of intersection $k \in I$ with conflicting through and left turning movements with the movement $i \in E(k)$
R	set of all concurrent through and right turn movement with adjacent movements
$F(k)$	set of movements of on-ramp $k \in M$
$L(k)$	Number of lanes on on-ramp $k \in M$
Decision (control) variables	
g_i^t	signal state of intersection cell; 0 for red, and 1 for green for cell $i \in C_i$ at time step $t \in T$
g_m^t	metering state of metering cell; 0 for metering (red), and 1 for no metering (green) for cell $m \in C_M$ at time step $t \in T$
Variables	
x_i^t	state variables; number of vehicles in cell $i \in C$ at time step $t \in T$

y_{ij}^t	number of vehicles advancing from cell $i \in C$ to cell $j \in S(i)$ at time step $t \in T$
Q_i^t	maximum saturation flow of intersection cell $i \in C_i$ at time step $t \in T$
Q_M^t	variable saturation flow of metering cell $m \in C_m$ at time step $t \in T$
Parameters	
D_i^t	demand of resource cell $i \in C_r$ at time step $t \in T$
Q_i^t	saturation flow rate in cell $i \in C$ at time step $t \in T$
N_i	capacity of cell $i \in C$ in terms of the number vehicles it can hold
β_i^t	portion of flow entering intersection cell $i \in C_i$ at time step $t \in T$ from the total flow leaving its upstream diverge cell
δ_{ij}	Kronecker delta ($\delta_{ij} = 1$ when $i = j$; otherwise $\delta_{ij} = 0$)
ρ	ratio of backward shockwave speed to the free flow speed
τ	prediction or optimization time steps in the MPC framework
G_{min}	minimum green time for signal
G_{max}	maximum green time for signal
G_{min}^{ramp}	minimum green time for on-ramp metering
G_{max}^{ramp}	maximum green time for on-ramp metering

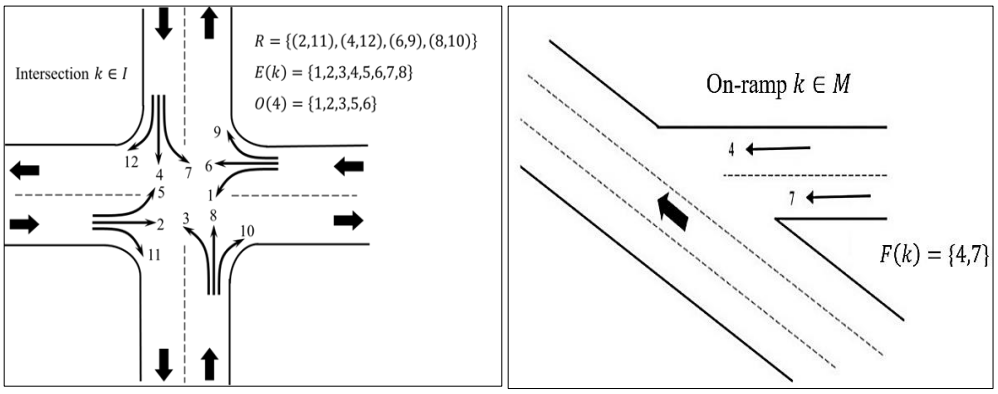

Figure 70: Intersection movements adopted from Mohebifard et al. (2019) and On-Ramp Movements

$$\sum_{j \in E(k)} g_j^t \leq 2 \qquad \forall k \in I, t \in T \qquad (5)$$

$$g_i^t = g_j^t \qquad \forall (i,j) \in R, t \in T \qquad (6)$$

$$g_i^t + g_j^t \leq 1 \qquad \forall k \in I, i \in E(k), j \in O(i), t \in T \qquad (7)$$

$$\sum_{\tau=t+1}^{t+G_{min}} g_i^\tau \geq \left(g_i^{t+1} - g_i^t\right) G_{min} \qquad \forall k \in I, i \in E(k), t \in T, t \leq |T| - G_{min} \qquad (8)$$

$$\sum_{\tau=t}^{t+G_{max}+1} g_i^\tau \le G_{max} \qquad \forall k \in I, i \in E(k), t \in T, t \le |T| - G_{max} \qquad (9)$$

$$q_i^t = g_i^t Q_i^t \qquad \forall i \in C_i, t \in T \qquad (10)$$

Constraints (8) and constraints (9) provides allowable limits for green time durations. Constraints (10) shows variable saturation flowrate for intersection cells. The flow rate equals to zero when signal indication is red, and the flow rate equals to maximum when signal is green.

Similar to signal timing constraints, constraints (11) - (14) represent constraints for on-ramp metering decisions. Constraints (11) allow all lanes on an on-ramp to receive green indications simultaneously. The maximum and the minimum green for on-ramp metering are presented by Constraints (12) - (13). Constraints (14) show variable saturation flow rate equation.

$$\textstyle\sum_{m \in F(k)} g_m^t \le L(\mathrm{k}) \qquad \forall k \in M, t \in T \qquad (11)$$

$$\sum_{\tau=t+1}^{t+G_{min}^{ramp}} g_m^\tau \ge (g_m^{t+1} - g_m^t)\, G_{min}^{ramp} \qquad \forall k \in M, m \in F(k), t \in T, t \le |T| - G_{min}^{ramp} \qquad (12)$$

$$\sum_{\tau=t}^{t+G_{max}^{ramp}+1} g_m^\tau \le G_{max}^{ramp} \qquad \forall k \in M, m \in F(k), t \in T, t \le |T| - G_{max}^{ramp} \qquad (13)$$

$$q_m^t = g_m^t Q_m^t \qquad \forall m \in C_M, t \in T \qquad (14)$$

Flow feasibility constraints are presented by constraints (15) - (19). Constraints (15) - (16) represents allowable outgoing flows of vehicles from a predecessor cell. The restrictions on flow come from available vehicles and saturation flow of the predecessor cell. Constraints (17) - (18) limits the incoming flow of vehicles to a successor cell based on saturation flow and available capacity. Constraints (19) distribute vehicles to successor cells proportionally (β_j^t) .

$$\sum_{j \in S(i)} y_{ij}^t \le x_i^t \qquad \forall i \in C \backslash C_s, t \in T \qquad (15)$$

$$\sum_{j \in S(i)} y_{ij}^t \le Q_i^t \qquad \forall i \in C \backslash C_s, t \in T \qquad (16)$$

$$\sum_{i \in P(j)} y_{ij}^t \le Q_j^t \qquad \forall j \in C \backslash C_r, t \in T \qquad (17)$$

$$\sum_{i \in P(j)} y_{ij}^t \le \rho\left(N_j - x_j^t\right) \qquad \forall j \in C \backslash C_r, t \in T \qquad (18)$$

$$y_{ij}^t = \beta_j^t \sum_{k \in S(i)} y_{ik}^t \qquad \forall j \in C_i, i \in P(j), t \in T \qquad (19)$$

Constraints (20)- (22) show the non-negativity constraints and integrality constraints for the optimization program.

$$x_i^t \geq 0, y_{ij}^t \geq 0 \qquad \forall i \in C, j \in S(i), t \in T \qquad (20)$$

$$g_i^t \in \{0,1\} \qquad \forall i \in C_i, t \in T \qquad (21)$$

$$g_m^t \in \{0,1\} \qquad \forall m \in C_m, t \in T \qquad (22)$$

4.2.2 Solution Technique

The optimization program has a complex formulation, and the traffic states changes with time. Based on these factors, a Model Predictive Control (MPC) framework is taken to solve the optimization program. The MPC framework collects initial cell occupancy, x_i^t of each cell, $i \in C$ at timestep, t. In our study, a microscopic simulation platform, PTV VISSIM (PTV Group, 2013) is used and VISSIM simulation provides the initial location coordinates of vehicles. These location coordinates are used to calculate cell occupancies of each cell of CTM network. Using the initial cell occupancies, traffic states up to a prediction horizon, T is estimated. Note that, traffic states are predicted up to T (<< Study period) and decisions are optimized up to that period. Therefore, prediction horizon, T is a set of timesteps $(t+1, t+2, \ldots., T)$ ahead of current timestep, t up to which the optimization model predicts system changes. Now, the predicted traffic data are used to solve the MILP. The MILP is solved using a commercial optimizer, CPLEX (CPLEX, 2009). The optimal solutions $(g_i^t = 0 \; or \; 1, g_m^t = 0 \; or \; 1)$ are implemented in VISSIM at the next timestep, $t+1$. A receding horizon control in MPC framework rolls on to the next timestep to repeat the process until the end of the study period.

Therefore, the solution technique followed in the study can be split into two modules: Simulation module and Optimization module (Figure *71*). The simulation module includes the VISSIM network. The VISSIM network provides network geometry, signal controller information, and vehicle location coordinates. The simulation module sends these data to optimization module via COM programming.

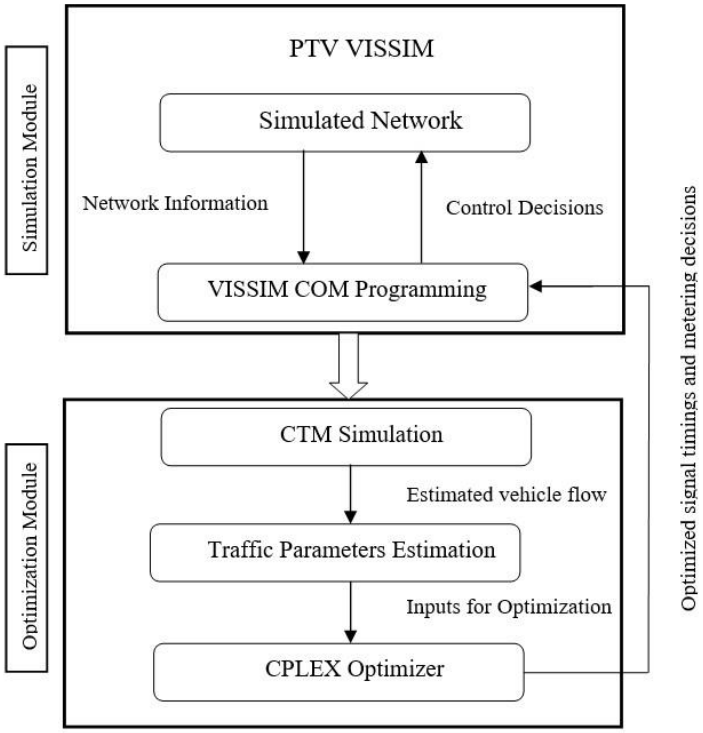

Figure 71: Solution technique used in the study

In optimization module, CTM network receives vehicle location coordinates and calculates initial cell occupancies. It is important to note that vehicle locations are exactly known from VISSIM, and no uncertainty is considered. It is assumed that the vehicles are connected, and accurate positions are known.

In addition to cell occupancies, the demand data is also processed and is converted from hourly rate (veh/hour) to discretized rate per timestep (veh/timestep). Discretized demand data and initial cell occupancies are required traffic parameters needed for the optimization program. The optimization program uses CTM simulation to find optimal solutions that maximizes vehicle throughput. Thus, the optimization is solved using CPLEX and the optimal decisions are sent back to the simulation module using COM programming for implementation. This process keeps on rolling up to the end of study period.

4.3 Case Study Network

A simulation network of a corridor from San Mateo, California is used in the study for evaluating the performances of our proposed methodology. This simulation network was calibrated as a part of FHWA Active Transportation and Demand Management project (Yelchuru et al., 2016). This report contains the calibration procedure of the testbed and also shows that the marginal error between field data and simulated data falls within the range of calibration targets. Therefore, this calibrated simulation model is used to test the methodology.

The corridor network has a freeway segment, an interchange with two on-ramps and two off-ramps, arterial road, and a few side streets (See Figure 72).

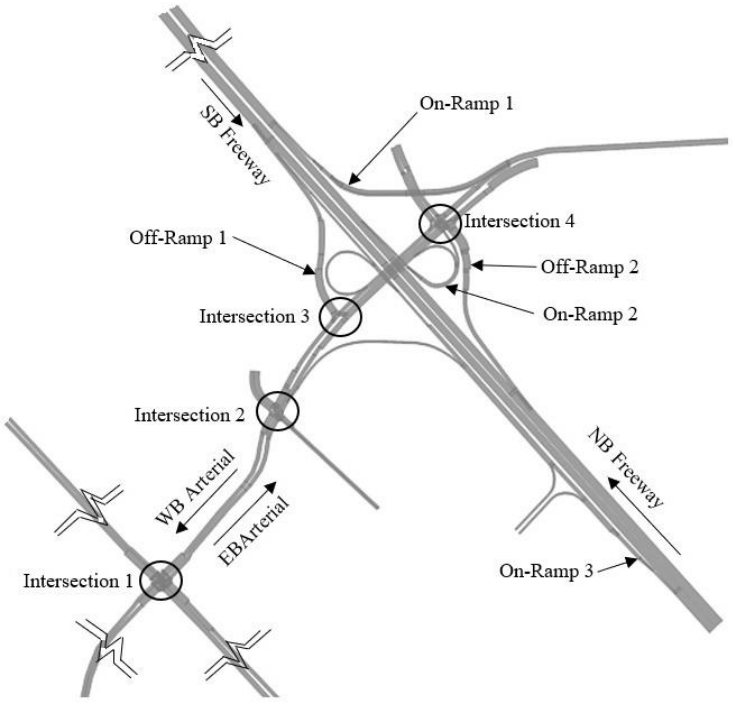

Figure 72: A Corridor from San Mateo County, California

The arterial road in the corridor includes four signalized intersections. The methodology is implemented on the four intersections and the two on-ramps of the interchange. In fact, five different scenarios are considered to test the effectiveness of the methodology:

I. Existing signal control with preset metering: The existing condition is tested in the simulation with no modification to signal controllers and ramp metering controls. The signal controllers have Ring Barrier Controllers (RBC), and they work as vehicle actuated controllers. Besides, the ramp metering controls have preset metering plans. This scenario is considered as the base scenario.

II. Existing signal control with no metering: This scenario is like scenario I except that the on-ramp metering is not implemented. Therefore, no metering is performed here. This scenario is specifically considered for comparison purpose with scenario I and scenario III.

III. Optimal Metering control: Optimal metering decisions are implemented on the ramp metering controls. However, the signal controllers are kept as before with no modification.

IV. Optimal Signal Control: Optimal signal timings are implemented in the simulation. Ramp controls have no metering plan.

V. Integrated Optimal Signal and Metering Control: All signal timings and ramp metering decisions are optimal solutions, and they are implemented. This scenario integrates the signal control decisions and metering decisions.

The first four scenarios are for benchmarking the performances of the integrated optimal signal and metering control. The above-mentioned scenarios are tested using a demand profile of six hours as shown in Table 19.

Table 19: Existing Demand (in veh/hour/lane) for Each Major Entry to Corridor

Time Duration (sec)	NB Freeway	SB Freeway	EB Arterial	WB Arterial	NB Side Street	SB-Side Street I	SB-Side Street II	EB Side Street	WB Side Street
0-1800	818	528	155	84	264	160	107	38	62
1800-3600	932	613	232	84	452	237	107	38	116
3600-5400	1260	959	232	163	453	268	178	64	15
5400-7200	1165	999	309	163	552	335	178	64	147
7200-9000	1185	1007	309	200	631	338	184	66	137
9000-10800	1145	984	386	200	687	383	184	66	257
10800-12600	1182	1064	386	200	342	424	180	64	219
12600-14400	1263	1081	309	200	443	366	180	64	117
14400-16200	1255	1012	309	200	438	368	125	58	79
16200-18000	1099	952	232	200	545	278	125	58	0
18000-21600	1115	838	232	150	683	234	100	55	0

Footnotes:
NB Side Street connects to Intersection 1; SB Side Street I connects to Intersection 1
SB Side Street II connects to Intersection 4; EB Side Street connects to on-ramp 3.
WB Side Street connects to Intersection 2

The demand profile is shown in Figure 73 for a clear understanding.

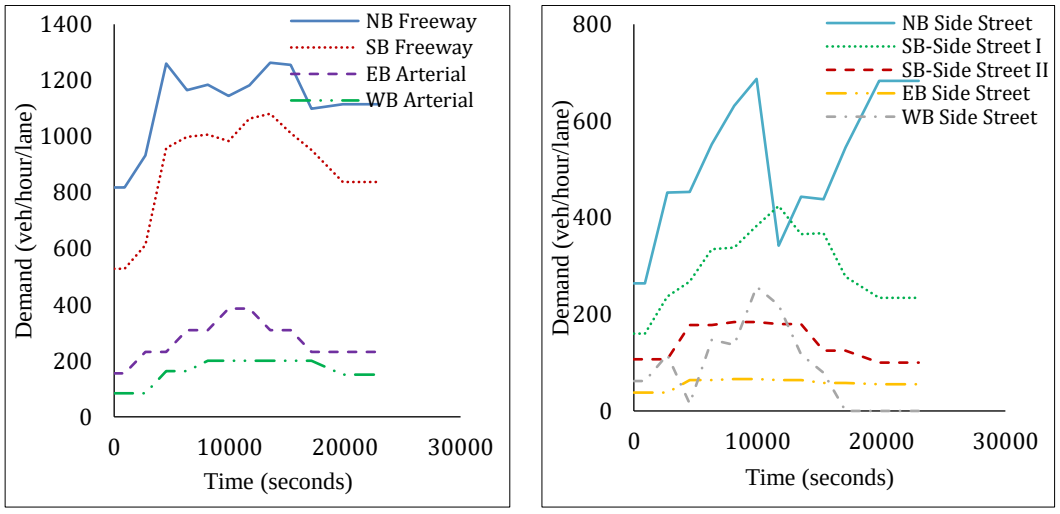

Figure 73: Six hours of demand profile used in the study

4.4 Results

In all performance measures (delay, stops, speed, travel time, throughput), the integrated control outperforms the base scenario (scenario I) by a large margin. Except for scenario IV which tend to produce identical results (only in terms of overall network delay) as integrated control, the performance improvements by integrated control are quite significant.

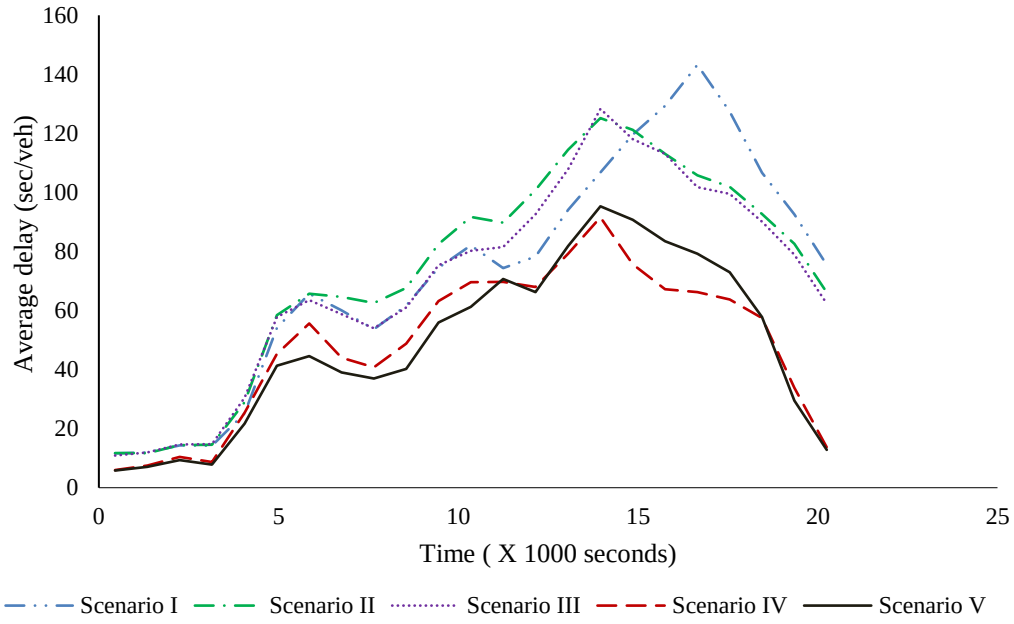

Figure 74: Average delay (sec/veh) during the study period

For instance, average vehicle delays for integrated control are significantly low during the study period as shown in Figure 74. It is evident that the average delays for the integrated control tend to remain minimum among other scenarios up to approximately 3.5 hours. After that, the average delay increases more than scenario IV, but it falls off soon and catches scenario IV. The overall network delay are pretty similar for Scenario IV and Scenario V. However, the significant differences and performance improvements of Integrated approach over Scenario becomes clear when we analyze directional performances as discussed in section 4.1.1. Besides, it is to be noted that the optimization program of Integrated control maximizes throughput of vehicles. Therefore, throughput is highest (79618) for integrated control among all the scenarios.

In addition to average delays, the other performance measures for the five scenarios are listed in Table 20.

Table 20: Network Performance for Tested Scenarios

Scenario No.	I	II	III	IV	V
Performance Measures	Existing Signal control with preset metering	Existing Signal control with No metering	Optimal Metering	Optimal Signal Control	Integrated

Average Delay (sec)	78.3	78.9	75.1	52.2	52.3
Average Stops	4.3	4.3	4.0	2.6	2.7
Average Speed (mph)	28.2	27.9	28.6	33.2	33.3
Throughput (vehicles)	79406	79374	79490	79612	79618
Total Delay (hours)	2121.65	2139.43	2029.64	1369.3	1374.14
Total Travel Time (hours)	4559.65	4583.6	4476.4	3806.7	3813.12
Total Stops (stops)	414957	415355	389762	240788	257511

The network results show that the integrated control reduces average delay, average stops, and travel time by 33.1%, 36%, and 16.4% respectively from the existing signal control and preset metering (scenario I). Besides, an 18.1% increase in average speed is also observed as compared to this base scenario. Also, a maximum number of completed trips (79618 vehicles) is observed in integrated control.

While integrated control outperforms the first three scenarios in all measures, the improvement is minimal when compared to optimal signal control (scenario IV). In fact, the results are almost identical for most measures. Except for vehicle stops, the result differences between the two scenarios are less than one present (<1%). In case of vehicle stops, the integrated control produces approximately 6.7% higher stops than scenario IV.

It is also noticeable in Table 20**:** that the implementation of optimal controls has been able to produce improvements over the first two scenarios with no optimization. While scenario II with no metering performs poor on performance measures compared to scenario I, the optimal metering control reduces delay, stops, and travel time by 4.1%, 5.6%, and 1.83% respectively from scenario I. An improvement in average speed (1.28%) and throughput (0.11%) are also achieved over scenario I.

4.4.1 Direction-wise and Intersection Level Performance Measures

The corridor-wide performances are broken down to direction-wise and intersection level performances to have insights into the improvement locations within the corridor. Table 21 shows the performance measures for various segments of the corridor for each scenario: Northbound freeway, southbound freeway, on-ramps, off-ramps, eastbound arterial, westbound arterial, and side-streets. (See Figure 73 for locations and directions of segments).

Table 21: Direction-wise Performance Measures

Scenario No. Performance Measures	Existing signal control and metering rates I	Existing signal control with no metering II	Optimal metering III	Optimal signal control IV	Integrated optimal signal and metering. V
NBFW (Northbound Freeway)					
Average Delay (sec/veh)	61.07	96.09	86.87	72.77	64.2
Average Stops (stops)	2.22	4.39	3.78	2.87	2.44
Average Speed (mph)	38.03	30.19	31.93	35.01	37.11
Total Travel Time (hours)	1561.03	1967.92	1864.79	1697.19	1602.36
SBFW (Southbound Freeway)					

Average Delay (sec/veh)	1.06	1.05	1.05	1.05	1.05
Average Stops (stops)	0.00	0.00	0.00	0.00	0.00
Average Speed (mph)	65.04	65.06	65.06	65.1	65.1
Total Travel Time (hours)	581.88	581.75	581.75	581.75	581.75
ONR (On-ramps)					
Average Delay (sec/veh)	63.50	45.01	47.32	33.21	39.65
Average Stops (stops)	8.30	5.78	6.01	4.04	4.96
Average Speed (mph)	12.37	15.9	15.36	19.5	17.37
Total Travel Time (hours)	251.22	199.58	206.37	159.06	179.65
OFR (Off-ramps)					
Average Delay (sec/veh)	5.24	5.30	5.31	5.39	7.54
Average Stops (stops)	0.34	0.34	0.34	0.17	0.3
Average Speed (mph)	40.1	39.95	39.94	39.7	36.5
Total Travel Time (hours)	37.68	37.79	37.8	38.01	41.44
EBArt (Eastbound Arterial)					
Average Delay (sec/veh)	424.10	333.14	320.52	49.32	87.9
Average Stops (stops)	24.50	19.41	18.67	4.56	7.73
Average Speed (mph)	4.11	5.03	5.18	16.4	12.55
Total Travel Time (hours)	1002.35	829.34	803.92	250.89	330.57
WBArt (Westbound Arterial)					
Average Delay (sec/veh)	26.78	32.05	33.67	6.17	7.11
Average Stops (stops)	0.87	1.02	1.05	0.3	0.35
Average Speed (mph)	24.71	23.1	22.61	34.29	33.92
Total Travel Time (hours)	179.03	191.93	195.91	128.91	129.51
Side Streets					
Average Delay (sec/veh)	50.82	20.47	22.92	49.63	50.9
Average Stops (stops)	1.87	0.49	0.64	1.8	1.83
Average Speed (mph)	13.47	16.4	16.18	13.33	13.37
Total Travel Time (hours)	822.63	677.76	689.5	815.3	819.15

The congested condition (average delay 78.3 sec/veh) observed in Table 20 for existing control (scenario I) is also visible in Table 21. It is seen that the Eastbound arterial road is highly congested (424 sec/veh) among other directions. As the eastbound arterial is connected to northbound freeway via the on-ramp, the performances of these segments need special attention. In scenario I, the on-ramp average delay is 63.5 sec/veh and the average delay of northbound freeway is 61.07 sec/veh. The northbound freeway delay is lowest among all scenarios. Therefore, the preset metering protects the northbound freeway at the expense of high delays on the on-ramp and eastbound arterial.

The integrated control makes significant improvement by reducing average delays, average stops, and travel time on eastbound arterial by 79.3%, 68. 5%, and 67.0% over scenario I. It also reduces average delay, average stops, travel time of on-ramp by 37.6%, 40.2%, 28.5% respectively. Such improvements are achieved at the cost of increasing the northbound freeway delay by a minimal amount of 5.13%. While scenario IV makes the most improvement on eastbound arterial (88.4% decrease in average delay), this improvement comes at the cost of increasing the delay of northbound freeway by 19.2% from the existing control (scenario I) and by 11.8% increment in average delay over Integrated control. Therefore, the integrated control

improves the conditions of eastbound arterial (79% reduction from Scenario I) and on-ramps with a minimal decrease of performance for the freeway. When Scenario IV is compared to Integrated control, It generates 12% more delay in the freeway and thus, it affects freeway operation significantly. Integrated control, on the other hand, keeps the delay much lower (5% more from preset timing of Scenario I) and also reduces arterial delay significantly.

Besides, the integrated control also improves the performances of other segments of the corridor over the benchmarks except scenario IV. The performances are slightly poor for integrated control in off-ramps, westbound arterial roads, and side streets as seen in Table 21. Also, the results of the side-streets say that integrated control has identical performances to scenario I. In fact, vehicles must wait longer in side streets before entering arterial roads and this situation has not changed even with integrated control. Therefore, an equity issue exists for the road users of side streets.

The average delay results are shown again in Figure 75.

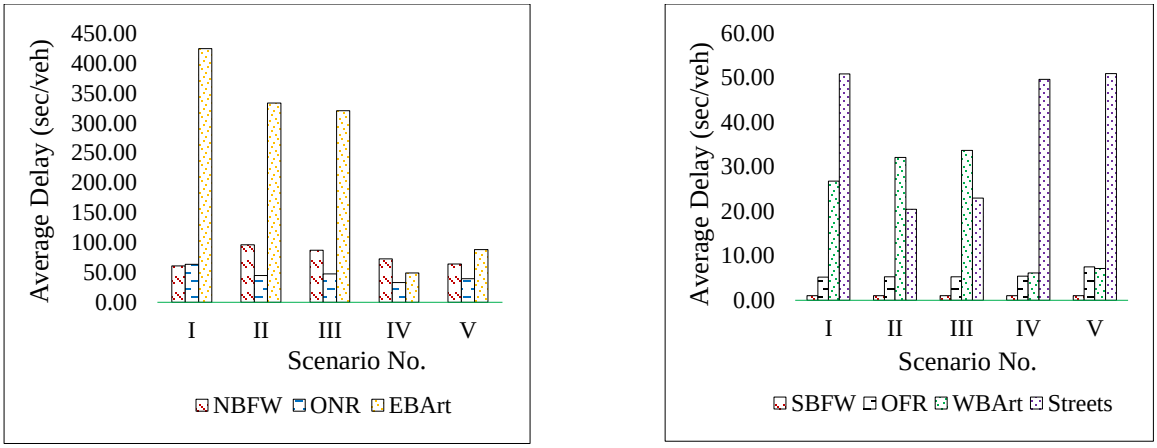

Figure 75: Direction-wise average delay for each scenario

Apart from direction-wise performances, the improvements integrated control is prominent at intersection level as shown in Figure 76.

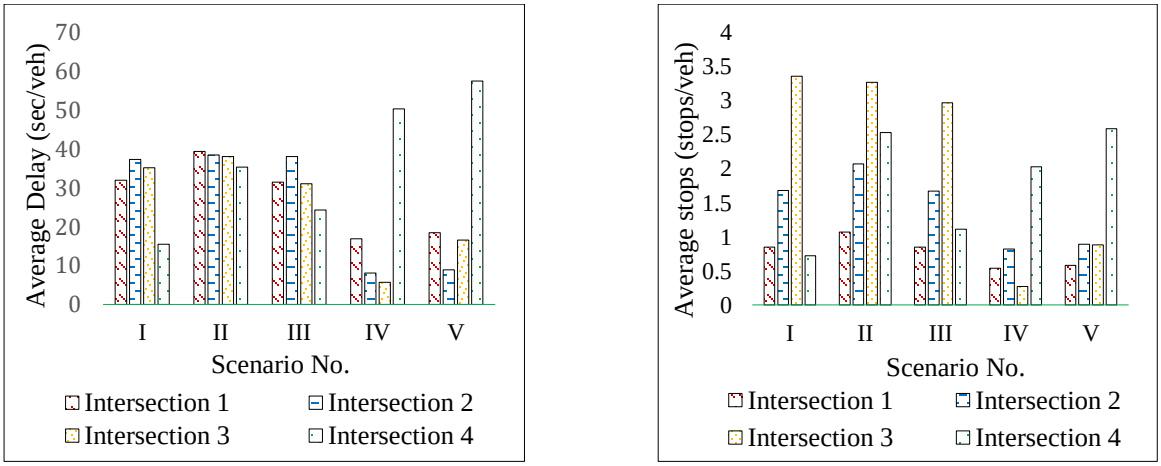

a. Average delay

b. Average number of stops

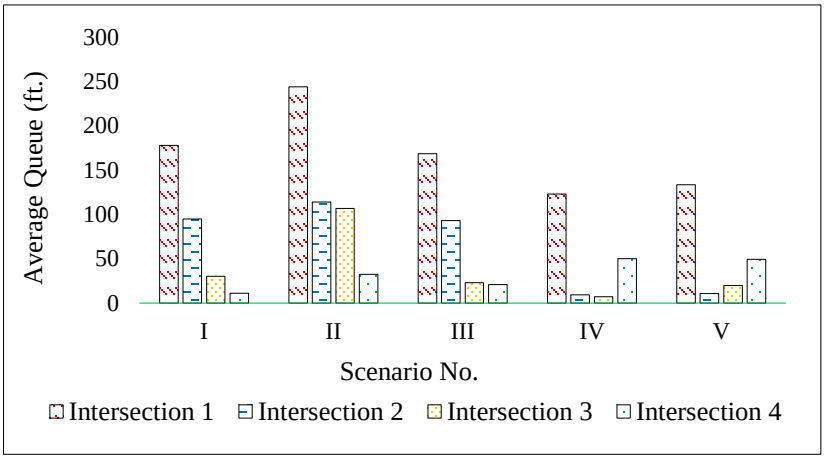

c. Average queue length

Figure 76: Performances of Each Intersection for Five Scenarios

It is seen that Integrated approach performs well in all measures for the first three intersections. However, the performances of integrated control for intersection IV and Intersection V are poor. These poor performances stem from restricting the right of ways for side streets vehicles. It is understandable as these intersections are near on-ramp 2 and the arterial road tend to have high demand of vehicles getting into on-ramp, the integrated control sets the optimum timings in a way to lessen already congested arterial by delaying vehicles from side streets.

4.4.2 Ramp Metering Flows

The ramp flows for each scenario are shown in Figure 77. As the on-ramp 2 is critical in for the study area, the ramp flows through this on-ramp are presented.

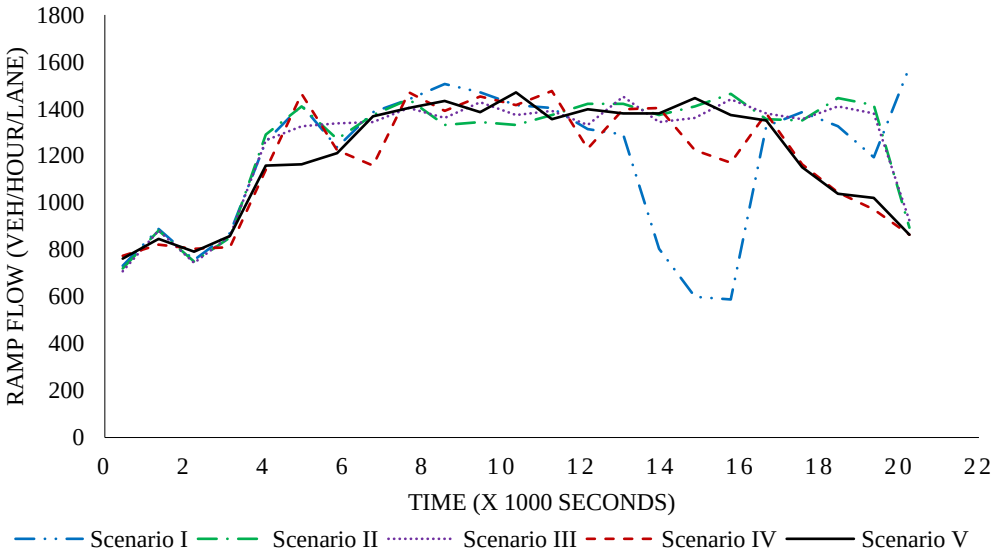

Figure 77: Ramp Flows (veh/hour/lane) through On-Ramp 2 for each Scenario

The ramp flows for integrated control keeps a relatively uniform flow of 1400 veh/hour/lane between 2 to 5 hours approximately. The other scenarios fluctuate around 1400 veh/hour/lane but scenario I has a preset metering that meters heavily approximately during (3.5- 4.5) hours as seen in Figure *77*.

4.4.3 Vehicle Accumulation in the Network

The active vehicles inside the network during the study period is shown in Figure 78.

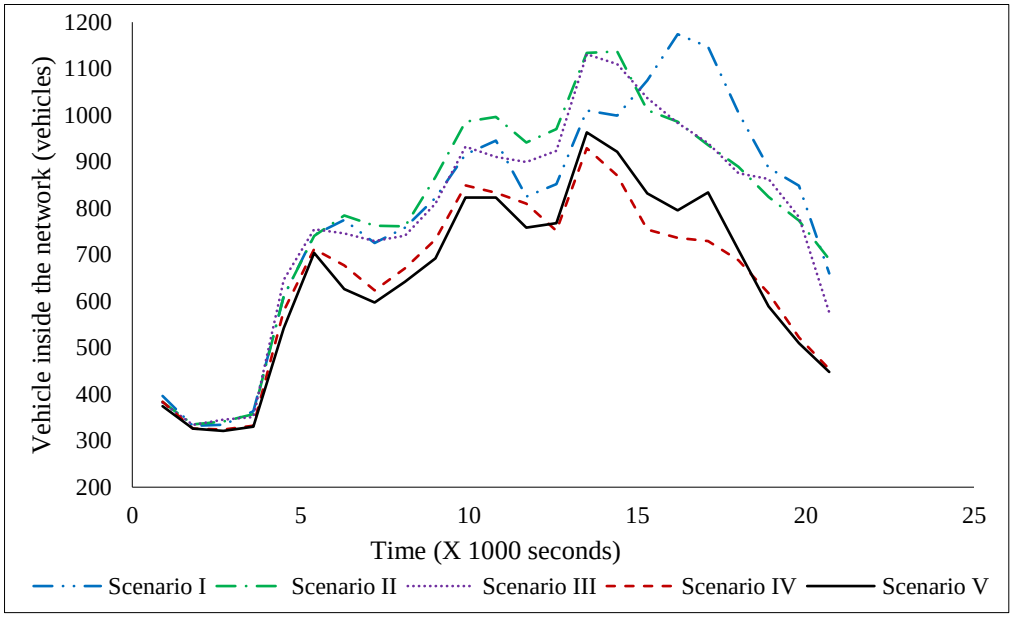

Figure 78 : Vehicle Accumulation in the Network over Study Period

The integrated control can keep least number of active vehicles up to approximately 3.5 hours. After that, the active vehicles go up more than scenario IV. However, active vehicles fall soon for the integrated control and become the minimum again before the end of the study period.

4.4.4 Computational Complexity of the Optimization Program

The run-time of our optimization program at each time step is shown in Figure 79. For a prediction horizon of two minutes, the average run-time is found to be 0.84 seconds with a standard deviation of 0.36 seconds (See Figure 79a).

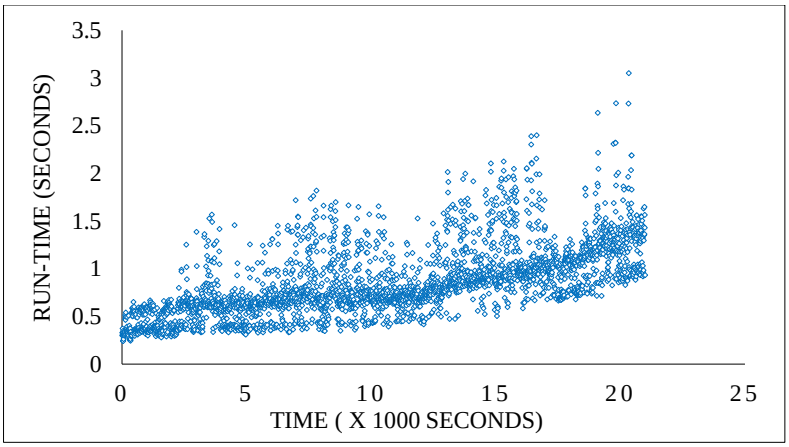

a. Computational Time for Two minutes of Prediction Period

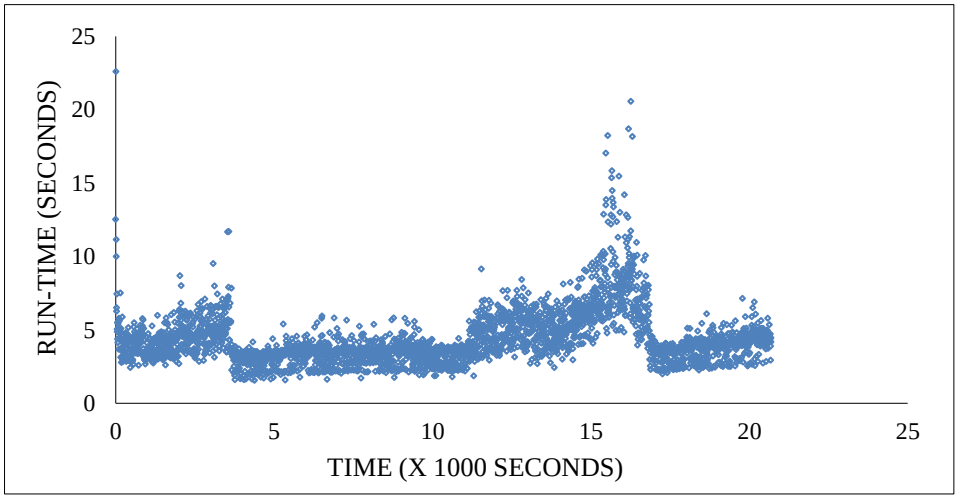

b. Computational Time for Five Minutes of Prediction Period

Figure 79: Computational Time of the Optimization Program

For a five minutes of prediction period, the average run-time is 4.4 seconds with a standard deviation of 1.8 seconds (See Figure 79a).

As each time step is six seconds and the optimal decision to implement next control is required to be computed before six seconds, the proposed methodology can be implemented in real-time with a prediction period of up to five minutes.

4.4.5 Vehicle Trajectories in Eastbound Arterial

It has already been shown that the heavily congested eastbound arterial of scenario I improves with implementing optimal controls. In fact, the Integrated control has achieved significant improvement over other scenarios. Such improvement is visible when vehicle trajectories are observed in Figure 80.

Vehicle trajectories are shown for the middle lane of eastbound arterial. Figure 80a shows severe delays for high demand of vehicles that are trying to get into the on-ramp 2. With no metering (scenario II), the congestion reduces but vehicles still experience higher delays near

on-ramp 2 (Figure 80b). With optimal control, the situation improves, and the traffic condition is the most ideal for scenario IV and scenario V (integrated control).

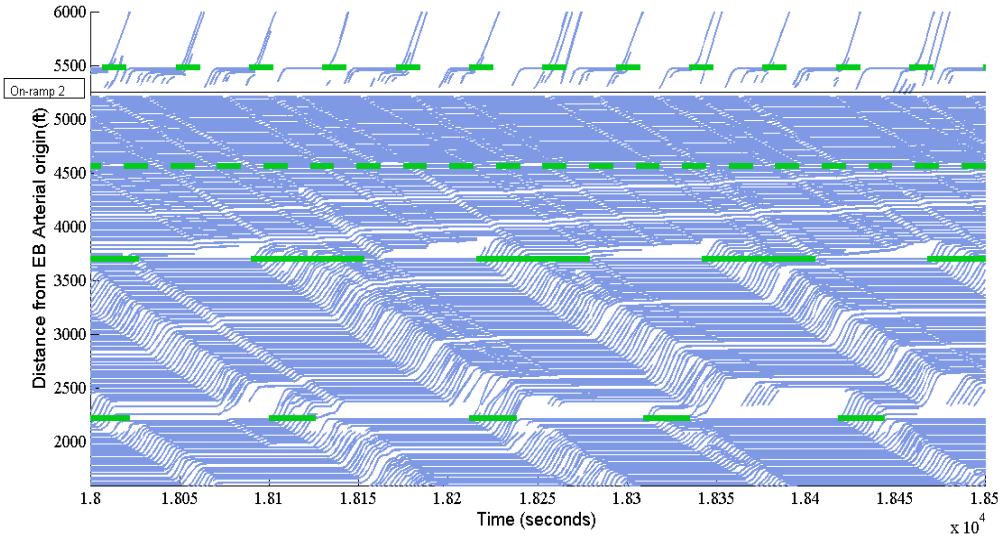

a. Scenario I

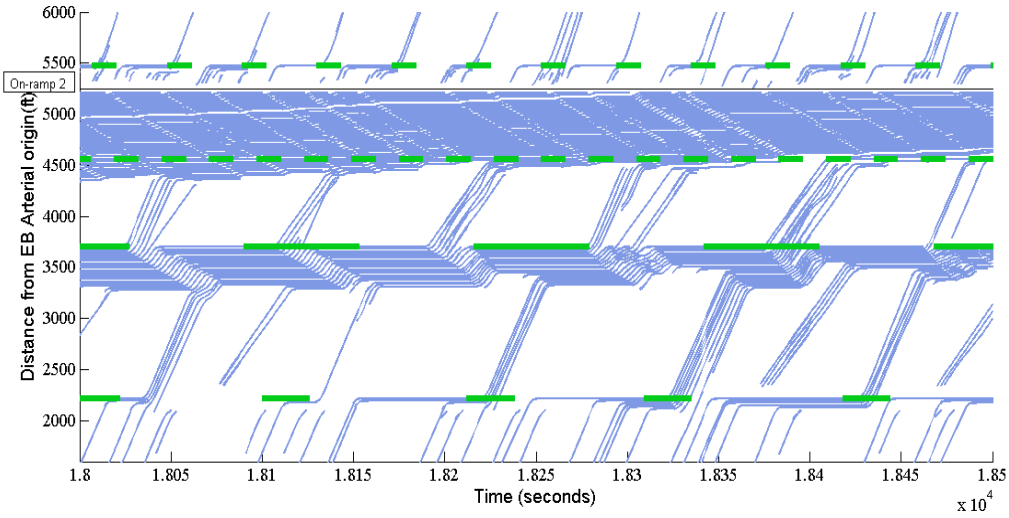

b. Scenario II

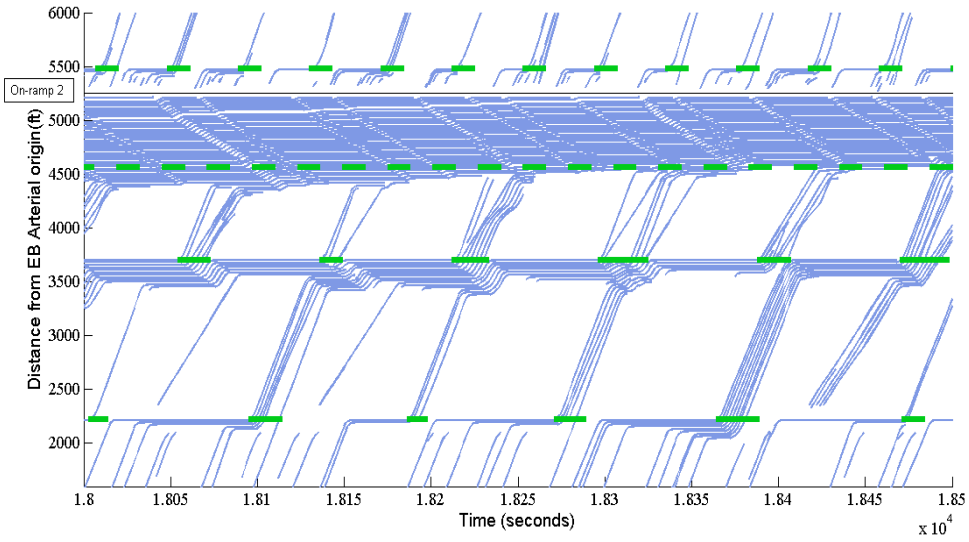

c. Scenario III

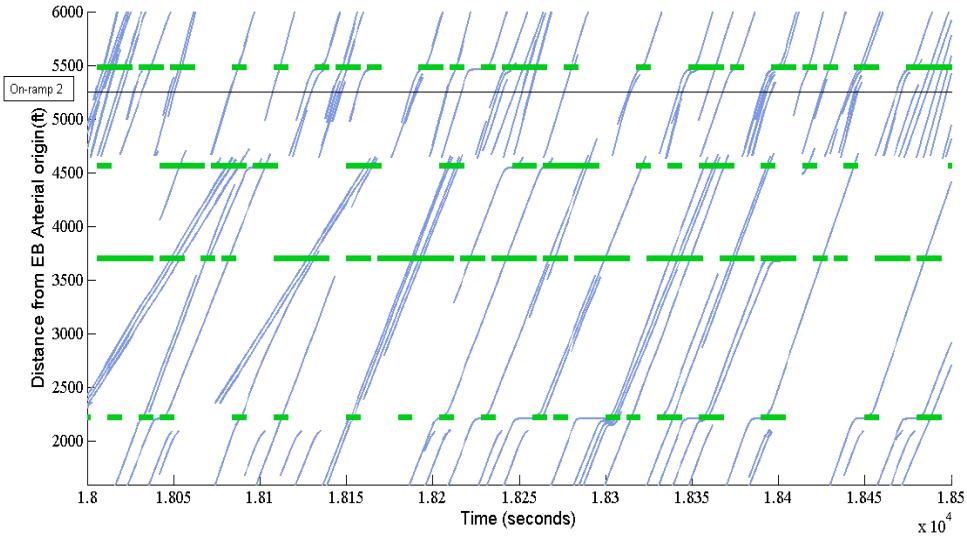

d. Scenario IV

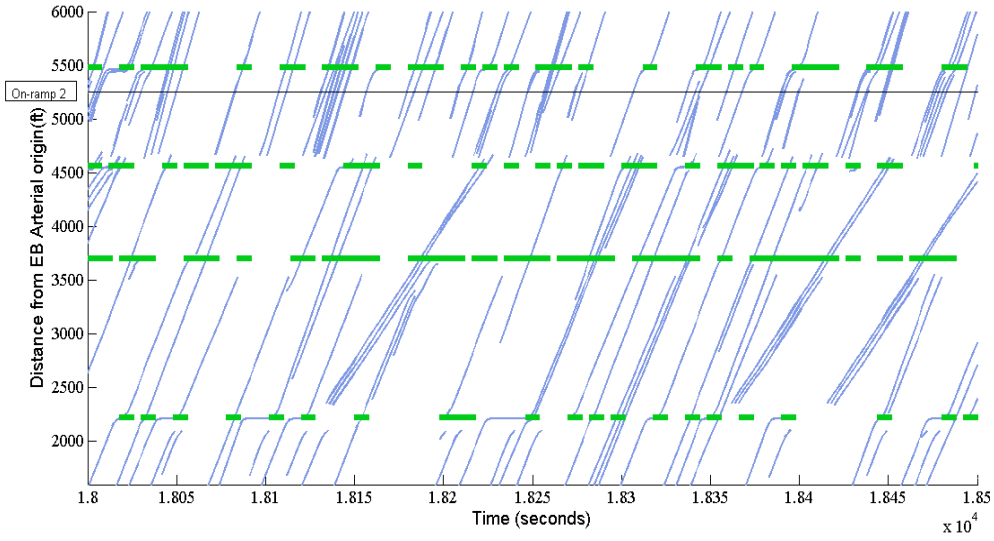

e. Scenario V

Figure 80: Vehicle trajectories for An Eastbound Arterial Lane

4.4.6 Latent Demand for each Scenario in the Simulated Network

Figure 81 shows the latent demands during the study period for each scenario. It is observed that the latent demand remains the minimum for scenario I. However, all scenarios are successful in diminishing the latent demand before the end of the study period.

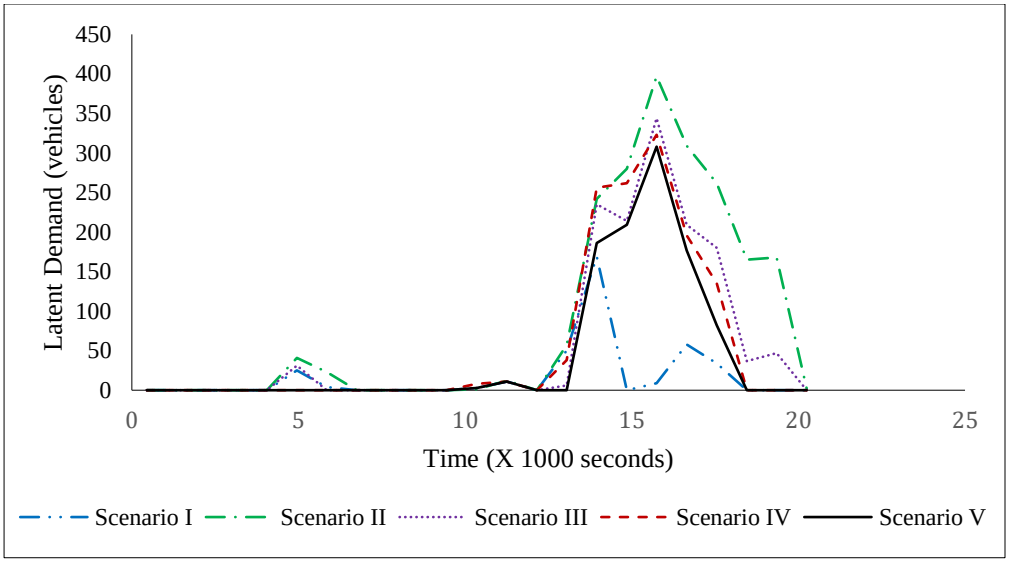

Figure 81: Latent Demand during the Study Period for each Scenario

Among the optimal controls, latent demand is lowest for the integrated control, and it can clear up any latent demand before five hours of the study period.

4.5 Conclusion

The study develops an integrated signal and metering control framework that optimizes signal timings and ramp metering timings simultaneously to improve the corridor performances. The optimization program is a mixed integer linear model (MILP) that sets optimal signal timings and metering decisions to maximize the completed number of trips over a prediction horizon. The model is incorporated inside a model predictive control framework that optimizes timings at each timestep, implements it, proceeds to next timestep, and repeats the process until the end of study period. The average run-time of the program for two minutes and five minutes of prediction periods are 0.8 seconds and 4.4 seconds, respectively. Using a cell transmission model resolution of six seconds, the optimization program can be implemented in real-time.

The integrated control framework together with four other benchmarking scenarios is tested in VISSIM simulation. The results show that the integrated control outperforms the existing signal control with preset metering significantly. The average delay, average stops, travel times is reduced by 33%, 36%, and 16%, respectively when compared to existing condition. Also, the highest number of completed trips (79618 vehicles) is achieved in integrated control. While improving the overall corridor level performances, the integrated control is successful in reducing the delay of a highly congested arterial by 79% with a minimum increase of the freeway delay of 5% as compared to existing condition. In other performance measures, the integrated control also performs efficiently when compared to benchmarks.

Overall, the study develops a promising methodology that integrates all signal control and metering control devices to jointly work together and achieve an efficient corridor network. However, the study still needs to address some limitations which are left for future studies. The

study assumes a full connectivity in the corridor as vehicle location coordinates are mapped precisely. Thus, accurate cell occupancy data are used in the optimization model. Nevertheless, a driving environment with partially connected vehicles will create complexities in estimating cell occupancies for cell transmission model. Uncertainty in mapping vehicle locations need to be addressed in future research. Besides, mixed driving scenarios with connected and automated vehicles is another challenge for the study.

In our study, the cycle time and signal phases are kept flexible. No specific phase sequence is maintained, and cycle times are free. The study can be extended to comply with specific phase sequences and cycles times. Another important limitation of the study is that there are no specific weights to different directional movements. This causes an equity issue as vehicles on the side streets experience higher delays. Such inequity can be avoided by assigning proper weights directional movements. Lastly, the methodology may need to be tested for a larger corridor network with high resolution of cell transmission model to have further insights into developing efficient optimization framework.

5 MACHINE LEARNING FOR PLAN ACTIVATION

5.1 Introduction

As stated earlier, in most cases, ramp metering restricts the vehicles from entering the freeway. This restriction improves the mainline freeway operations but can result in long queues on the on-ramps. These queues can fill the ramp at the peak period and spillback to the feeding intersecting arterials. The spillback from the ramps can disrupt the intersecting arterial operations and reduce their capacities. Most existing adaptive ramp metering algorithms have a queue override feature to relax the ramp metering control by increasing the metering rate when the queue approaches the upstream end of the ramp. However, this relaxation of the metering rate can reduce the effectiveness of this strategy in mitigating congestion on the freeway mainline. In addition, this queue override feature is generally reactive, and the dissipation of the access ramp queue length and the spillback to upstream intersections can take some time.

Given the above, a strategy that predicts the queue spillback before it occurs can effectively reduce the impact of the ramp queues. Suppose the spillback to upstream intersections can be predicted before it occurs in real-time operations. In that case, it will be possible to implement an integrated signal timing and ramp metering control strategy such as those presented in Chapters 3 and 4 to reduce the probability of queue spillback.

The potential actions to address the forecasted spillback do not only involve relaxing the ramp metering rate but also constraining the vehicles from entering the on-ramp(s) by modifying the signal timing parameters of upstream signal(s) on the intersecting arterial streets. Managing vehicle entry to the ramp through upstream signals can reduce the queue spillback from the ramp with less impact on ramp metering operations, improving the operations of the arterial, ramp, and freeway segments. However, queue spillback is stochastic and does not happen every day and at the same time within the peak period. A signal timing plan to mitigate spillbacks should be activated only for those periods when there is a potential for queue spillback. This research develops and investigates machine learning-based approaches to predict the drop in capacity at signalized intersections caused by queue spillbacks from the on-ramps due to ramp metering two signal timing cycles before such drops in capacity. Such prediction can be used as an important component of proactive management strategies to reduce the impacts of queue spillbacks.

5.2 Study Network

The study network of this research is a segment of Southbound I-95, the intersecting arterial street (NW 119th St), and the on-ramp from NW 119th St to Southbound I-95 in Miami-Dade County, Florida, as shown in Figure 82. Detailed analysis of the queue detector data at the upstream end of the on-ramp indicates frequent queue backups during the peak period. The ramp metering signals are activated in the morning peak for the southbound direction of I-95 in Miami-Dade County. The NW 119th St links upstream of the on-ramp have high demands, particularly in the eastbound direction during the AM peak. Data are available for the modeled facility, including high-resolution controller data and estimated travel times based on crowdsourced data from a private sector vendor (HERE) are available for NW 119th St. Volume, occupancy, and speed for the I-95 mainline and on-ramp detector measurement are available, as archived in the Regional Integrated Transportation Information System (RITIS). Another available dataset is an archive of the ramp metering rates implemented by the adaptive ramp metering obtained from the traffic management center of the Florida Department of Transportation, District 6. The research team obtained the data available from the above sources for use in the preparation, calibration, and validation of the traffic simulation model to replicate the real-world scenario.

Figure 82 Study network in Miami, FL

5.3 Methodology

This research aims to predict the reduction in capacity at upstream signalized intersections due to spillback from metered on-ramps, two signal timing cycles before such capacity reductions occur. The research explored using two categories of machine learning techniques. The first category utilizes classification machine learning techniques that predict a range of the

drop in capacity as a categorical variable rather than a specific value for the drop in capacity. The second category utilizes machine learning techniques that predict specific values for the drop as a continuous variable. Machine learning requires a large amount of data to train and test the developed models. In the absence of good quality and detailed data for all possible scenarios, a well-calibrated traffic microscopic simulation model can be used to generate the required data. An advantage of the use of simulation models is that they can also be used to test the benefits of the application of traffic control strategies in response to the predicted drop in capacity. Thus, this research used a microscopic model that had been well calibrated for the case study facility using high-resolution controller data in combination with the commonly used traffic data like travel times and volumes in a previous study using a multi-objective optimization technique. The details of the calibration of the model developed for the case study are presented by Tariq et al. in (Tariq et al., 2021). The evaluation of this calibrated model showed that the proposed optimized technique based on high-resolution controller improved the calibration process (Tariq et al., 2021). The model was developed using VISSIM (PTV AG, Karlsruhe, 2021). The research team conducted further examination of the model demands and signal timing based on information obtained from an FDOT report on the corridor operations (Brusa et al., 2018).

Figure 83 shows the framework of the utilized methodology to generate the required data from the simulation model and to use the data in developing and testing the machine learning models. The obtained data from simulation includes travel time measurements that emulate data obtained from a third-party vendor or vehicle matching technology like Bluetooth readers. In addition, the obtained data from simulation includes high-resolution controller data that is used to calculate measures like green occupancy ratio (GOR) and turn movement volume counts. Other data obtained from the simulation are occupancy and volume measurements from the queuing detectors located at the upstream end of the metered ramps and the passage detectors located downstream of the ramp metering stop line. As shown in Figure 83, the study investigated two variations. The first variation includes the GOR and occupancy of the upstream movements that feed the on-ramp, flow rate and occupancy of the on-ramp queue detector and the passage detector, and flow rate and travel time of the arterial segments upstream of the on-ramp. Significant increases in GOR and travel time due to capacity reduction may not happen until the reduction in capacity occurs. Thus, they may not be ideal for forecasting congestion. This consideration led the researchers to develop a second variation of models that excluded these two variables.

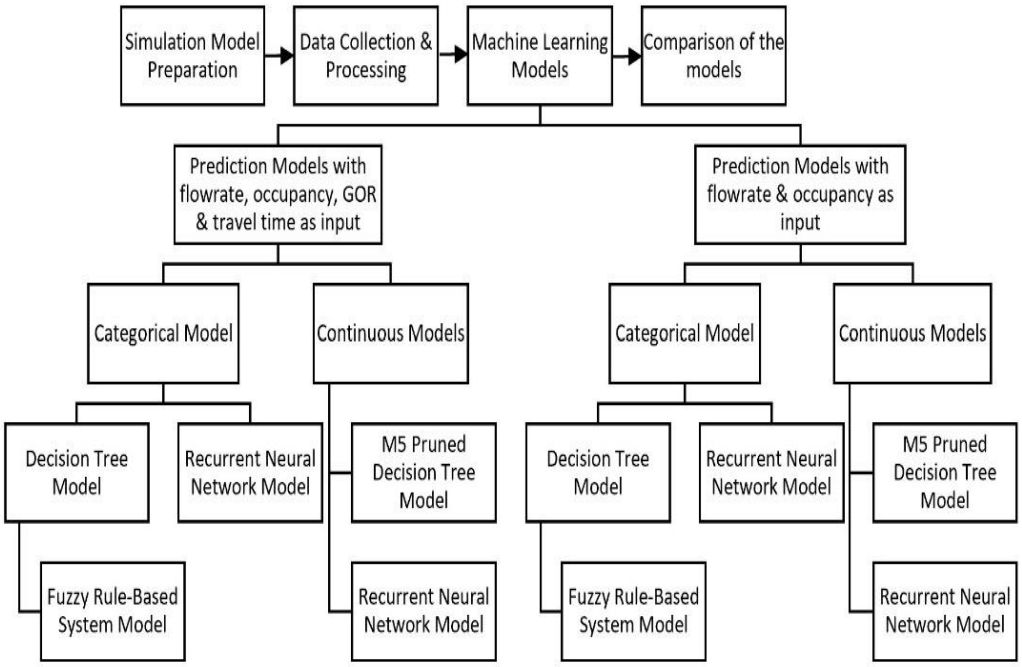

Figure 83 Methodology framework

As indicated in Figure 83, the study compared two types of categorical models. The first type is a decision tree (DT) model combined with a fuzzy rule-based system (FRBS). The decision tree identified the significant variables and their contribution in predicting the category of the capacity reduction rate. The method converted the results from the decision tree into crisp rules, which might affect the accuracy of the findings considering the uncertainty associated with rules. For this reason, this study converts the decision tree's output to fuzzy rules by identifying the fuzzy set membership functions in FRBS model based on the crisp rules from the decision tree. The second categorical model used a recurrent neural network (RNN) to predict a time series of capacity reduction considering the temporal effect of the input variables over time. This study also used two types of machine learning for the continuous models that predict capacity reduction as a continuous variable. The first type is M5 pruned (M5P) decision tree model, which can have multivariate linear equations at their leaves, improving the model's prediction capability. The second type utilizes the RNN to estimate the time series dataset of the capacity reduction rate at the upstream intersection, as a continuous variable.

5.4 Data Generation from Simulation

The study used the outputs from the calibrated microscopic simulation model to estimate performance measures to use as inputs for the machine learning algorithms. The midblock traffic flow rates and occupancy data were collected using the 'Data Collection Point' feature in the VISSIM software for the eastbound (EB) and westbound (WB) movement of the intersection of NW 119th St at NW 7th Ave, and the intersection of NW 119th St at NW 6th Ave. The real-world and simulation data examination indicates that the capacity of the EB

through movement of the NW 119th St and NW 7th Ave intersection decreased with the queue spillback from the on-ramp to the upstream arterial intersection. For this reason, the flow rate and occupancy in the EB direction of NW 119th St was collected from data collection points representing traffic sensors at further upstream intersections to reflect the demand of the traffic flow in the eastbound direction since the volumes at the NW 7th Ave intersection can be constrained by the spillback and this does not reflect demands. This study also collected flow rate and occupancy measurements from data collection points located in the simulation at the real-world locations of the ramp queue detector and passage detector on the metered ramps. The travel times of EB and WB movement were generated using the 'Vehicle Travel Time' feature in VISSIM. Besides these data, the study calculates the GOR measures for each turning movement using high-resolution controller data from the simulation. GOR is defined as the stop bar detector occupancy during the green interval (Day and Bullock, 2010). As the GOR value increases, the utilization of the green time also increases.

The machine learning prediction is made at two cycle intervals in this research. Thus, all measures calculated from the simulation that are used as inputs to the models were generated for an interval of two cycles (a total of 290 seconds). All the generated variables including GOR of EB and WB directions, total and right lane flow rate of EB direction, travel time up to one upstream intersection and up to two upstream intersections of EB direction, total and left lane flow rate of WB direction, travel time up to one upstream intersection of WB direction, flow rate and occupancy of ramp queue detector, and flow rate and occupancy of passage detector were used as independent or input variables for the machine learning models.

The goal of the developed machine learning models is to predict the capacity reduction rate of the EB direction at the intersection of NW 119th St and NW 7th Ave due to queue spillback from the ramp to the feeding arterial since field observations and examination of real-world data indicate that the reduction in capacity occurs mainly for this movement. This capacity reduction rate was calculated as follows:

$$\text{Capacity Reduction Rate} = \frac{Base\ Capacity\ - Capacity\ during\ spillback}{Base\ Capacity} \quad (23)$$

This analysis selected the threshold value of the GOR that indicates spillback as 0.9 and the base capacity as 575 vehicles per hour (veh/hr) based on the fundamental diagram of the flow rate vs. GOR for the EB movement at the NW 7th intersection, generated based on the high-resolution controller data from the simulation model as shown in Figure 84. The maximum capacity in the diagram is around 575 vehicles per hour and occurs around a GOR of 0.9. At GOR values higher than 0.90, Figure 84 shows that the maximum throughput starts decreasing reaching values close to 230 veh/hr due to the spillback impact.

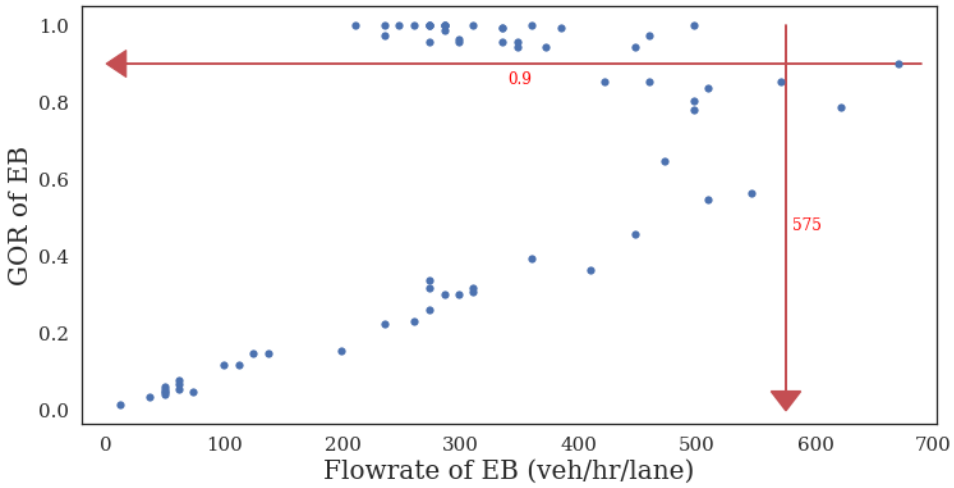

Figure 84 Fundamental diagram of the eastbound direction of NW 119th Street Intersection with NW 7th Ave (Note: The arrows in the figure indicate the estimated capacity of the movement and the corresponding GOR)

For the categorical models, the capacity reduction rate calculated according to Equation 1 was classified into three distinct categories with intervals of zero to 0.2, 0.2 to 0.5, and 0.5 to 1. These categories of capacity reduction rate are referred to in this paper as Category 1, Category 2, and Category 3, respectively, and were selected based on the examination of the fundamental diagram.

5.5 Machine learning Model Development

This section describes the development of the models developed to predict the capacity reduction rate at upstream intersection movements due to queue spillback from metered ramps. The study randomly selected 80% of the dataset generated using the simulation model to train the model and 20% to test the model.

5.5.1 The Decision Tree (DT) Model

The study utilized a classification and regression trees (CART) algorithm to develop a decision tree model to predict capacity drop as a categorical variable. CART creates binary trees by using the threshold and the features that result in the most significant information gain at each node. The decision tree model was developed using a python programming language with the SKlearn library. When developing the model, the Gini Index was applied as the decision tree classifier's criterion to measure the input set's impurity. This index measures the degree or probability of a particular variable being wrongly classified when it is randomly chosen (Tangirala, 2020). The range of the Gini Index can be zero to one, where zero means that all elements belong to a certain class, and one means that the elements are randomly distributed across various classes. A Gini Index of 0.5 denotes equally distributed elements into classes.

When all variables were used as inputs, the results of the decision tree development indicate that the most significant variables for predicting the category of the capacity reduction rate

were occupancy and flow rate of the ramp queue detector, and the travel time and green occupancy ratio (GOR) of the eastbound direction (the peak direction of travel on the case study arterial in the analyzed period). When excluding the GOR and travel times from the set of input models, as discussed earlier, the significant variables were the occupancy measurements of the ramp queue detector and the passage detector.

5.5.2 Fuzzy Rule-Based System (FRBS) Model

The output of the decision tree model was then used to identify the fuzzy membership functions and rules in the FRBS model based on the Mamdani Fuzzy model (Dubois and Prade, 1980). The resulting decision tree structure was first converted into crisp (if-then) rules (Hall and Lande, 1996). Table 22 shows the converted crisp rules from the decision tree models to predict the category of the capacity reduction rate, first using the GOR, travel time, flow rate, and occupancy as inputs and then using only the flow rate and occupancy as inputs. From the output of the DT model, the threshold value of the occupancy of the ramp queue detector that indicates significant spillback impacting intersection movement capacity is 22.7% since this value separates low-capacity reduction rate (Category 1) from moderate to high capacity reduction rate (Categories 2 and 3). The difference between Category 2 (capacity reduction rate is from 20% to 50%) and Category 3 (capacity reduction rate is higher than 50%) is that Category 2 has travel time of the eastbound direction less than or equal to 36.8 seconds or the GOR of the eastbound direction less than or equal to 0.97. When using only flow rate and occupancy as inputs, there are two rules to obtain Category 1 and 2, and one rule to obtain Category 3 based on the occupancy of ramp queue detector and passage detectors, as shown in Table 22.

Table 22 Crisp Rules from the Decision Tree Model to Predict Capacity Reduction as a Categorical Variable

Category	Rules
Crisp Rules from DT Model with all variables as inputs	
1	if Oc_rq ≤ 22.7
2	if Oc_rq > 22.7 & Fl_rq ≤ 726 & TT_eb ≤ 36.8
2	if Oc_rq > 22.7 & Fl_rq > 726 & G_eb ≤ 0.97
3	if Oc_rq > 22.7 & Fl_rq ≤ 726 & TT_eb > 36.8
3	if Oc_rq > 22.7 & Fl_rq > 726 & G_eb > 0.97
Crisp Rules from DT Model with excluding GOR and travel times from inputs	
1	if Oc_rq ≤ 22.7
1	if Oc_rq > 22.7 & Oc_rq ≤ 49.2 & Oc_rq > 40.9 & Oc_p > 17.5
2	if Oc_rq > 22.7 & Oc_rq ≤ 49.2 & Oc_rq ≤ 40.9
2	if Oc_rq > 22.7 & Oc_rq ≤ 49.2 & Oc_rq > 40.9 & Oc_p ≤ 17.5
3	if Oc_rq > 22.7 & Oc_rq > 49.2

where,
Oc_rq= Occupancy of the ramp queue detector (sec)
Oc_p= Occupancy of the passage detector (sec)
Fl_rq= Flow rate of the ramp queue detector (veh/hr)
TT_eb= Travel time up to two upstream intersections of eastbound direction (sec)
G_eb= GOR of eastbound direction

The FARBS model was developed using the Fuzzy Logic Toolbox of MATLAB (The MathWorks Inc., 2022). Each membership function in the fuzzy logic models has parameters and shapes for both the input and output variables (Lee, 1990). This study applied the most widely used shapes, the triangular and trapezoid shapes, for the input and output variables. The crisp rules in Table 22 were used to set the parameters and threshold values of the membership functions. The defuzzification process was done to obtain crisp values from the fuzzy output set using the weighted average method in the defuzzification.

5.5.3 Recurrent Neural Network (RNN) Model

RNN is an advanced machine learning method for time series data that utilizes the temporal effect of the input variables over time through a hidden layer. Long Short-Term Memory (LSTM) based RNN performs better than traditional RNNs on tasks involving long time lags (Hochreiter, 1997). The LSTM unit consists of three gates: forget gate layer, input gate layer, and output gate layer. How much of the previous data will be forgotten and how much of the previous data will be used in next steps is decided by the forget gate layer (Akin et al., 2019). The output of this forgets gate falls between 0 and 1, with "0" forgetting the preceding data and "1" using it.

This study used the Python programming language with Keras library and Tensorflow library in the backend to train and validate the RNN model. In this study two different LSTM-based RNN models were developed. The first RNN model predicts the category of the capacity reduction rate, and the second model predicts the capacity reduction rate, as a continuous variable. For the RNN model that predicts the category of the capacity reduction rate, the loss function of the RNN model was set to the 'sparse_categorical_crossentropy' in the utilized libraries, as commonly used in the development of classification models that predict categorical variables (Gultepe and Duru, 2019). In this loss function the cross-entropy loss ranges between 0 and 1 (Liu et al., 2020). As the predicted probability value departs from the actual value, the cross-entropy loss increases. The utilized tool fine-tuned the hyper parameters of the model to optimize the loss function value, targeting the achievement of the best results in the prediction. The optimal batch size for feeding input was found to be ten for 200 epochs. For the second RNN model that predicts the reduction in capacity as a continuous variable, the loss function for predicting the capacity reduction rate on the arterial utilized in this study was the root mean squared error (RMSE). The optimal batch size for feeding the input was found to be thirty-two for 500 epochs. All the data were normalized using the max-min normalization for both types of RNN models.

5.5.4 M5 Pruned (M5P) Decision Tree Model

This study also used the M5P decision tree model to predict the capacity reduction rate as a continuous variable. M5P decision tree models produced two linear regression equations at the leaf nodes associated with two different rules. Table 23 shows that when considering all variables as inputs, the M5P model includes a regression equation for the situation when the

occupancy of the ramp queue detector is less than or equal to 22.7%. This equation is based on the occupancy of the ramp queue and passage detectors, and the GOR of the eastbound and westbound movements. When occupancy of the ramp queue detector is greater than 22.7% indicating a higher congestion on the ramp, the variables of the regression equation are the GOR of the eastbound movement, travel time of the eastbound and westbound movements, and the occupancy of the ramp metering passage detector. The second prediction model, prepared using only the flow rate and occupancy variables as inputs as shown in Table 23, generated two linear model equations at the leaf node corresponding to two different rules based on the occupancy of the ramp queue detector. In this case when the occupancy of the ramp queue detector is less than or equal to 22.7%, the variables of the linear regression equation to predict capacity reduction rate are occupancy of the ramp queue detector and the passage detector. On the other hand, when the occupancy of the ramp queue detector is greater than or equal to 22.7%, the variables in the linear regression equation are the volume of the ramp queue detector, total eastbound direction, and total eastbound right lane.

Table 23 Rules produced using the M5P Decision Tree Model

M5P decision tree model with all variables as inputs	**M5P decision tree model with excluding GOR and travel times from inputs**
Rule: 1 **If**, Occupancy_RQ <= 22.7 **Then**, CapRed_rate = - 0.0027 + 0.0314 * GOR_EB + 0.0538*GOR_WB + 0.0007 * Occupancy_RQ - 0.0015*Occupancy_P **Rule: 2** **If**, Occupancy_RQ > 22.7 **Then**, CapRed_rate = - 0.5885 + 0.6464 * GOR_EB + 0.0004 * TT_EBR_alt_prev + 0.0252 * TT_WBL_prev - 0.0423 * Occupancy_P	**Rule:1** **If,** Occupancy_RQ <= 22.7 **Then,** CapRed_rate = - 0.0031 + 0.0012 * Occupancy_RQ - 0.0009 * Occupancy_P **Rule: 2** **If,** Occupancy_RQ > 22.7 **Then,** CapRed_rate = 0.8472-0.0009 * Flowrate_RQ + (0.0008 * Flowrate_EB_D - 0.0023 * Flowrate_EBR_D)

where,
CapRed_rate= Capacity Reduction Rate
Occupancy_RQ= Occupancy of the ramp queue detector (sec)
Occupancy_P= Occupancy of the passage detector (sec)
GOR_EB= GOR of eastbound direction
GOR_WB= GOR of westbound direction
TT_EBR_alt_prev= Travel time up to two upstream intersections of eastbound direction (sec)
TT_WBL_prev= Travel time up to one upstream intersection of westbound direction (sec)
Flowrate_RQ= Flow rate of the ramp queue detector (veh/hr)
Flowrate_EBR_D= Flow rate of the eastbound right lane (veh/hr)
Flowrate_EB_D= Flow rate of the eastbound direction (veh/hr)

5.6 Model Testing

The trained categorical prediction models (DT, FRBS and RNN) were evaluated using the test dataset based on the Precision, Recall, F1-Score, and overall accuracy. Precision is the number of true positive results divided by the number of all indicated positive results (sum of true positive and false positive), as shown in Equation 24. A perfect Precision score of 1.0 means that every produced result is true.

$$\text{Precision} = \frac{True\ Positive}{True\ Positive + False\ Positive} \quad (24)$$

Recall is the number of true positive results divided by the number of all samples that should have been identified as positive, as indicated in Equation 25. A perfect Recall score of 1.0 means that all true instances are identified.

$$\text{Recall} = \frac{True\ Positive}{True\ Positive + False\ Negative} \quad (25)$$

The F1-Score is a measure of a test's accuracy and is calculated as the weighted harmonic mean of the Precision and Recall. The value of F1-score ranges from 0 to 1, where high values of F1-score indicate good classification performance (Tharwat, 2018). F1-score is estimated using the following equation:

$$\text{F1-score} = 2 * \frac{Precision * Recall}{Precision + Recall} \quad (26)$$

Accuracy (Tharwat, 2018) is the ratio between the correctly predicted instances and all the instances in the dataset, as presented in Equation 27:

$$\text{Accuracy} = \frac{True\ Positive + True\ Negetive}{True\ Positive + True\ Negative + False\ Positive + False\ Negative} \quad (27)$$

The evaluations of the continuous models (M5P decision tree and RNN) use two different performance measures: the root mean squared error (RMSE) and the mean absolute error (MAE).

5.7 Model Evaluation Results

Table 24 shows the test results of the categorical models using Precision, Recall, F1-Score and Accuracy measures. From Table 24, the performance of the models was similar in the case of using all variables as input and the case with excluding the GOR and travel time from the input. The LSTM-based RNN models gave the highest values of these parameters in both cases (when using all parameters and subset of the parameters as inputs). The FRBS model showed improvement over the basic DT model only when excluding GOR and travel time.

Table 24 Comparison of the Performance of the Categorical Models

	Weighted Average	Accuracy

		Precision	Recall	F1-score	
Prediction models with all variables as inputs	**DT**	0.93	0.89	0.90	0.89
	FRBS	0.91	0.89	0.90	0.89
	RNN	0.98	0.97	0.97	0.97
Prediction models with excluding GOR and travel time from input	**DT**	0.92	0.86	0.88	0.86
	FRBS	0.94	0.93	0.93	0.93
	RNN	0.98	0.97	0.97	0.97

Comparison among the continuous models to predict the capacity reduction rate as a continuous variable (M5P decision tree and RNN) is shown in Table 25. Better results were obtained when using all variables in the model. The RNN produced the best results both when excluding the GOR and travel time from the input of the model and when including these two variables compared to the M5P decision tree models.

Table 25 Comparison of the Continuous Models

		RMSE	MAE
Prediction models with all variables as inputs	**M5P Decision Tree**	0.024	0.012
	RNN	0.024	0.008
Prediction Models with excluding GOR and travel Time from Input	**M5P Decision Tree**	0.082	0.032
	RNN	0.028	0.009

Figure 85 shows an example of a time series of ground truth capacity reduction rates obtained from a simulation model run versus a time series of the predicted capacity reduction rate as a continuous variable using the M5P and RNN models. The capacity reduction rate is predicted for two cycles in the future. Figure 85 shows that both M5P and RNN models were able to predict the increment of capacity reduction rate for the provided example.

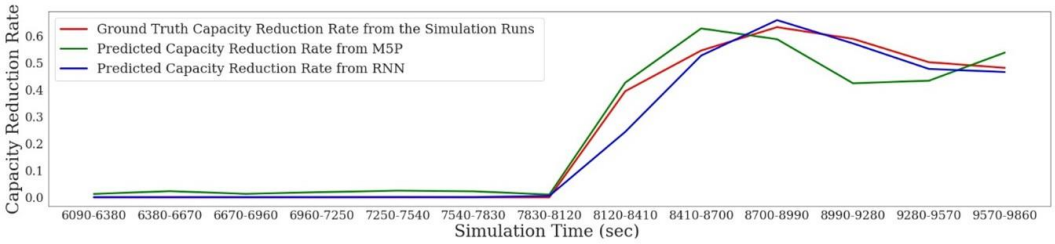

a) M5P and RNN model with all variables as inputs

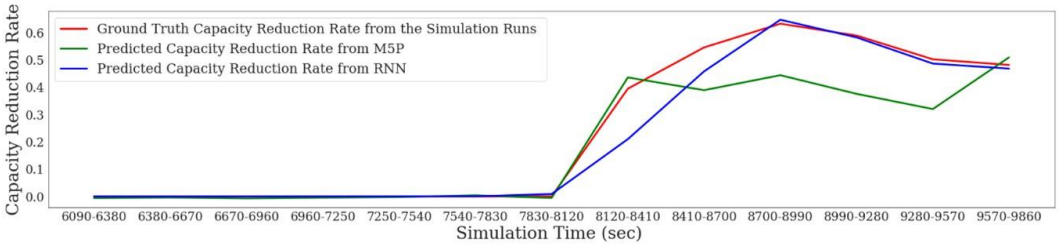

b) M5P and RNN model with excluding GOR and travel times from inputs

Figure 85 Time series of the capacity reduction rate for continuous prediction models

5.8 Comparison of Continuous and Categorical RNN Models

The RNN models produced the best results in predicting the capacity reduction rate in the case of expressing this rate as a categorical variable as well as the case of expressing the rate as a continuous variable. This section includes a comparison of the performance of the RNN models for these two cases. For a fair comparison, the evaluation is conducted one time to determine how far the prediction is from the ground truth category of the capacity drop and the second time how far the prediction is from the ground truth value of the capacity drop as a continuous variable. To achieve this comparison, the output of the categorical output model was converted to continuous values using the median value of each category. The output of the continuous RNN model was converted to categorical values by using the same category intervals used when developing the categorical models. The comparison was based on the mean absolute percentage error (MAPE) and category prediction accuracy measure.

When using the continuous value as the criterion to predict the capacity drop, Table 26 shows that the RNN models that predict the capacity rate as a continuous variable have only 7.4% and 8.6% errors depending on whether all the variables or a subset of the variables are used as inputs. Using the median values of the categorical model outputs result in 24.7% and 25.0% errors, respectively. When evaluating based on the prediction of the category of the capacity drop, the prediction accuracy was similar when comparing the results of the continuous and categorical RNN models, as shown in Table 26.

Table 26 Comparison of the Categorical RNN Model and Continuous RNN model

		Mean Absolute Percentage Error	Category Prediction Accuracy
Prediction models with all variables as inputs	**Continuous RNN Model Outputs**	7.4 %	96.8 %
	Median of Categorical RNN Model Outputs	24.7 %	99.4 %
Prediction models with excluding	**Continuous RNN Model Outputs**	8.6 %	95.5 %

GOR and travel times from inputs	**Median of Categorical RNN Model Outputs**	25.0 %	98.1 %

5.9 Conclusions

Five machine learning algorithms were developed and compared in this study. Three algorithms (decision tree, FRBS, and LSTM-based RNN) predict capacity drop as a categorical variable. Two additional algorithms (M5P decision tree and LSTM-based RNN) were used to predict capacity reduction as a continuous variable. From this study continuous models provide better prediction of capacity reduction rate, compared to categorical models. In addition, the LSTM-based RNN models produced better results than the other models tested in this study The findings of this study can be used to conduct additional research to activate signal timing plans to prevent capacity drop and to integrate signal timing models with ramp metering models.

6 CONCLUSION AND RECOMMENDATIONS

6.1 Conclusion

The study develops two control strategies that aim to reduce queue spillback effects from on-ramps to the upstream roads and improve the freeway-arterial street network performance. The first strategy can be considered as a traffic responsive strategy since the signal timing plans are developed off-line and stored in a library to select from when spillback occurs or is predicted. The second can be considered as an adaptive signal control strategy since it calculates the signal timing plan in real-time when activated. In addition to these strategies, this study developed machine learning based models that can predict capacity reduction due to queue spillbacks from on-ramps. An integrated control framework is proposed to combine these three methods for use in real-time to improve the corridor performance, particularly when on-ramp queues are predicted to spill to upstream arterial intersections.

Firstly, a traffic responsive methodology is proposed to mitigate the effect of queue spillback from the on-ramp to the affected upstream signalized intersections of the connected arterial road. The method involves the determination of oversaturated locations followed by balancing of queue lengths while improving the network performance through the adjustment of ramp metering and/or signal controllers at the affected upstream intersections. Three case studies were conducted to test the method using microsimulation. The intended objectives were achieved using the method. Although there was an improvement in the overall network performance in terms of average speed and total travel time per vehicle, there were some tradeoffs of delay, queue lengths and better operations of the freeway segment. Also, it is important to select a scope area since the methodology does not solve bottlenecks outside the scope section.

This study also developed an adaptive traffic control methodology for joint signal timing and ramp metering rate optimization for corridor networks. The methodology was based on mathematical programming, which was solved and implemented in real-time by using Model Predictive Control. The average computation time of the optimization program is 4.4 seconds with five minutes of prediction period and 0.84 seconds with two minutes of prediction period. Therefore, the methodology can be implemented in real-time using a cell transmission model resolution of 6 seconds. The findings in San Mateo, CA show that the integrated control can outperform existing benchmark condition significantly. Specifically, the integrated control reduces average delay, average stops, travel times by 33%, 36%, and 16%, respectively when compared to existing control condition. Also, it reduces highly congested arterial delay by 79% with an increase of the freeway delay of 5%. While the optimal signal control reduces arterial delay by 88% at the expense of 19% increase in Freeway delay, optimal signal control has 12% more delay in freeway than Integrated control. Overall, the integrated control improves and balances the overall congestion condition from the benchmarks.

The study developed models that can predict capacity drop at upstream signalized intersections due to spillbacks from metered on-ramps. The study can make this prediction two cycle lengths ahead of time to allow ample time for implementing remedial actions. This study developed and compared five machine learning algorithms. Three algorithms predict the capacity drop as a categorical variable. These algorithms are classification decision tree, FRBS, and LSTM-based RNN. Two additional algorithms were used that predict capacity reduction as a continuous variable, which are M5P decision tree and LSTM-based RNN. The models developed to predict the reduction in capacity as a continuous variable could provide better prediction of the capacity reduction compared to the categorical models. In addition, the LSTM-based RNN models produced better results than the other models tested in this study. Excluding GOR and travel time variables from the input did not change the performance of the RNN models. The research presented in this paper can be used for further research to activate signal timing plans to prevent capacity drop and to integrate signal timing models with ramp metering models.

It can be concluded thar the proposed methodologies to mitigate the effect of queue spillback are more effective when:

- The selected scope area includes a merge/on-ramp and the intersecting arterial with as many signalized intersections as may be affected by the spillback.
- The study period covers the onset of oversaturation to dissipation.
- The selected scope involves either an on-ramp entrance bottleneck or a freeway merge bottleneck resulting to queue back up to the intersections of the connected road.
- The typical values for maximum and minimum green times given in the Chapter 10 of FHWA Signal Timing Manual are taken into consideration while adjusting the signal controllers at the affected signalized intersections.
- The demand proportions of different are approaches are used to guide the signal timing plan adjustments.
- The constraints of capacity of the on-ramp or the freeway merge are taken into account.

6.2 Recommendations

It is recommended that the two control strategies and the machine-learning-based predictive models are integrated in a real-time decision support tool for use in traffic management center operations. The decision support tool would monitor the traffic performance on the freeway mainline, freeway on-ramps, and the signalized intersections at the freeway interchanges. In addition, it would predict the potential drops in capacities due to spillbacks from on-ramps at least two cycles before they occur. Based on this monitoring and prediction, the decision support tool would suggest actions to implement the traffic responsive strategy or traffic adaptive strategy developed in this study. It is recommended that this tool is implemented, tested, evaluated, and modified as necessary based on an implementation in real-world traffic management center application.

Future research can investigate the impact the queue spillback mitigation method has on traffic progression in segments with coordinated intersections. Also, future studies can consider expanding the scope area to resolve several bottlenecks. The traffic responsive methodology focused on manually calculating and changing the splits within the cycle length based on demands and expected throughputs to attain an improved network performance. Considering the splits, cycle lengths and offsets, and developing an algorithm to automate the generation of optimal values to achieve the optimal network performance is another area of future research.

As for the integrated control framework, the study finds that significant improvement happens when integrated control framework is implemented. Therefore, demand-responsive integrated control can greatly improve the traffic operations of the corridor. Apart from the findings, the study has some limitations which are kept for future research. As our approach does not consider any specific phase sequence and fixed cycle times, such constraints can be studied in the future. Another challenge for the future would be incorporating the effects of connected and automated vehicles in setting up integrated control framework. Lastly, a larger portion of the corridor can be studied with suitable methodology to have better insights into optimum signal timing and ramp metering solutions.

The prediction model developed in this research is location specific. The method used in this research can be used to prepare models for other on-ramp locations. However, it may be useful to test the developed models' transferability to locations with similar characteristics. The prediction interval in this study is two cycles in the future to allow time for the implementation of proactive management strategy. Further research is needed to investigate the reduction in capacity with longer prediction interval.

7 REFERENCE LIST

Akin, C., Kacar, U., Kirci, M., 2019. Twins recognition using hierarchical score level fusion, in: ArXiv, Cornell University.

Arnold, E.D., 1998. Report Ramp Metering: A Review of the Literature, Virginia Transportation Research Council.

Arun, A., Madhu, E., Velmurugan, S., 2016. Selection of a Suitable Service Measure and Determination of LOS Criteria for Indian Multilane Interurban Highways: A Methodological Review. Transp. Dev. Econ. 2, 1–12. https://doi.org/10.1007/s40890-016-0021-x

Bellemans, T., De Schutter, B., De Moor, B., 2006. Model predictive control for ramp metering of motorway traffic: A case study. Control Eng. Pract. 14, 757–767. https://doi.org/10.1016/j.conengprac.2005.03.010

Bhouri, N., Haj-Salem, H., Kauppila, J., 2013. Isolated versus coordinated ramp metering: Field evaluation results of travel time reliability and traffic impact. Transp. Res. Part C Emerg. Technol. 28, 155–167. https://doi.org/https://doi.org/10.1016/j.trc.2011.11.001

Brusa, E., Calà, A., Ferretto, D., 2018. Operational analysis. Stud. Syst. Decis. Control 134, 115–145. https://doi.org/10.1007/978-3-319-71837-8_5

Carlson, R.C., Papamichail, I., Papageorgiou, M., Messmer, A., 2010a. Optimal Motorway Traffic Flow Control Involving Variable Speed Limits and Ramp Metering. Transp. Sci. 44, 238–253. https://doi.org/10.1287/trsc.1090.0314

Carlson, R.C., Papamichail, I., Papageorgiou, M., Messmer, A., 2010b. Optimal mainstream traffic flow control of large-scale motorway networks. Transp. Res. Part C Emerg. Technol. 18, 193–212. https://doi.org/https://doi.org/10.1016/j.trc.2009.05.014

Cassidy, M.J., Anani, S.B., Haigwood, J.M., 2002. Study of freeway traffic near an off-ramp. Transp. Res. Part A Policy Pract. 36, 563–572. https://doi.org/10.1016/S0965-8564(01)00016-7

Cheng, Y., Chang, G.L., 2021. Arterial-friendly local ramp metering control strategy. Transp. Res. Rec. 2675, 67–80. https://doi.org/10.1177/0361198121994581

Comert, G., Khan, Z., Rahman, M., Chowdhury, M., 2021. Grey models for short-term queue length predictions for adaptive traffic signal control. Expert Syst. Appl. 185, 115618. https://doi.org/10.1016/j.eswa.2021.115618

CPLEX, I.B.M.I., 2009. V12. 1: User's Manual for CPLEX. Int. Bus. Mach. Corp. 46, 157.

Daganzo, C.F., 1995. The cell transmission model, part II: Network traffic. Transp. Res. Part B Methodol. 29, 79–93.

Daganzo, C.F., 1994. The cell transmission model: A dynamic representation of highway traffic consistent with the hydrodynamic theory. Transp. Res. Part B Methodol. 28, 269–287.

Day, C.M., Bullock, D.M., 2010. Final Report Volume 1 Performance Based Management of Arterial Traffic Signal Systems.

Dong, J., Lu, C., Liu, C., Hawkins, N., 2016. Assessing Segment- and Reliability on Urban Freeways.

Dubois, D., Prade, H., 1980. Fuzzy sets and systems: theory and applications. New York: Academic Press.

Elefteriadou, L., 2014. An Introduction to Traffic Flow Theory. https://doi.org/10.1007/978-1-4614-8435-6

Filipovska, M., Mahmassani, H.S., 2020. Traffic Flow Breakdown Prediction using Machine Learning Approaches. Transp. Res. Rec. 2674, 560–570. https://doi.org/10.1177/0361198120934480

Frejo, J.R.D., Camacho, E.F., 2012. Global Versus Local MPC Algorithms in Freeway Traffic Control With Ramp Metering and Variable Speed Limits. IEEE Trans. Intell. Transp. Syst. 13, 1556–1565. https://doi.org/10.1109/TITS.2012.2195493

Friedrich, M., 2016. Evaluating the Service Quality in Multi-modal Transport Networks. Transp. Res. Procedia 15, 100–112. https://doi.org/10.1016/j.trpro.2016.06.009

Geroliminis, N., Haddad, J., Ramezani, M., 2013. Optimal Perimeter Control for Two Urban Regions With Macroscopic Fundamental Diagrams: A Model Predictive Approach. IEEE Trans. Intell. Transp. Syst. 14, 348–359. https://doi.org/10.1109/TITS.2012.2216877

Gultepe, Y., Duru, A., 2019. Using Convolutional Neural Networks for Handwritten Digit Recognition, in: International Conference on Data Science, Machine Learning and Statistics - 2019 (DMS-2019), Turkey. pp. 305–307.

Haj-Salem, H., Papageorgiou, M., 1995. Ramp metering impact on urban corridor traffic: Field results. Transp. Res. Part A Policy Pract. 29, 303–319. https://doi.org/https://doi.org/10.1016/0965-8564(94)00034-8

Hajbabaie, A., 2012. Intelligent dynamic signal timing optimization program. University of Illinois at Urbana-Champaign.

Hajbabaie, A., Benekohal, R.F., 2011. Does traffic metering improve network performance efficiency?, in: 2011 14th International IEEE Conference on Intelligent Transportation Systems (ITSC). IEEE, pp. 1114–1119.

Hall, L.O., Lande, P., 1996. Generating fuzzy rules from data, in: IEEE International Conference on Fuzzy Systems. pp. 1757–1762. https://doi.org/10.1109/fuzzy.1996.552635

Han, Y., Ramezani, M., Hegyi, A., Yuan, Y., Hoogendoorn, S., 2020. Hierarchical ramp metering in freeways: An aggregated modeling and control approach. Transp. Res. Part C Emerg. Technol. 110, 1–19. https://doi.org/https://doi.org/10.1016/j.trc.2019.09.023

Hashemi, H., Abdelghany, K.F., 2016. Real-time traffic network state estimation and prediction

with decision support capabilities: Application to integrated corridor management. Transp. Res. Part C Emerg. Technol. 73, 128–146. https://doi.org/https://doi.org/10.1016/j.trc.2016.10.012

Hegyi, A., De Schutter, B., Hellendoorn, H., 2005. Model predictive control for optimal coordination of ramp metering and variable speed limits. Transp. Res. Part C Emerg. Technol. 13, 185–209. https://doi.org/https://doi.org/10.1016/j.trc.2004.08.001

Hochreiter, S., 1997. Long Short-Term Memory. Neural Comput. 9, 1735–1780. https://doi.org/10.1162/neco.1997.9.8.1735

Iqbal, M.S., Hadi, M., Xiao, Y., 2017. Predicting arterial breakdown probability: A data mining approach. J. Intell. Transp. Syst. Technol. Planning, Oper. 21, 190–201. https://doi.org/10.1080/15472450.2017.1279543

Jacobson, L., Stribiak, J., Nelson, L., Sallman, D., 2006. Ramp Management and Control Handbook.

Kan, X. (David), Lu, X.-Y., Skabardonis, A., 2018. Increasing Freeway Capacity by Efficiently Timing Its Nearby Arterial Traffic Signals. Transp. Res. Rec. 2672, 27–34. https://doi.org/10.1177/0361198118782796

Kan, Y., Wang, Y., Papageorgiou, M., Papamichail, I., 2016. Local ramp metering with distant downstream bottlenecks: A comparative study. Transp. Res. Part C Emerg. Technol. 62, 149–170. https://doi.org/https://doi.org/10.1016/j.trc.2015.08.016

Keyvan-Ekbatani, M., Yildirimoglu, M., Geroliminis, N., Papageorgiou, M., 2015. Multiple concentric gating traffic control in large-scale urban networks. IEEE Trans. Intell. Transp. Syst. 16, 2141–2154.

Keyvan Ekbatani, M., Gao, X., Gayah, V. V, Knoop, V.L., 2016. Combination of traffic-responsive and gating control in urban networks: Effective interactions, in: Proceedings of the 95th Annual Meeting of the Transportation Research Board, Washington (USA), 10-14 Jan. 2016; Authors Version.

Kotsialos, A., Papageorgiou, M., 2004. Nonlinear optimal control applied to coordinated ramp metering. IEEE Trans. Control Syst. Technol. 12, 920–933. https://doi.org/10.1109/TCST.2004.833406

Kouvelas, A., Triantafyllos, D., Geroliminis, N., 2018. Hierarchical Control Design for Large-Scale Urban Road Traffic Networks, in: Transportation Research Board 97th Annual Meeting,.

Kwon, E., Ambadipudi, R.-P., Bieniek, J., 2003. Adaptive coordination of ramp meter and intersection signal for optimal management of freeway corridor, in: Proc. 82th Annu. Meeting Transp. Res. Board.

Lee, C.C., 1990. Fuzzy Logic in Control Systems: Fuzzy Logic Controller, Part II. IEEE Trans. Syst. Man Cybern. 20, 419–435. https://doi.org/10.1109/21.52552

Lim, K., Kim, J.H., Shin, E., Kim, D.-G., 2011. A signal control model integrating arterial

intersections and freeway off-ramps. KSCE J. Civ. Eng. 15, 385–394.

Liu, J.-W., Wang, Y.-F., Lu, R.-K., Luo, X.-L., 2020. Multi-View Non-negative Matrix Factorization Discriminant Learning via Cross Entropy Loss. Present. 2020 Chinese Control Decis. Conf.

Lu, C., Elefteriadou, L., 2013. An investigation of freeway capacity before and during incidents. Int. J. Transp. Res. 5.

Lu, X.-Y., Su, D., Spring, J., 2013. Coordination of Freeway Ramp Meters and Arterial Traffic Signals Field Operational Test (FOT). CONTRACT 65, 3763.

Massahi, A., Hadi, M., Cutillo, M.A., Xiao, Y., 2017. Estimating the effects of urban street incidents on capacity. Transp. Res. Rec. 2615, 55–61. https://doi.org/10.3141/2615-07

Mata, H., Hadi, M., 2021. Supervised and Unsupervised Data Analytic Techniques to Support Integrated Facility and Segment Level of Service Analysis, in: 100th Annual Meeting of the Transportation Research Board,Washington, D.C., 2021. Washington DC, United States.

Medina, J.C., Hajbabaie, A., Benekohal, R. (Ray) F., 2013. Effects of Metered Entry Volume on an Oversaturated Network with Dynamic Signal Timing. Transp. Res. Rec. J. Transp. Res. Board 2366, 53–60. https://doi.org/10.3141/2356-07

Mohebifard, R., Hajbabaie, A., 2019. Distributed Optimization and Coordination Algorithms for Dynamic Traffic Metering in Urban Street Networks. IEEE Trans. Intell. Transp. Syst. 20, 1930–1941. https://doi.org/10.1109/TITS.2018.2848246

Mohebifard, R., Hajbabaie, A., 2018a. Real-Time Adaptive Traffic Metering in a Connected Urban Street Network, in: Transportation Research Board 97th Annual Meeting.

Mohebifard, R., Hajbabaie, A., 2018b. Dynamic traffic metering in urban street networks: Formulation and solution algorithm. Transp. Res. Part C Emerg. Technol. 93, 161–178. https://doi.org/10.1016/j.trc.2018.04.027

Mohebifard, R., Islam, S.M.A.B. Al, Hajbabaie, A., 2019. Cooperative traffic signal and perimeter control in semi-connected urban-street networks. Transp. Res. Part C Emerg. Technol. 104, 408–427. https://doi.org/https://doi.org/10.1016/j.trc.2019.05.023

Muñoz, J.C., Daganzo, C.F., 2002. The bottleneck mechanism of a freeway diverge. Transp. Res. Part A Policy Pract. 36, 483–505. https://doi.org/10.1016/S0965-8564(01)00017-9

Muñoz, J.C., Daganzo, C.F., 2000. Experimental characterization of multi-lane freeway traffic upstream of an off-ramp bottleneck. Univ. California, Berkeley 94720, 1–63.

Pang, M., Yang, M., 2020. Coordinated control of urban expressway integrating adjacent signalized intersections based on pinning synchronization of complex networks. Transp. Res. Part C Emerg. Technol. 116, 102645. https://doi.org/https://doi.org/10.1016/j.trc.2020.102645

Papageorgiou, M, Kotsialos, A., 2002. Freeway ramp metering: an overview. IEEE Trans. Intell. Transp. Syst. 3, 271–281. https://doi.org/10.1109/TITS.2002.806803

Papamichail, I., Kotsialos, A., Margonis, I., Papageorgiou, M., 2010. Coordinated ramp metering for freeway networks – A model-predictive hierarchical control approach. Transp. Res. Part C Emerg. Technol. 18, 311–331. https://doi.org/https://doi.org/10.1016/j.trc.2008.11.002

Papamichail, I., Papageorgiou, M., 2008. Traffic-Responsive Linked Ramp-Metering Control. IEEE Trans. Intell. Transp. Syst. 9, 111–121.

Papamichail, I., Papageorgiou, M., Vong, V., Gaffney, J., 2010b. Heuristic Ramp-Metering Coordination Strategy Implemented at Monash Freeway, Australia. Transp. Res. Rec. 2178, 10–20. https://doi.org/10.3141/2178-02

PTV AG, Karlsruhe, G., 2021. PTV VISSIM 2021 User Manual 265–297.

PTV Group, 2013. PTV Vissim 7 User Manual. PTV AG.

Rahman, R., Hasan, S., 2021. Real-time signal queue length prediction using long short-term memory neural network. Neural Comput. Appl. 33, 3311–3324. https://doi.org/10.1007/s00521-020-05196-9

Ramezani, M., Haddad, J., Geroliminis, N., 2015. Dynamics of heterogeneity in urban networks: aggregated traffic modeling and hierarchical control. Transp. Res. Part B Methodol. 74, 1–19.

Shaaban, K., Khan, M.A., Hamila, R., 2016. Literature Review of Advancements in Adaptive Ramp Metering. Procedia Comput. Sci. 83, 203–211. https://doi.org/https://doi.org/10.1016/j.procs.2016.04.117

Smaragdis, E., Papageorgiou, M., 2003. Series of New Local Ramp Metering Strategies. Transp. Res. Rec. 74–86. https://doi.org/10.3141/1856-08

Su, D., Lu, X.-Y., Horowitz, R., Wang, Z., 2014. Coordinated ramp metering and intersection signal control. Int. J. Transp. Sci. Technol. 3, 179–192.

Tangirala, S., 2020. Evaluating the impact of GINI index and information gain on classification using decision tree classifier algorithm. Int. J. Adv. Comput. Sci. Appl. 11, 612–619. https://doi.org/10.14569/ijacsa.2020.0110277

Tariq, M.T., Hadi, M., Saha, R., 2021. Using high-resolution signal controller data in the calibration of signalized arterial simulation models. Transp. Res. Rec. 2675, 1043–1055. https://doi.org/10.1177/03611981211031882

Tariq, M.T., Massahi, A., Saha, R., Hadi, M., 2020. Combining Machine Learning and Fuzzy Rule-Based System in Automating Signal Timing Experts' Decisions during Non-Recurrent Congestion. Transp. Res. Rec. 2674, 163–176. https://doi.org/10.1177/0361198120918248

Tharwat, A., 2018. Classification assessment methods. Appl. Comput. Informatics 17, 168–192. https://doi.org/10.1016/j.aci.2018.08.003

The MathWorks Inc., 2022. Fuzzy Logic Toolbox ™ User's Guide R2022a.

Tian, Z., 2007. Modeling and Implementation of an Integrated Ramp Metering-Diamond

Interchange Control System. J. Transp. Syst. Eng. Inf. Technol. 7, 61–69.

Urbanik, T., Tanaka, A., Lozner, B., Lindstrom, E., Lee, K., Quayle, S., Beaird, S., Tsoi, S., Ryus, P., Gettman, D., Sunkari, S., Balke, K., Bullock, D., 2015. Signal Timing Manual - Second Edition, Signal Timing Manual - Second Edition. https://doi.org/10.17226/22097

Wang, C., Xu, Y., Zhang, J., Ran, B., 2022. Integrated Traffic Control for Freeway Recurrent Bottleneck Based on Deep Reinforcement Learning. IEEE Trans. Intell. Transp. Syst. 1–14. https://doi.org/10.1109/TITS.2022.3141730

Wang, Y., Kosmatopoulos, E.B., Papageorgiou, M., Papamichail, I., 2014. Local Ramp Metering in the Presence of a Distant Downstream Bottleneck: Theoretical Analysis and Simulation Study. IEEE Trans. Intell. Transp. Syst. 15, 2024–2039. https://doi.org/10.1109/TITS.2014.2307884

Wang, Y., Yu, X., Zhang, S., Zheng, P., Guo, J., Zhang, L., Hu, S., Cheng, S., Wei, H., 2021. Freeway Traffic Control in Presence of Capacity Drop. IEEE Trans. Intell. Transp. Syst. 22, 1497–1516. https://doi.org/10.1109/TITS.2020.2971663

Wu, J., Jin, X., Horowitz, A.J., 2008. Methodologies for estimating vehicle queue length at metered on-ramps. Transp. Res. Rec. 75–82. https://doi.org/10.3141/2047-09

Yang, X., Cheng, Y., Chang, G.-L., 2018. Integration of adaptive signal control and freeway off-ramp priority control for commuting corridors. Transp. Res. Part C Emerg. Technol. 86, 328–345. https://doi.org/https://doi.org/10.1016/j.trc.2017.11.019

Yelchuru, B., Nevers, B., Dowling, R., Zohdy, I., Kamalanathsharma, R., 2016. Analysis, Modeling, and Simulation (AMS) Testbed Development and Evaluation to Support Dynamic Mobility Applications (DMA) and Active Transportation and Demand Management (ATDM) Programs - San Mateo Testbed Analysis Plan.